TECHNISCHE UNIVERSITÄT MÜNCHEN

TUM School of Life Sciences

Deciphering the roles of hypothalamic oxytocin neurons and astrocytes in the regulation of systemic glucose homeostasis

Franziska Maria Lechner

Vollständiger Abdruck der von der TUM School of Life Sciences
der Technischen Universität München zur Erlangung des akademischen Grades einer

Doktorin der Naturwissenschaften (Dr.rer.nat.)

genehmigten Dissertation.

Vorsitz:	Prof. Julijana Gjorgjieva
Prüfende der Dissertation:	1. Prof. Dr. Ilona Grunwald Kadow
	2. Prof. Dr. Cristina García-Cáceres

Die Dissertation wurde am 13.12.2023 bei der Technischen Universität München eingereicht und durch die TUM School of Life Sciences am 22.03.2024 angenommen.

I. Abstract

Obesity, along with its associated comorbidities like type 2 diabetes (T2D), has escalated to pandemic proportions. Consequently, there are currently intensified efforts focused on identifying more effective pharmacological targets to manage this widespread prevalence. The brain, particularly the hypothalamus, is known to play a pivotal role in regulating glucose homeostasis by overseeing systemic glucose levels and influencing peripheral organs involved in glucose regulation. However, the cellular and molecular mechanisms through which the hypothalamus maintains control over glucose metabolism, and how it is impacted in obesity and diabetes, remain largely unknown. Given the significant gaps in our knowledge, I focused my investigations on comprehending how both neuronal and non-neuronal cells (astrocytes) contribute the regulation of systemic glucose levels, understanding their distinct roles, and uncovering regulatory mechanisms that could potentially be the target of future pharmacological interventions. Specifically, I focused my investigations on: (1) how the neuropeptide oxytocin (OT) improves glucometabolism via central versus peripheral signaling (pancreatic β-cell), aiming to clarify the exact neural and humoral pathways by which the OT system modulates glucose disposal and pancreatic hormone secretion; and (2) how hypothalamic astrocytes, via glucose transporter 1 (GLUT-1), regulate hepatic glucose output in response to glucopenia via the peripheral nervous system.

More specifically I found that chemogenetically activating hypothalamic OT neurons induces an increase in circulating OT levels, glucose disposal and first-phase insulin secretion. Supporting the importance of oxytocin signaling in glucoregulation, a region-specific OTR KO in the glucoregulatory ventromedial hypothalamus (VMH) led to altered glucose tolerance. To distinguish β-cell- from brain- OT signaling, we generated a β-cell-specific OTR-KO mouse model and found that these mice failed to improve glucose tolerance and insulin secretion relative to control mice upon systemic but not central administration. Intriguingly, central OT application in control mice triggered a lesser insulin secretion than systemic OT injection, suggesting that the neuronal circuits involving OT signaling operate through a distinct glucoregulatory mechanism. In HFHS diet-fed mice, the effect of centrally administered OT was blunted, while peripheral OT still improved glucose tolerance.

Interestingly, we found that mice with astrocyte-specific postnatal ablation of GLUT1 exhibit an excessive hepatic glucose output in response to glucoprivation relative to littermate controls, hence overcompensating, possibly due to a potentiated central glucopenia. This difference in hepatic glucose output was lost by pharmacologically blocking the nicotinergic acetylcholine receptor of the peripheral nervous system, revealing these effects are mediated by direct innervation. Mechanistically, in acute brain slices, we could reveal that in hypothalamic astrocytes devoid of GLUT-1, a glucoprivic stimulus failed to increase intracellular Ca^{2+},

otherwise observed in astrocytes from control mice. Furthermore, I demonstrated a reduced glycolytic capacity, increased capacity to metabolize glutamate and elevated basal respiration in primary GLUT1-KO astrocytes compared to controls.

In summary, these findings support the critical role of the hypothalamus in orchestrating counterregulatory processes crucial for maintaining systemic glucose levels — a function particularly affected in metabolic diseases like obesity and T2D. Furthermore, my research elucidates the active contribution of specific hypothalamic cell populations, such as OT and OTR expressing neurons and GLUT-1 expressing astrocytes, to the regulation of systemic glucose levels through distinct mechanisms, dependent on peripheral glucose levels. Understanding the intricate roles played by different cell populations within the hypothalamus presents opportunities for tailored interventions addressing glucose dysregulation in diverse metabolic conditions.

II. Zusammenfassung

Das Auftreten von Übergewicht zusammen mit Begleiterkrankungen wie Typ 2 Diabetes (T2D) hat pandemische Ausmaße angenommen. Schlussfolgernd haben sich die derzeitigen Anstrengungen verstärkt, effektive pharmakologische Ziele zur Bekämpfung dieser weitverbreiteten Prävalenz zu identifizieren. Das Gehirn, im Spezifischen der Hypothalamus, spielt eine entscheidende Rolle in der Regulation des Energie- und Glukosestoffwechsels, indem es den Blutzucker im Zusammenspiel mit anderen blutzuckerregulierenden Organen im Gleichgewicht hält. Allerdings sind die zellulären und molekularen Mechanismen, welche dem Hypothalamus die Kontrolle über die Glukosehomöostase ermöglichen, weitestgehend unbekannt. Ebenso unklar ist bisher, wie dieses Zusammenspiel durch Übergewicht beeinflusst wird und letztendlich zu Diabetes führt. Daher sollten Zellpopulationen und Signalwege im Gehirn als pharmakologisches Ziel neuer Wirkstoffe in Betracht gezogen werden. Ausgehend von den Wissenslücken habe ich mich in meiner Dissertation damit beschäftigt zu verstehen, wie sowohl Neuronen und als auch nicht-neuronaler Zellpopulationen im Gehirn (Astrozyten) zu der Regulation des systemischen Blutzuckerspiegels beitragen. Außerdem habe ich deren individuellen Rollen untersucht, um potenzielle Mechanismen und Angriffspunkte für zukünftige, breitgefächerte Behandlungsmöglichkeiten zu eruieren. Im Genaueren habe ich mich bei meiner Arbeit auf Folgendes fokussiert: (1) Wie sich die Wirkungsweise des Neuropeptids Oxytozin (OT) auf die Verbesserung des Glukosemetabolismus aus zentraler Signalweiterleitung und peripherer Wirkung an den β-Zellen des Pankreas zusammensetzt, wodurch ein genaueres Bild der neuralen versus humoralen Wirkungsweisen des OT-Systems auf Glukosespeicherung und Insulinsekretion des Pankreas entstanden ist; Und (2) Wie hypothalamische Astrozyten mithilfe des Glukosetransporter 1 (GLUT-1) die Glukosefreisetzung der Leber nach Glukopenie durch das periphere Nervensystem reguliert.

Chemogenetische Aktivierung von Oxytozinneuronen während eines hyperglykämischen Clamps, und damit endogene Freisetzung von Oxytozin, führte zu einem Anstieg von zirkulierendem Oxytozin, gesteigerter Glukoseeinlagerung und erhöhter Insulinsekretion in der Startphase. Ein regional begrenzter KO des Oxytozinrezeptors (OTR) in dem glukoregulatorischem ventromedialem Hypothalamus (VMH) führte zu einer Verschlechterung der Glukosetoleranz, was die wichtige Rolle von zentraler Oxyotozinsignalgebung unterstreicht. Um die Oxytozinwirkung durch β-Zell-induzierte Signalgebung von Gehirn-induzierter Signalgebung zu unterscheiden, generierten wir ein β-Zell-spezifischen OTR KO-Mausmodell und konnten zeigen, dass Mäuse ohne OTR in β-Zellen nicht auf systemisch (subkutan) verabreichtes OT reagieren, aber dass zentral (intranasal) verabreichtes OT weiterhin die Glukosetoleranz verbessert. Interessanterweise löst zentral verabreichtes OT

kaum Insulinsekretion aus, was darauf hinweist, dass neuronal vermittelte Oxytozin-Signalgebung auf einen separaten glukoregulatorischen Mechanismus zurückgreift. In Mäusen, die mit einer Hochfettdiät gefüttert wurden, ist die zentrale Wirkung von OT abgeschwächt während periphere OT-Verabreichung weiterhin zu einer Verbesserung der Glukosetoleranz führt.

Bemerkenswerterweise konnten wir zeigen, dass ein Astrozyten-spezifischer, postnataler KO von GLUT-1 einen exzessive hepatische Glukoseproduktion als Antwort auf Glukopenia im Vergleich zu Kontrollen zur Folge hat, möglicherweise verursacht durch zentrale Glucopenia. Dieser Unterschied in der Glukoseproduktion der Leber konnte durch pharmakologische Inhibierung der nikotinergischen Acetylcholinrezeptoren ausgeglichen werden, was aufzeigt, dass der Effekt durch direkte Innervierung bedingt ist. Auf mechanistischer Ebene konnten wir herausfinden, dass hypothalamische Astrozyten ohne GLUT1 in *ex-vivo* Gehirnschnitten einen angestiegenen intrazellulären Ca^{2+} Spiegel aufweisen und auf einen Glucopenia-induzierenden Stimulus nicht wie Wildtypastrozyten im Vergleich mit einem Anstieg des intrazellulären Ca^{2+} reagieren. Weiterhin konnten wir sowohl eine reduzierte Glykolyse und glykolytische Kapazität nachweisen als auch eine erhöhte Basalatmung und eine angestiegene Abhängigkeit und Kapazität Glutamat zu verstoffwechseln.

Zusammenfassend unterstützen diese Erkenntnisse die zentrale Rolle des Hypothalamus die gegensteuernden Prozesse zu dirigieren, die zur Erhaltung des Gleichgewichts des systemischen Blutglukosespiegels notwendig sind – eine Funktion, die speziell in stoffwechselbedingten Krankheitsbildern wie Übergewicht und Diabetes, beeinträchtigt ist. Weiterhin hat meine Forschung das Wissen über die aktive Regulation des Blutglukosespiegels durch spezifische hypothalamische, neuronale Populationen wie OT- und OT Rezeptor exprimierende Neurone sowie GLUT-1 exprimierende Astrozyten vertieft, welche als Reaktion auf steigende oder sinkende Blutglukose reagieren indem sie durch spezialisierte Signalweiterleitung eine Gegenregulation in Gang setzen. Das Verstehen dieser verzweigten Rollen verschiedener Zellpopulationen innerhalb des Hypothalamus schafft neue Möglichkeiten zur angepassten Behandlung von Regulationsstörungen der Blutglukose bei Stoffwechselerkrankungen.

III. Table of Contents

IV. List of figures

V. List of tables

VI. Glossary of terms

2DG	2-Deoxy-Glucose
2DGTT	2-Deoxy-Glucose tolerance test
AAV	Adeno-associated virus
aBNST	anterior bed nucleus of the stria terminalis
AgRP	Agouti related protein
ARC	Arcuate nucleus of the hypothalamus
BAT	Brown adipose tissue
BBB	Blood brain barrier
BMI	Body mass index
BW	Body weight
CART	Cocain- and amphetamine-regulated transcript
CCK	Cholecystokinin
CeA	Central amygdala
CNO	Clozapine N-oxide
CNS	Central nervous system
DCA	Dichloroacetate
DIO	Diet-induced obesity
DMX	Dorsal motor nucleus of the vagus
DREADD	Designer receptors exclusively activated by designer drugs
ECAR	Extracellular acidification rate
FI	Food intake
G6pase	Glucose-6-phosphatase
GFAP	Glial fibrillary acidic protein
GIP	Glucose-dependent insulinotropic polypeptide
GLP1	Glucagon-like peptide 1
GLUT	Glucose transporter
GTT	Glucose tolerance test
i.c.v.	intracerebroventricular
i.n.	intranasal(ly)
IL-6	Interleukin 6
IR	Insulin receptor
IRS	Insulin receptor substrate
ITT	Insulin tolerance test
K_{ATP}	ATP sensitive potassium channel
KO	Knockout

MBH	Mediobasal hypothalamus
MCT	Monocarboxylate Transporter
NcA	Nucleus accumbens
NPY	Neuropeptide Y
NTS	Nucleus tractus solitarius
OCR	oxygen consumption rate
PCR	Polymerase chain reaction
PEPCK	Phosphoenolpyruvate carboxykinase
PI3K	Phosphoinositide kinase
PKB/Akt	Protein kinase B
POA	Preoptic area
POMC	Proopiomelanocortin
PVN	Paraventricular nucleus
s.c.	subcutaneous(ly)
SGLT	Sodium glucose linked transporter
SNS	Sympathetic nervous system
STAT3	Signal transducer and activator of transcription 3
T1D	Type I Diabetes
T2D	Type II Diabetes
VMH	Ventromedial nucleus of the hypothalamus
WHO	World Health Organization
WT	Wildtype

1 Introduction

1.1 Obesity and diabetes

Obesity is a global pandemic, long considered to have no treatment capable of slowing its steady progression. From 1980 to 2015, the prevalence of obesity has roughly doubled in more than 70 countries, and the rate of increase among children surpassed that of adults (GBD 2015 Obesity Collaborators et al., 2017). According to the most recent numbers of the World Health Organization (WHO), 39% of the adult population worldwide are overweight with a body mass index (BMI) of 25 or more and 13% are obese (BMI $\geq$30), which translates to 650 million people with obesity (WHO report, 2016). The WHO also reported a shocking count of 39 million children overweight or obese in 2020. In 2015, around 4 million deaths were attributed to obesity, mostly due to its wide range of comorbidities that include cardiovascular disease, non-alcoholic fatty liver disease, chronic kidney disease, and diabetes (GBD 2015 Obesity Collaborators et al., 2017).

Diabetes itself affected approximately 415 million people in 2015 and is estimated to increase by 50% by 2040 (Ogurtsova et al., 2017). The term diabetes is commonly used to refer to diabetes mellitus, a metabolic disorder characterized by insufficient insulin effectiveness that leads to chronic hyperglycemia and consequent vascular and neuropathic damages (Padhi et al., 2020). *Diabetes mellitus* summarizes two major sub-types: type I diabetes (T1D), which results from reduced or abolished insulin secretion following autoimmune destruction of β-cells, and type II diabetes (T2D), defined by multi-organ insulin resistance and often associated with obesity (Padhi et al., 2020). While lifestyle interventions such as increased physical activity and dietary weight management are promising for the treatment of T2D (Churuangsuk et al., 2022, Jaramillo et al., 2023), patient adherence is extremely discouraging. Currently, the most successful treatment against obesity and its comorbidities, such as T2D, is bariatric surgery (van den Broek-Altenburg et al., 2022). However, it is only conducted in extreme cases of a BMI >40 or a BMI >35 with severe comorbidities, as it requires life-long eating restrictions and nutrient supplementation. Other therapeutical options are targeting insulin availability, insulin action or limit blood glucose artificially (Padhi et al., 2020). Nevertheless, the need for frequent dosing (due to the short half-life of the drugs) and the side effects often lead to a lack of compliance from patients (Padhi et al., 2020). Therefore, ongoing research is aiming at advancing our understanding of the defective mechanisms to refine therapeutical options.

1.2 Glucose homeostasis and insulin resistance

In a healthy population, the blood glucose level is maintained within a tight range of around 3.9-5.6mM (70-100mg/dl) by multiple mechanisms and organs involved in glucose homeostasis. Ingestion of food is followed by a release of incretins from intestinal L- and K-

cells, glucagon like protein 1 (GLP-1), and glucose-dependent insulinotropic polypeptide (GIP), which stimulate insulin secretion (Bano, 2013). Digestion and absorption of food also leads to a rise in blood glucose, which, after glucose uptake at the level of the pancreas, stimulates insulin secretion itself. Insulin acts on several effector tissues to decrease blood glucose: it inhibits gluconeogenesis in the liver which leads to storage of glucose in the form of glycogen, it increases glucose uptake in muscle and adipose tissue, and inhibits glucagon secretion in the pancreas (Bano, 2013). However, when blood glucose levels fall to hypoglycemic conditions (<3.9mM), counterregulatory mechanisms are triggered to bring the blood glucose back into the normal range. These counterregulatory mechanisms include hepatic glucose production (HGP), release of hormones like epinephrine, norepinephrine, glucagon, and corticosteroids that mobilize endogenously stored glucose and fatty acids as alternative energy sources (Watts and Donovan, 2010, Cato et al., 1990). Furthermore, increased food intake including improved digestion and absorption leads to an elevated uptake of exogenous nutrients.

Table 1 – Regulatory response to fluctuations in blood glucose and pathologic defects promoting diabetes Summarized from (Bano, 2013)

Organ	Hyperglycemia	Hypoglycemia	Obesity/Prediabetes
Pancreas	Insulin secretion	Glucagon secretion	Progressive β-cell dysfunction, mitochondrial disfunction
Liver	Inhibition of gluconeogenesis, glycogen storage	Gluconeogenesis, Glycogenolysis	Insulin resistance, fat accumulation, mitochondrial dysfunction, inflammatory response
Muscles	Glucose uptake, Glycogen storage	Glycogenolysis	Insulin resistance, fat accumulation, mitochondrial dysfunction
Adipose Tissue	Glucose uptake; De-novo lipogenesis	Lipolysis	Inflammatory response, Increased adipokine/ cytokine release
Adrenals		Corticosteroids, Catecholamines	
Kidney		Gluconeogenesis	

While it is not entirely clear what the fundamental changes are that lead to a chronic dysregulation of blood glucose as in diabetes, several obesity-related changes are associated with the disruption of glucose homeostasis. Within adipose tissue, a hypercaloric diet and obesity lead to stress and apoptosis of adipocytes, consequently followed by increased

inflammation and release of adipokines and cytokines (Deng and Scherer, 2010). With obesity, the adipose tissue, skeletal muscle, and liver become insulin resistant, thus, glucose uptake and inhibition of gluconeogenesis induced by insulin are blunted (Martyn et al., 2008, Bano, 2013). Increased release of free fatty acids by adipose tissue further decreases glucose uptake (Boden, 1997). In obesity, fat accumulates in other tissues such as liver and muscle (Larson-Meyer et al., 2011), leading to a decrease in both mitochondrial mass and function (Bournat and Brown, 2010), which further interferes with insulin signaling. After long-term maximal activation of pancreatic cells, which attempt to compensate by increasing insulin secretion, β-cells and/or islets can become critically damaged. With advancing islet damage, insulin secretion is progressively reduced (Prentki and Nolan, 2006).

Until now, the high emphasis put on insulin, whether regarding resistance, β-cell damage/exhaustion, or replacement, has led to an islet-centric view that pushed aside the contribution of insulin-independent glucoregulatory mechanisms, also referred to as “glucose effectiveness” (Mirzadeh et al., 2022). Studies showed that this so-called glucose effectiveness is significantly decreased (around 40%) in T2D patients. Linked to changes in both glucose tolerance and insulin sensitivity, it can be found significantly reduced as early as 10 years before the onset of T2D (Welch et al., 1990, Bergman et al., 1981, Martin et al., 1992). The mechanisms regulating blood glucose levels include adjustments in food consumption, digestion, nutrient (re)absorption, energy storage, and energy expenditure, all of which are orchestrated by the brain as illustrated in figure 1 (Roh et al., 2016). The brain can not only integrate information about glucose levels per se, but it also responds to hormonal cues that are assessing the body’s energy status such as GLP-1, GIP, the hunger-hormone ghrelin, leptin, and insulin, among others. Moreover, it exerts its influence on effector organs both, through direct innervation and indirectly by stimulating hormone secretion. Several studies have documented pathological changes in the central nervous system (CNS) during the early stages of obesity and diabetes (Gonzalez Olmo et al., 2023, Stevenson et al., 2020, Henn et al., 2022, Lutomska et al., 2022). If this marks the earliest starting point in diabetic pathophysiology within the homeostatic regulatory circuits of the CNS, it raises the question of whether obesity and diabetes should be considered a brain disease. The implication would then suggest that pharmacological treatments for diabetes could target respective neuronal circuits and other involved brain cell communities. Consequently, we are interested in unraveling the brain cell populations or circuits involved which could potentially represent relevant future targets.

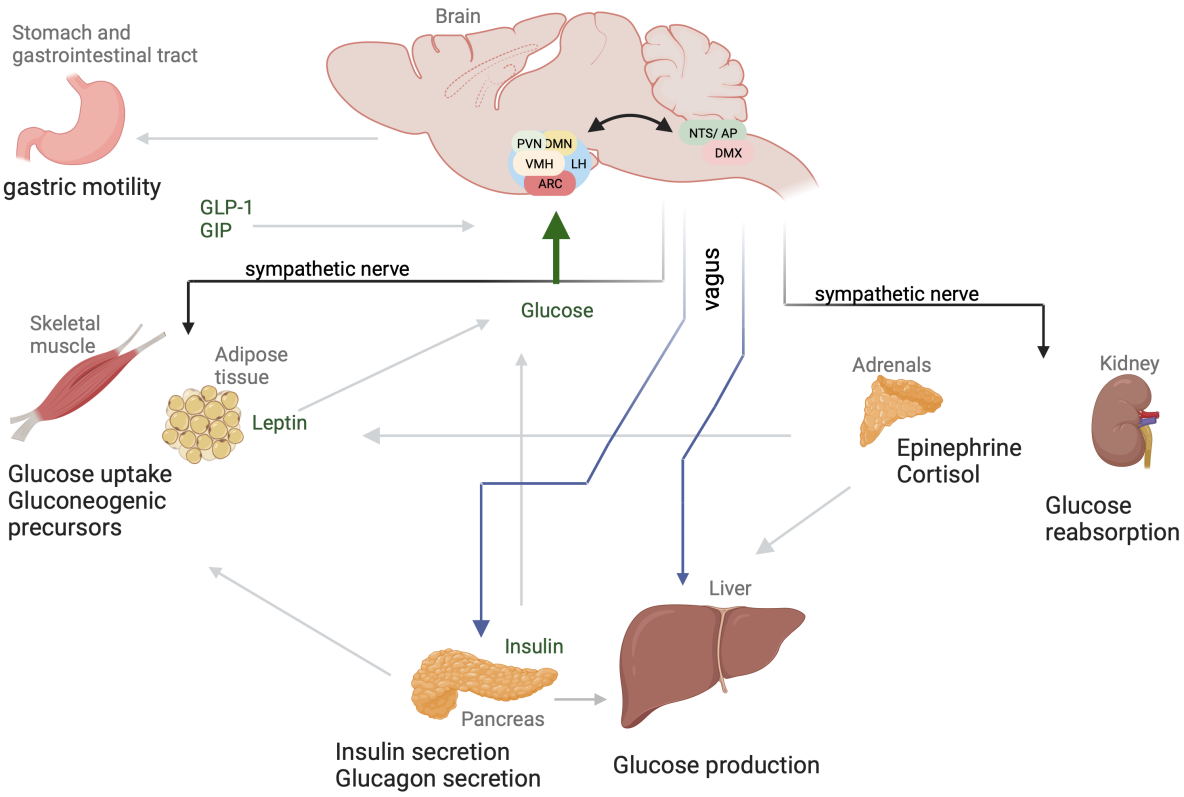

Figure 1 – Regulatory outputs of the central nervous system (CNS) to control glucose homeostasis

The brain, specifically the hypothalamus and the hindbrain sense glucose and cues of energy status (GLP-1, GIP, leptin, insulin) and communicate with peripheral tissues via sympathetic and parasympathetic nerves to induce glucoregulatory responses. GLP-1: glucagon like peptide 1; GIP: glucose-dependent insulinotropic polypeptide; DMN: dorsomedial nucleus; LH: lateral hypothalamus; PVN: paraventricular nucleus; VMH: ventrolateral hypothalamus; ARC: arcuate nucleus; DMX: dorsal motor nucleus of the vagus; NTS: nucleus tractus solitarius; AP: area postrema (Created with Biorender.com, adapted from (Roh et al., 2016))

1.3 Glucose sensing in the brain

Being able to assess glucose availability (glucose sensing) is of major importance for the regulation of glucose homeostasis. This is especially true for the brain, where appropriate glucose supply is essential and tight control of glucose levels is imperative. Brain glucose levels vary within a range from 0.1-5mM depending on species, brain region, and blood glucose concentration, as the brain glucose concentration represents 15-30% of peripheral blood glucose levels (Silver and Erecinska, 1994, McNay and Gold, 2002, Abi-Saab et al., 2002). Besides important sensors in the hepatic portal-mesenteric veins, glucose sensing neurons have been found in the hindbrain and the hypothalamus (Routh et al., 2012). Different types of neurons are involved in the fine-tuning of glucose sensing and are defined by their given capacity in changing their activity in response to changes in extracellular glucose levels (Routh et al., 2014). There are neurons which are either glucose-excited (GE) or glucose-inhibited (GI), amongst which some neurons are active in low glucose conditions (hypoglycemia) and others in high glucose conditions (hyperglycemia).

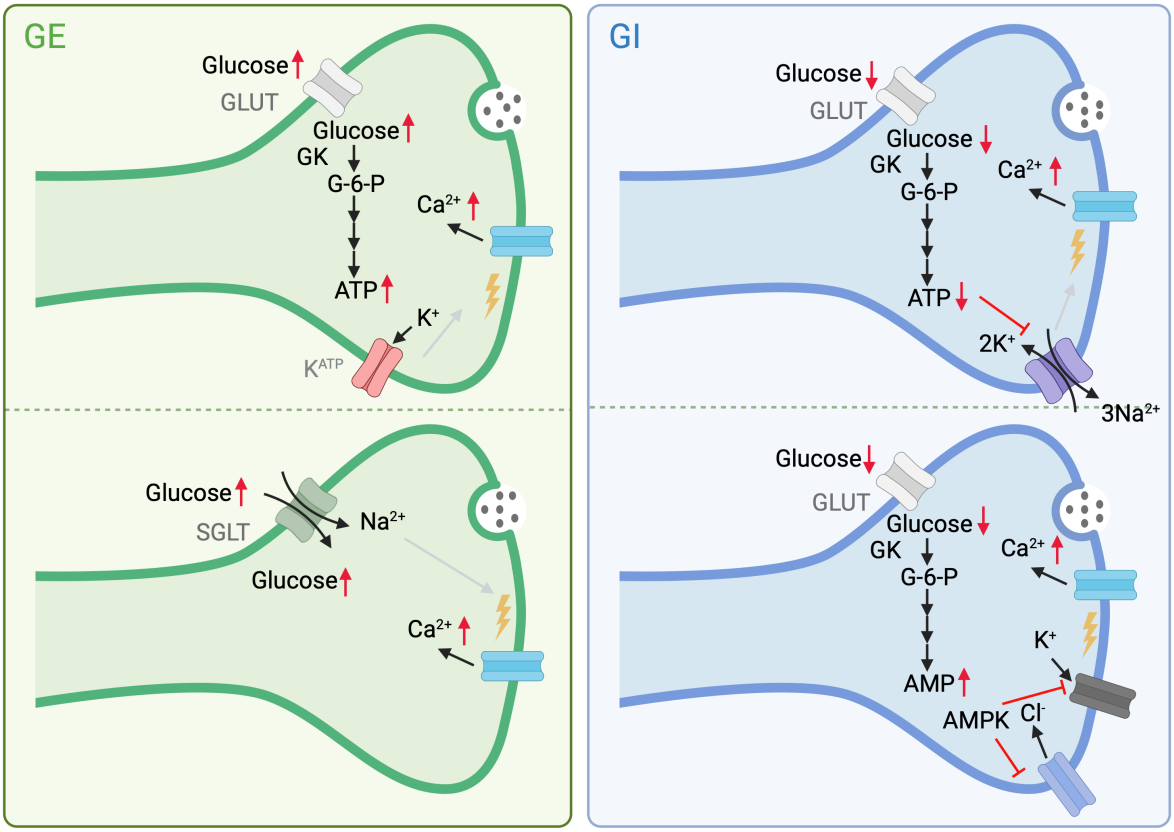

Figure 2 – Mechanism of glucose sensing

GK: Glucokinase; G-6-P: Glucose-6-Phosphate; GLUT: Glucose transporter; SGLT: sodium-dependent glucose co-transporter; ATP: Adenosine triphosphate; AMP: Adenosine monophosphate; AMPK: AMP-activated protein kinase; (created with Biorender.com, adapted from:(Koepsell, 2020))

Interestingly, pancreatic islet cells developed from neuronal progenitor cells, which explains the similarities concerning glucose sensing from a phylogenetic standpoint (Arntfield and van der Kooy, 2011). In the brain, two types of sensing can be distinguished, as summarized in figure 2: metabolism-dependent, involving glucose transporters (GLUTs), and metabolism-independent, based on sodium-dependent glucose cotransporter-1 (SGLT-1) transporters. In GE neurons, the described mechanism based on GLUTs is the same as in the pancreatic β-cell: glucose is metabolized to generate ATP via glucokinase (GK), an increase in the ATP/ADP ratio inhibits ATP-sensitive potassium channels (K_{ATP}) leading to a change in membrane potential (V_M). Consequently, the opening of voltage-dependent Ca^{2+} channels induces an increase in intracellular Ca^{2+}. When the transport of glucose is achieved by SGLTs, it is the transport itself which induces changes in V_M as it depends on the co-transport of Na^{2+} and H^+. In both cases, the change in V_M leads to release of neurotransmitters. In GI neurons, there are two described mechanisms, 1) decreasing ATP inhibits sodium potassium pump (Na^{+}/K^{+}-ATPase), which slows down transport, leads to changes in V_M and, thus intracellular Ca^{2+}, and 2) elevated AMP activates AMP-activated protein kinase (AMPK) which inhibits potassium (K^+) and chloride (Cl^-) channels, which again alters V_M.

The hypothalamus is, next to the brain stem, the most important region in the brain controlling energy and glucose homeostasis (Haspula and Cui, 2023). The proximity to the median eminence as a circumventricular organ allows direct contact to circulating nutrients and hormones. In contrast to most parts of the brain, where the blood brain barrier (BBB) tightly controls the flux from blood to brain, blood vessels in these areas are fenestrated to allow increased exchange of nutrients/hormones which allows sensing of the peripheral energy status. As far as hypothalamic areas are concerned, the paraventricular nucleus (PVN), the arcuate nucleus (ARC), and the ventromedial hypothalamus (VMH) are specifically linked to glucose regulation and have been shown to play a major role in glucoregulatory circuits. Within the hindbrain, the area postrema (AP), nucleus tractus solitarius (NTS), and dorsal motor nucleus of the vagus (DMX) (summarized as the dorsal vagal complex (DVC)) are involved in detection of hypoglycemia and induction of a counterregulatory response to the latter (A summary of main brain areas involved glucose homeostasis is shown in figure 3).

1.3.1 Hindbrain

2-deoxyglucose (2DG) is a compound that is taken up by cells like glucose but cannot be metabolized leading to an intracellular energy deficit and is often used to induce glucopenia/glucoprivation. Within the hindbrain, application of 2DG in the fourth ventricle (4V) led to an increase in blood glucose levels, food intake, and cFos[1] expression, in ARC and PVN (Sato et al., 2021). Catecholaminergic neurons in the A1/C1 region of the ventrolateral medulla (VLM), in the C2 and C3 of the dorsal medulla, and in the A6 area of the pons have been found to be activated in response to 2DG (Ritter et al., 1998, Damanhuri et al., 2012). However, Li and colleagues showed, using a chemogenetic[2] approach in different VLM regions, that only dual transfection and activation of medial C1 and rostral C1 in the VLM induces elevations in blood glucose and corticosterone (Li et al., 2018). Zhao and colleagues confirmed that chemogenetic activation of neurons in the rostral VLM, more specifically catecholaminergic neurons, was able to induce hyperglycemia via spinal cord projections and sympathetic activation of the adrenals (Zhao et al., 2017). Also, chemogenetic activation of neurons in the NTS increased blood glucose, glucagon, and hepatic PEPCK mediated by parasympathetic innervation (Boychuk et al., 2019). In terms of glucose sensing mechanistics, it has been shown that GLUT-2-expressing GI neurons projecting to the DMX are activated via AMPK-mediated closure of K_{ATP} channels which leads to parasympathetic signaling and glucagon secretion (Lamy et al., 2014). In summary, several neuronal populations in the hindbrain respond to glucose deprivation and activation of these neurons can induce increases in blood glucose, glucagon, and corticosteroids by stimulating autonomic innervation.

[1] an immediate early gene used as surrogate for neuronal activity
[2] genetically expressed Designer Receptors Exclusively Activated by Designer Drugs (DREADDs) which can be either activating or inhibiting of cells expressing them upon binding of their ligand Clozapine N-oxide (CNO)

1.3.2 Arcuate Nucleus

The ARC is home to the well-characterized feeding circuit, the melanocortin system which includes the anorexigenic proopiomelanocortin (POMC)/ cocaine- and amphetamine-regulated transcript (CART) co-expressing neurons and orexigenic agouti-related protein (AgRP)/neuropeptide Y (NPY) co-expressing neurons that counteracts each other to regulate hunger and satiety (Wess et al., 2013).

GK, an enzyme important for glucose sensing as seen in figure 2, has been shown to be expressed in both AgRP and POMC neurons (Stanley et al., 2013). Furthermore, deletion of AMPK in POMC or AgRP neurons prevented their responses to changes in glucose levels in electrophysiological studies on *ex vivo* brain slices, indicating its necessity for glucose sensing (Claret et al., 2007). Interestingly, the metabolic regulation of both mouse models was disrupted: AMPK KO in POMC neurons led to obesity by increased food intake and decreased energy expenditure, while AMPK KO in AgRP neurons elevated the sensitivity to melanocortin signaling (Claret et al., 2007). These results highlight the importance of glucose sensing in ARC neurons in the regulation of energy balance. Genetically interfering with the K_{ATP} channel function in POMC neurons, which is also involved in glucose sensing, caused glucose intolerance in mice (Parton et al., 2007). This suggests that glucose sensing in POMC neurons is a crucial part of the control of glucose homeostasis. Intriguingly, disrupting insulin signaling in astrocytes reduces the activation of POMC neurons by glucose, suggesting astrocytes are involved in the glucose sensing of POMC neurons as another regulatory layer, which allows fine-tuning of glucose homeostasis (Garcia-Caceres et al., 2016). Interestingly, optogenetic[3] activation of POMC neurons increases HGP via increased gene expression of gluconeogenic enzymes PEPCK and G6Pase, which indicates a participation of POMC neurons in the counterregulatory response to low blood glucose (Kwon et al., 2020). Indeed, insulin-induced hypoglycemia was demonstrated to increase POMC intracellular Ca^{2+} (visualized through the expression of the genetically encoded the Ca^{2+} sensor GCaMP6 in POMC neurons) indicating an increase in these neurons' activation (Kwon et al., 2020). Furthermore, AgRP- and POMC-expressing neurons located in the ARC have been shown to participate in glucoregulatory processes by modulating glucose reabsorption in the kidney and glucose uptake in the BAT (Chhabra et al., 2016, Steculorum et al., 2016). More specifically, activation (chemogenetic and optogenetic) of AgRP neurons induces insulin resistance and reduced glucose uptake in BAT (Steculorum et al., 2016). In the pathological context of diet-induced obesity, glucose sensing in POMC neurons is impaired, which hints towards a role of glucose detection in the brain in the development of T2D (Parton et al., 2007). In summary, both AgRP and POMC

[3] a method where light-sensitive channels or enzymes are expressed in specific cells to allow their light-induced activation (or inhibition)

neurons are involved in glucose sensing and can affect peripheral glucose levels. However, integration and relay of signaling mostly takes place in the PVN (Cowley et al., 1999)

1.3.3 Paraventricular Nucleus

The function of the PVN is often described as a control center integrating signals from other hypothalamic nuclei, pons, and hindbrain. In response, it sends signals to the hindbrain and spinal cord to activate autonomic responses and/or releases neuroendocrine hormones via the pituitary (Ferguson et al., 2008). They are also involved in glucose homeostasis, as parvocellular neurons, the non-neuroendocrine neuronal type in the PVN, are activated by glucoprivation as demonstrated by studies looking at the immunoreactivity for cFos (Sanders and Ritter, 2000). Electrophysiological studies in *ex vivo* brain slices showed that parvocellular neurons in the PVN can detect glucopenia, with 24% GE vs 26% GI neurons (Melnick et al., 2011). However, compounds blocking or opening K_{ATP} channels did not affect the neuronal response, suggesting K_{ATP}-independent glucose sensing (Melnick et al., 2011). Interestingly, GK is highly expressed in the PVN (Ma et al., 2020). Virally overexpressing GK or glucose injection into the PVN improves glucose tolerance in an oral glucose tolerance test (oGTT) via an elevated release of the incretin GLP-1. Conversely, a knockdown of GK or a 2DG injection into the PVN decreased glucose tolerance during an oGTT (Ma et al., 2020), proving direct glucose sensing and a regulatory effect of GK-expressing neurons in the PVN on glucose homeostasis. Intriguingly, insulin- and glucose-induced oxytocin (OT) secretion from OT neurons, located in the PVN and the supraoptic nucleus (SON), has been shown to be blunted by GK inhibitors, suggesting OT neurons are one of the glucose-sensing neuronal population in the PVN (Song et al., 2014).

More indirectly, MC4R-expressing neurons in the PVN (PVN^{MC4R}) are inhibited by catecholaminergic input from the NTS, a connection that is important for feeding in response to fasting or hypoglycemia (Sayar-Atasoy et al., 2023). Accordingly, following glucoprivation, PVN^{MC4R} neurons are inhibited via an increased GABA release from AgRP-expressing neuronal projections emanating from the ARC, which triggers food intake (Sayar-Atasoy et al., 2023). In line with these observations, infusing catecholamines or NPY into the PVN induced food intake (Leibowitz et al., 1988). In the absence of food, infusion of catecholamines or NPY induced a counterregulatory response in the form of release of corticosteroids and vasopressin and increased blood glucose (Leibowitz et al., 1988). However, studies investigating the effect of PVN lesions on glucopenia-induced food intake did not show any difference in comparison to control conditions (Calingasan and Ritter, 1992). In sum, neurons in the PVN integrate signals from the ARC to modulate blood glucose accordingly, however, a subset of PVN neurons are also able to sense and influence glucose levels.

1.3.4 Ventromedial nucleus of the hypothalamus

The VMH is recognized as central in regulation of glucose homeostasis. Early studies using electrical stimulation of this region found activation of mechanisms to elevate glucose levels, including increased HGP, glycogen breakdown, and decreased insulin and glucagon levels but also mechanisms to reduce blood glucose levels, including glucose uptake in various peripheral tissues (Shimazu and Ogasawara, 1975, Shimazu et al., 1966, Frohman and Bernardis, 1971). Those results emphasize the presence of glucose increasing as well as glucose lowering neuronal circuits. On the contrary, lesion studies in the VMH were shown to increase circulating insulin, decrease glucagon levels, and suppress the counterregulatory response to hypoglycemia via parasympathetic and sympathetic pathways (Inoue et al., 1977, Berthoud and Jeanrenaud, 1979). A closer examination of the activity in the VMH of rats revealed that 14% of neurons were directly GE and 3% were GI (Song et al., 2001). In addition to this classification, other glucose-responsive subtypes in the VMH are not intrinsically glucose sensing but are presynaptically excited by decreased extracellular glucose (14%), and another part are presynaptically driven to respond to glucose elevations (19%) (Song et al., 2001). Another mechanism that appears to be involved is mitochondrial adaptation in the VMH in response to changes in systemic glucose availability (Toda et al., 2016). The study found that uncoupling protein 2 (UCP2) regulates the activity of GE neurons in the VMH by increasing mitochondrial numbers and reducing reactive oxygen production in response to elevated glucose levels - a circuit that enhances insulin-induced glucose uptake into peripheral tissues (Toda et al., 2016).

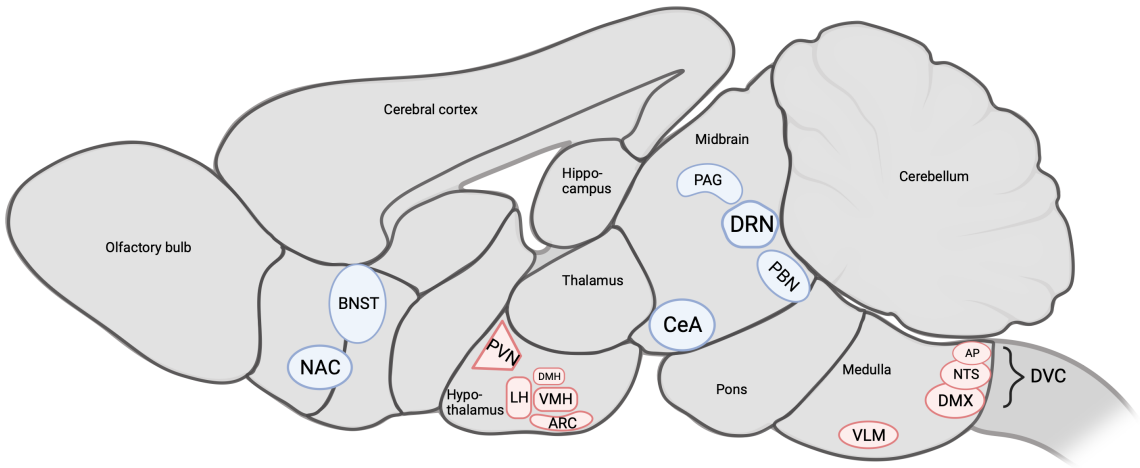

Figure 3 – Brain regions involved in glucose sensing

In red: areas of glucose sensing and regulation; In blue: areas which projections to have been shown to play a role. BNST: bed nucleus of the stria terminalis; NAC: nucleus accumbens; PAG: periaqueductal grey; DRN: dorsal raphe nucleus; PBN: parabrachial nuclei; CeA: central nucleus of the amygdala; PVN: paraventricular nucleus; VMH: ventrolateral hypothalamus; ARC: arcuate nucleus; DMX: dorsal motor nucleus of the vagus; NTS: nucleus tractus solitarius; AP: area postrema; DVC: dorsal vagal complex (Created with Biorender.com)

Several studies have been carried out to investigate the neuronal populations in the VMH involved in glucose sensing (discussed areas depicted in figure 3) and the peripheral consequences of their activation or inhibition. Infusing 2DG, a nonmetabolizable glucose analog, into the VMH via microdialysis showed that sensing energy deficits specifically in the VMH can significantly induce counterregulatory responses such as an increase in plasma levels of glucoregulatory hormones (epinephrine, norepinephrine, glucagon) and elevated blood glucose (Borg et al., 1995). On the other hand, infusing glucose into the VMH blunted hormonal counterregulation to a peripheral hypoglycemic condition by 85%, reaffirming the VMH as a key regulator of systemic glucose homeostasis (Borg et al., 1997).

The activity of different neuronal subpopulations within the VMH and projections to various regions seem to be integrated for a functional glucose homeostasis. Meek and colleagues observed that optogenetic inhibition of steroidogenic factor 1 (SF1) neurons blunts the counterregulatory response to insulin and stimulates glucagon and corticosterone release (Meek et al., 2016). On the other hand, the optogenetic stimulation of SF1 neurons resulted in an increase in blood glucose via a counterregulatory response including increases in glucagon, corticosterone, and expression of gluconeogenic genes (PEPCK and G6Pase) in the liver (Meek et al., 2016). Intriguingly, stimulating the SF1 neurons innervating the anterior bed nucleus of the stria terminalis (aBNST), but not those projecting to the PVN, CeA, or periaqueductal gray (PAG), led to increased blood glucose (Meek et al., 2016). However, when targeting nitric oxide synthase 1 (NOS1) expressing neurons, stimulating projections to the aBNST and PAG both elevated blood glucose while the first increased glucagon secretion and the later inhibited insulin secretion (Faber et al., 2018). Consequently, activating all VMH^{NOS} neurons resulted in an additive effect regarding blood glucose increase (Faber et al., 2018). Furthermore, investigations on estrogen receptor α-positive neurons in the ventrolateral VMH ($vlVMH^{ER\alpha}$) showed that $vlVMH^{ER\alpha}$ neurons projecting to the medioposterior (mp)ARC are activated by insulin but inhibited by glucose, while $vlVMH^{ER\alpha}$ neurons projecting to the dorsal raphe nuclei (DRN) respond in an opposite manner (He et al., 2020). Consequently, stimulating mpARC or inhibiting DRN projections both elevate blood glucose levels (He et al., 2020).

Regulatory circuits downstream of glucose sensing by SF1- and NOS1-expressing neurons were mostly shown to not change insulin levels. Only increased blood glucose via activation of VMH^{NOS} neurons projecting to PAG was accompanied by a lowering of insulin levels (Faber et al., 2018). Moreover, Khodai and colleagues found that chemogenetically activating the neuronal subpopulation expressing the pituitary adenylate cyclase activating peptide (PACAP) resulted in decreased insulin levels and significant glucose intolerance (Khodai et al., 2018).

Furthermore, the optogenetic activation of CCK_BR-expressing neurons in the VMH (VMH^{CCKBR}) resulted in strong hyperglycemia without changes in insulin levels; inversely, a tetanus toxin-induced silencing impaired HGP, which also included a blunted counterregulatory response to

insulin and 2DG (Flak et al., 2020). Interestingly, these effects of VMH^{CCKBR} silencing even led to controlled blood glucose levels and body weight in streptozotocin-induced diabetic mice (Flak et al., 2020).

In sum, glucoregulatory circuits branching from the VMH are extremely specialized and fine-tuned, which highlights the importance of glucose homeostasis.

1.4 Brain-organ crosstalk in the regulation of glucose homeostasis

The brain participates in the glucose regulation by signaling to certain organs implicated in the regulation of glucose homeostasis in the periphery, such as the liver, skeletal muscle, adipose tissue, pancreas, adrenal glands or gastrointestinal tract. The brain not only directly senses glucose availability, but also receives information from the periphery via both hormonal feedback and the autonomic innervation of peripheral organs.

While the communication between the periphery and the CNS occurs continuously, but also according to metabolic changes, research aimed to understand the specific pathways in the different tissues by which glucose metabolism is regulated.

1.4.1 Central glucoregulation via signaling to the liver

In the early 2000s, the laboratory of Rossetti investigated the role of hypothalamic nutrient sensing on the regulation of HGP. They were able to demonstrate that insulin signaling, specifically in the hypothalamus, is able to suppress HGP independently from blood insulin levels. This mechanism entailed phosphoinositide-3-kinase (PI3K) as a downstream target of the insulin receptor (IR) as well as K_{ATP}, as shown in figure 4 (Obici et al., 2002, Pocai et al., 2005a). The involvement of PI3K was confirmed by others through intracerebroventricular (i.c.v.) infusion of a PI3K inhibitor which led to a decreased insulin response (Gelling et al., 2006). Furthermore, overexpression of insulin receptor substrate 2 (IRS-2) and phosphokinase B (PKB) in the hypothalamus doubled the effect of insulin (Gelling et al., 2006). Similarly to insulin, when nutrients like glucose or lactate injected into the hypothalamus, HGP was also inhibited (Lam et al., 2005). As the effect is blocked by a K_{ATP} channel blocker, K_{ATP} signaling is also necessary for HGP suppression by those nutrients (Lam et al., 2005). The importance of central K_{ATP} channels was further highlighted in both rats and humans, where the i.c.v. injection of a K_{ATP} agonist was able to prevent both the reduction in endogenous glucose production and the increase in the expression of key gluconeogenic enzymes (phosphoenolpyruvate carboxykinase (PEPCK) and glucose-6-phosphatase (G6Pase)) in the liver otherwise induced by systemic application of a K_{ATP} channel antagonist (Carey et al., 2020). Interestingly, in another brain region, the dorsal vagal complex (DVC), it was found that HGP can be inhibited in a K_{ATP} channel-dependent manner both by insulin signaling (Filippi et

al., 2012) and through neuronal activation secondary to inhibition of hypothalamic fatty acid oxidation, dependent on vagal[4] innervation (Obici et al., 2003, Pocai et al., 2005b).

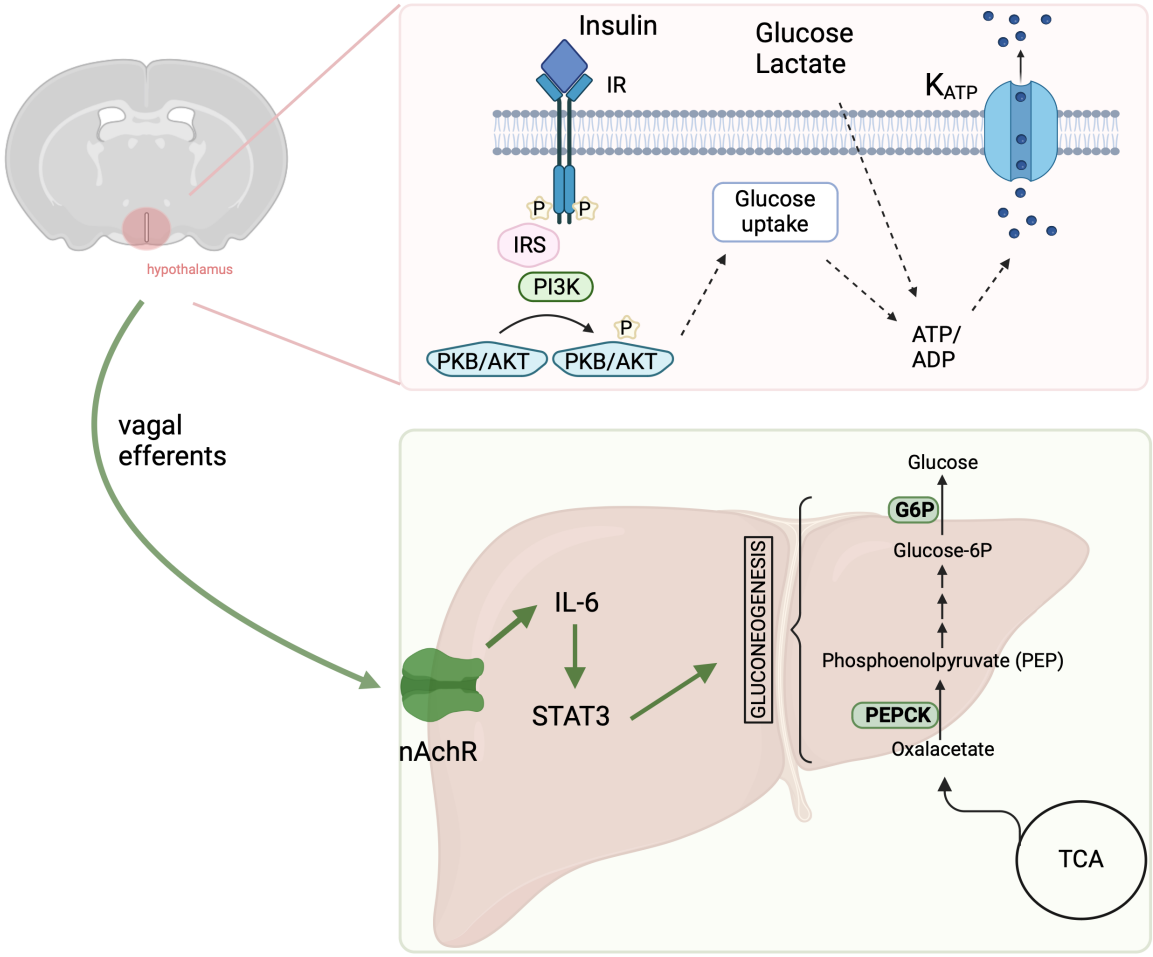

Figure 4 – Hypothalamic insulin signaling, and nutrient sensing regulates hepatic gluconeogenesis

Hypothalamic insulin signaling via IR, PI3K, PKB and K_{ATP} affects hepatic IL-6/STAT3 signaling via the vagus nerve. nAchR/IL-6/STAT3 signaling in the liver leads to gluconeogenic gene expression and HGP. IR: insulin receptor; IRS: insulin receptor substrate; PKB/Akt: Phoshokinase B; K_{ATP}= ATP dependent potassium channel; PI3K: phosphoinositide-3-kinase; IL-6: interleukin 6; STAT3: signal transducer and activator of transcription 3; G6P: glucose-6-phosphatase; PEPCK: phosphoenolpyruvate carboxykinase; TCA: tricarboxylic acid cycle; (Created with Biorender.com)

Another signaling pathway, linking the brain and the liver in the context of regulation of HGP, involves signal transducer and activator of transcription 3 (STAT3) and interleukin 6 (IL-6). Over several studies it was found that hypothalamic insulin signaling, via the vagus nerve, affects IL-6 expression in the liver, which activates STAT3 to induce gluconeogenic gene expression as illustrated in figure 4 (Inoue et al., 2006, Inoue et al., 2004, Kimura et al., 2016). Specifically, vagotomy, pharmacological inhibition of cholinergic receptors, or nAChR deficiency, could all prevent the activation of IL-6/STAT3 signaling in the liver and its

[4] The vagus nerve is the 10th cranial nerve, and is regarded as the main nerve of the parasympathetic nervous system and is influencing the digestive system

consequent induction of gluconeogenic signaling (Kimura et al., 2016). Interestingly, in obese and diabetic mice, central insulin signaling was blunted (Kimura et al., 2016). In diabetic rats, hypothalamic expression of PKB, is decreased which hints towards a disruption in central insulin signaling in a diabetic state (Gelling et al., 2006). In summary, central glucoregulatory circuits effectively inhibit HGP, and this pathway might be interrupted in diabetes.

1.4.2 Central glucoregulation via signaling to endocrine pancreas

Early studies investigated the effect of lesions in the hypothalamus on the release of pancreatic hormones, specifically in the VMH. Using different stimuli on pancreata isolated from rats with or without lesions showed a general “hyperresponsiveness” as secretion of insulin, glucagon, and somatostatin were increased in rats with VMH lesions (Goto et al., 1980, Rohner-Jeanrenaud and Jeanrenaud, 1980). Berthoud and Jeanrenaud observed this hyperinsulinemia *in vivo*, and demonstrated the involvement of the vagus nerve by reversing the effect through vagotomy (Berthoud and Jeanrenaud, 1979). Yoshimatsu and colleagues showed that lesions in several hypothalamic areas (VMH, dorsomedial hypothalamus (DMH), and PVN) led to an augmented vagal nerve activity and a reduction in splanchnic nerve activity (includes mostly sympathetic nerves), which was also observed when glucose was given intravenously (i.v.) (Yoshimatsu et al., 1984). Using retrograde tracing, Rosario and colleagues showed that the pancreas receives signals from the hindbrain regions NTS and DMX and midbrain regions periaqueductal grey (PAG), central amygdala (CeA), and A5, which themselves receive projections emanating from hypothalamic regions (PVN, ARC, VMN, and LH) (Rosario et al., 2016). Aiming to dissect the contribution of hypothalamic nuclei to glucose homeostasis at the level of the pancreas, the research group demonstrated that inhibiting glucose sensing (by interfering with GK activity) in the ARC or the VMH leads to deficits in insulin secretion, although glucose intolerance was only observed when the ARC was targeted (Rosario et al., 2016). Looking at the regulation of glucose homeostasis via a brain-pancreas connection, other investigators confirmed that glucose sensing in the brain (intracarotid administration), and more specifically in the VMH (directly injected into the VMH) led to decreased glucagon secretion (Borg et al., 1997, Biggers et al., 1989). On the other hand, 2DG, a compound that induces intracellular energy deficits and leads to glucopenia, can induce glucagon secretion when given centrally (i.c.v. or directly into the VMH) (Marty et al., 2005, Borg et al., 1995). In sum, these results illustrate the bidirectional communication between brain glucoregulatory circuits and the pancreas to keep blood glucose levels under tight control.

1.4.3 Central glucoregulation via signaling to the kidney and adrenal glands

Glucose infusion into the VMH also blunted catecholamine secretion by adrenal glands while 2DG-mediated glucoprivation induced the opposite response (Borg et al., 1997, Borg et al., 1995). Interestingly, retrograde tracing from the kidneys resulted in labeling of both POMC and

AgRP neurons in the ARC, suggesting involvement of the melanocortin system (Bell et al., 2018). Intriguingly, $POMC^{ARC}$-deficient mice exhibited reduced renal catecholamine content. Surprisingly, the melanocortin system also influences renal glucose reabsorption, which can participate in the regulation of blood glucose levels. Indeed, POMC deficiency in the ARC, although associated with obesity and insulin resistance, was accompanied by glycosuria which improves glucose tolerance (Chhabra et al., 2016). This effect can be abolished by central administration of a melanocortin receptor agonist (Melanotan II) while antagonizing the melanocortin system with AgRP infusion improved glucose tolerance (Chhabra et al., 2016).
Of note, the improvement in glucose tolerance associated with glycosuria was also recapitulated in mice with hypothalamic MC4R ($MC4R^{HPT}$) deficiency (de Souza Cordeiro et al., 2021). Treatment with epinephrine was able to revert the glycosuria observed in $POMC^{ARC}$-deficient mice, implying sympathetic nervous system (SNS) activation in this crosstalk between hypothalamus and kidney to regulate blood glucose levels (Chhabra et al., 2016). This was later confirmed when it was shown that improved glucose tolerance in $MC4R^{HPT}$ deficient mice was linked to lower renal sympathetic nerve activity, decreased levels of circulating adrenaline and norepinephrine, and reduced expression of renal GLUT2 (de Souza Cordeiro et al., 2021). In sum, signaling of the melanocortin system modulates glucose reabsorption via sympathetic innervation and regulation of catecholamine release.

1.4.4 Central glucoregulation via signaling to adipose tissue and skeletal muscle

The ability of certain tissues such as adipose tissue or skeletal muscle to perform glucose uptake serves as another homeostatic lever for glucoregulation. The injection of glucose directly in the hypothalamus (PVN or VMH) leads to an increase in sympathetic activity and an elevated outflow to, e.g., brown adipose tissue (BAT) (Sakaguchi and Bray, 1987, Sakaguchi and Bray, 1988).
POMC signaling has been shown to promote BAT thermogenesis by activating the SNS outflow to BAT (Tang et al., 2022) and to stimulate browning of WAT, which is opposed by AgRP signaling (Ruan et al., 2014, Dodd et al., 2015). Accordingly, deletion of MC4R in extra-hypothalamic cholinergic neurons, both sympathetic and parasympathetic, interfered with glucose homeostasis, which can be partly explained by dysregulated thermogenesis in BAT and WAT (Berglund et al., 2014). Interestingly, the recovery of MC4R signaling in the LH in MC4R KO mice has been shown to ameliorate glucose tolerance by increasing BAT glucose uptake via an elevation of sympathetic nerve activity and elevated GLUT4 expression in BAT (Morgan et al., 2015). On the other hand, the activation of AgRP neurons has been demonstrated to cause insulin resistance by impairing glucose uptake in BAT, which is linked to decreased sympathetic nerve activity and acute reprogramming of gene expression (Steculorum et al., 2016). Several studies have highlighted the participation of the melanocortin system in the VMH to glucoregulation through adaptations of adipose tissue and muscle

physiology (Toda et al., 2009, Gavini et al., 2016). Indeed, its activation results in acute glucose uptake in different skeletal muscles, BAT and heart (Toda et al., 2009), which is accompanied by an increase in sympathetic outflow to different tissues (e.g., adipose depots, liver, and skeletal muscle) (Gavini et al., 2016). In skeletal muscle specifically, activation of melanocortin receptors in the VMH induced changes in the muscle molecular profile and metabolism, leading to increased physical activity, lipid metabolism, and heat production (Gavini et al., 2016). The injection of another hypothalamic neuropeptide, orexin A, into the VMH has been shown to induce both increased glucose uptake and glycogen production in skeletal muscle through activation of the SNS (Shiuchi et al., 2009). In summary, the CNS controls glucose uptake and metabolism in adipose tissue and skeletal muscles by modulating the sympathetic outflow they receive.

1.5 Oxytocin (OT) and oxytocin receptor (OTR) – adding new angles to diabetes therapy?

Over the last couple of decades, considerable advances have been made in our understanding of how hypothalamic neurocircuits govern whole-body glucose homeostasis. Various neuronal cell types have been suggested to play important roles in sensing acute changes in blood glucose concentration as summarized above. However, the exact wiring and signaling modalities employed by these networks to coordinate a vast range of counterregulatory responses (i.e., behavioral, hormonal, and autonomic) remain incompletely understood.

Among the large array of hypothalamic signaling molecules, the neuropeptide OT and its receptor OTR have attracted particular interest, and several lines of evidence support their pertinent role in glucoregulation. For instance, several studies have linked OTR gene polymorphisms with increased diabetes risk (Amin et al., 2023, Saravani et al., 2015). In line, one of OTR gene polymorphisms was shown to influence the negative correlation between OT blood levels and the markers used as indicators for diabetes: fasting blood glucose, fasting insulin, and the calculated HOMA-IR[5] (Chang et al., 2019). These observations thus strongly suggest that OT signaling is implicated in diabetes pathogenesis and the regulation of whole-body glucose homeostasis in humans.

1.5.1 OT neurons and OTR

OT, a nine-amino acid neuropeptide hormone, is mainly known for its actions affecting labor, lactation, and bonding behavior. Notably, however, increasing evidence now indicates that the OT system is also involved in metabolic homeostasis (McCormack et al., 2020). Endogenous OT production is mainly found in OT neurons situated in the PVN and the supraoptic nucleus (SON) of the hypothalamus (Swanson and Sawchenko, 1983). Two types of OT neurons have

[5] a parameter calculated from fasting glucose and fasting insulin values used as a surrogate for insulin resistance (see methods part for calculation)

been described, parvocellular OT neurons, roughly 70 neurons in the rat brain, located in the PVN and magnocellular OT neurons summing up to around 8000 neurons in the rat brain, located in the PVN and SON (Swanson and Sawchenko, 1983, Althammer and Grinevich, 2017). Magnocellular OT neurons store OT in vesicles for release into the systemic circulation via the posterior pituitary. Additionally, magnocellular OT neurons signal in an autocrine and paracrine fashion through somato-dendritic secretion of OT, e.g., to adjunct brain areas such as the VMH (Brown et al., 2020). More recently, magnocellular OT neurons have been shown to form bifurcations and directly innervate numerous forebrain and hindbrain regions (Zhang et al., 2021, Hung et al., 2017, Knobloch et al., 2012). Conversely, parvocellular OT neurons project to various regions of the brain, including the ARC, ventral tegmental area (VTA), nucleus accumbens (NAc), CeA, NTS and the spinal cord (Kerem and Lawson, 2021). Thus, OT signaling is involved in the regions responsible glucose sensing, glucose homeostasis and energy balance as summarized in Fig. 5 (ARC and NTS as part of the hindbrain). Interestingly, VTA, NAc and CeA are brain areas that are part of the reward network, giving OT the opportunity to influence not only homeostatic regulation of food intake, but also the hedonic pathways (Kerem and Lawson, 2021, Leng and Sabatier, 2017).

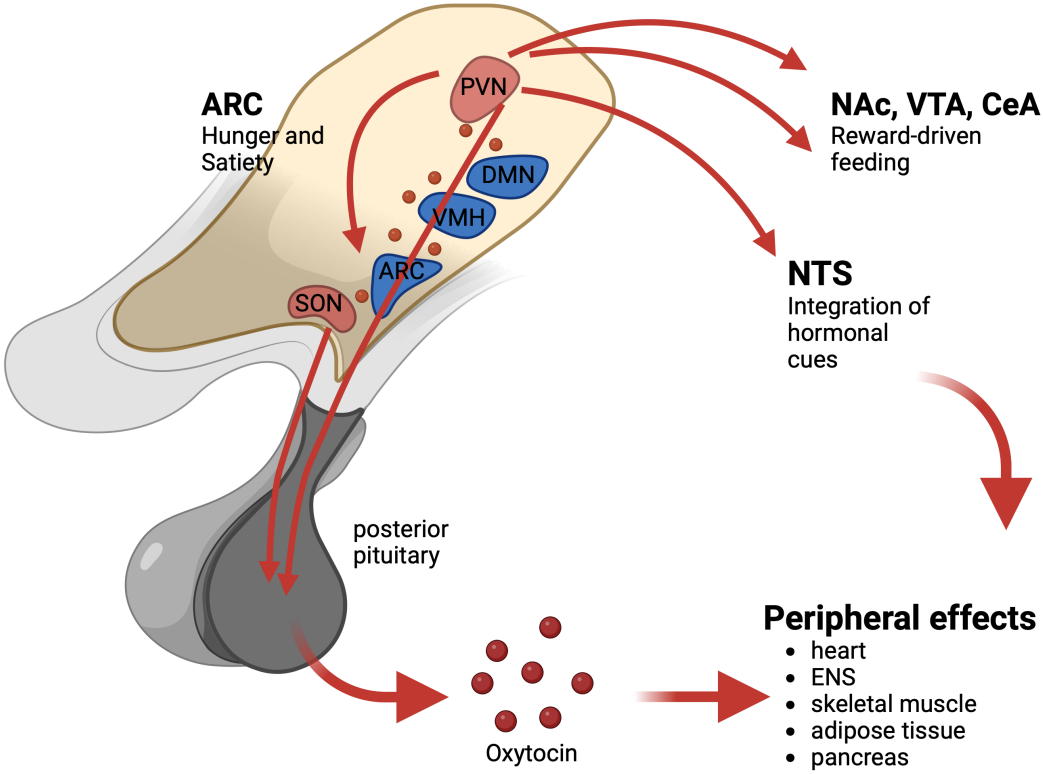

Figure 5 – Multiple routes of OT signaling

Magnocellular OT neurons situated in the SON and the PVN release OT via the posterior pituitary. Circulating OT acts on OTR receptors of the heart, ENS, skeletal muscle, adipose tissue and pancreas, amongst others. Magnocellular and parvocellular OT neurons project to various regions within the brain, including the ARC, NAc, VTA, CeA and NTS. Thus, OT has multiple routes to act on e.g. metabolic regulation. OT: oxytocin; NAC: nucleus accumbens; VTA: ventral tegmental area; DMN: dorsal medial nucleus of the hypothalamus; CeA: central nucleus of the amygdala; PVN: paraventricular nucleus; VMH: ventrolateral hypothalamus; ARC: arcuate nucleus; NTS:

nucleus tractus solitarius; ENS: enteric nervous system (Created with Biorender.com, adapted from (McCormack et al., 2020))

Notably, oxytocinergic neurons have been shown to co-express glutamate as a fast-acting neurotransmitter alongside OT (Pinol et al., 2014, Rinaman, 1998, Osakada et al., 2022). However, the physiological relevance of this co-transmission, especially in glucoregulation, remains elusive.

The OTR belongs to the rhodopsin-type (class I) G protein-coupled receptor (GPCR) family, with seven transmembrane α-helix domains (Gimpl and Fahrenholz, 2001). Intracellularly, OTR is coupled to a $G_{q/11}$ class GTP binding protein which, together with $G\beta\chi$ and upon OT binding, stimulates phospholipase C_β isoforms. Following this, inositol triphosphate, which triggers intracellular Ca^{2+} release, and 1,2-diacylglycerol, which activates protein kinase C to phosphorylate target proteins, are generated. Increases in intracellular Ca^{2+} can have different effects depending on the respective tissue. In neuronal cells it affects cellular excitability, firing patterns, and neurotransmitter release (Gimpl and Fahrenholz, 2001).

OTR is expressed in various peripheral tissues including the reproductive tissues, but also several metabolically active tissues such as adipose tissue, skeletal muscle, cardiac tissue, the enteric nervous system, and pancreatic ß-cells (Kerem and Lawson, 2021, Jurek and Neumann, 2018). Within the rodent brain, the OTR expression pattern matches, at large, with regions that exhibit substantial innervation of oxytocinergic axon terminals (Kerem and Lawson, 2021). Furthermore, several cortical and hippocampal regions express OTR, suggesting an impact on neuronal populations involved in decision-making and cognitive control (Kerem and Lawson, 2021, Tribollet et al., 1989, Quintana et al., 2019, Jurek and Neumann, 2018). Interestingly, an especially strong expression can be found in the VMH of the hypothalamus, in mice and humans (Tribollet et al., 1989, Quintana et al., 2019). This finding suggests a potential role in regulating glucose homeostasis through the OTR-expressing neurons in the VMH.

This data collectively reinforces the notion that OT constitutes a pleiotropic signaling molecule that can expert multifaceted actions through multiple routes of communication. How parallel OT signaling pathways affect energy and glucose homeostasis remains largely unclear.

1.5.2 OT impacts energy homeostasis

As mentioned before, more recent evidence has demonstrated that OT is involved in the regulation of energy homeostasis, more specifically in body weight and food intake control. Previously, various gene mutations that involved a reduction in OT expression in the PVN coincided with hyperphagic obesity ((Swaab et al., 1995, Kublaoui et al., 2008). Several studies have shed light on OT's specific routes of action. In diet-induced obese rats, a 7-day OT treatment (intraperitonial (i.p.)) led to a dose-dependent reduction in food intake and body fat, which intriguingly exceeded that of pair-fed controls, thus suggesting an effect on energy

expenditure (Morton et al., 2012). Consistent with this notion, another study conducted in obese rhesus monkeys found that systemic OT administration increased energy expenditure alongside a reduction in food intake and body weight, as well as improved plasma fatty acids and plasma glucose levels (Blevins et al., 2015). Interestingly, these effects could be recapitulated by central (i.c.v.) delivery of OT (Morton et al., 2012). In line with these findings, central OTR antagonism induced hyperphagia (Kublaoui et al., 2008), suggesting that central signaling pathways play a major role in OT's effect on food intake.

In humans, intranasal administration of OT significantly decreased body weight over a period of 8 weeks in an obese cohort, which was represented by a significantly lower BMI, decreased waist and hip circumference, and a normalization of total cholesterol and LDL, thus showing great potential as a weight loss agent (Zhang et al., 2013). The observed weight loss is likely a consequence of OT-induced reduction in caloric intake ((Ott et al., 2013, Lawson et al., 2015), which is accompanied by increased insulin sensitivity ((Lawson et al., 2015).

In sum, OT treatment effectively lowers body weight in mice and humans and OTR signaling in the brain seems to play a major role in OT's effect on energy homeostasis.

1.5.3 Glucoregulatory properties of OT

In isolated murine islets, OT has been shown to robustly potentiate glucose-induced insulin secretion (Maejima et al., 2015). Watanabe and colleagues could showed that systemic OT administration prevents stress-induced cell death in pancreatic islets and increased OT and OTR expression in islets and brain (Watanabe et al., 2016). Following this interesting result, they demonstrated that $OTR^{-/-}$ mice, along with impaired glucose tolerance, exhibit an augmented cell death rate and ER stress response in islets - possibly due to impaired EKR-CREB signaling.

Several studies demonstrated that OT could affect glucose homeostasis by directly binding to OTRs on pancreatic islets. Gao and colleagues observed a dose-dependent augmenting effect of OT on the release of somatostatin, glucagon, and insulin from isolated murine islets (Gao et al., 1991). Interestingly, while somatostatin and glucagon were released independently of glucose, OT increased insulin secretion only under high glucose concentrations (Gao et al., 1991). Another study found that the insulinotropic effect of OT on *ex vivo* pancreata is dose-dependent in a physiological range with a similar response to OTR agonism (Bobbioni-Harsch et al., 1995). The effect of OT is blunted by OTR antagonists which strengthens the idea that OT-OTR signaling is responsible for insulin secretion from pancreatic islets (Bobbioni-Harsch et al., 1995).

Injecting OT i.p. into mice led to increased neuronal activity in various hypothalamic and hindbrain nuclei including the PVN, ARC, LC, NTS, DMX, and AP (Maejima et al., 2011). Continuous s.c. injections (17 days) resulted in decreased food intake and bodyweight. Intriguingly, OT administration also lowered the respiratory exchange ratio (RER), i.e., the ratio

between amount of exhaled CO_2 and inhaled O_2, which is an indicator of preferential oxidation of lipids. Lastly, this study also reassuringly found that OT administration robustly improves glucose tolerance (Maejima et al., 2011). While lowering of blood glucose and insulin was not found to be significant in obese humans after intranasal OT, Zhang and colleagues observed a robust improvement in glucose tolerance and fasting insulin in prediabetic DIO mice as well as in streptozotocin-induced T1D mice by OT and analogs (Zhang et al., 2013). This suggests that OT and its analogs exhibit multifaceted effects holding potential for improved weight management, insulin sensitivity, and insulin secretion. In sum, a large body of pre-clinical and clinical studies support the notion of OT being a promising candidate for the development of therapeutic peptides targeting obesity and diabetes.

1.6 Astrocytes as part of glucoregulation

1.6.1 Astrocytes and their functions

A reasonable question to ask is if neurons are the only brain cells involved in the sensing and regulation of glucose levels. In recent years, it has become clear that glia cells are not merely supportive but fulfill important roles concerning processes within the brain. Astroglial processes cover neuronal synapses, forming a tripartite synapse or, taking into account the contribution of other cell types such as microglia, a multipartite synapse. Functions attributed to astrocytes include the regulation of various physiological components such as blood flow, pH, synaptogenesis, synaptic transmission, and the provision of energy substrates to neurons, which are discussed elsewhere (Sofroniew and Vinters, 2010). Astrocytes respond to neuronal signaling with activity-related intracellular Ca^{2+} increases and the release of signaling compounds that impact synaptic transmission making them part of the signaling machinery (Araque et al., 1999). In this context, astrocytes influence synaptic transmission by regulating the extracellular levels of neurotransmitters. In particular, the excitatory neurotransmitter glutamate, which has the potential to cause neurotoxicity through overstimulation, and is efficiently removed from the synaptic cleft by astrocytic glutamate transporters glutamate transporter 1 (GLT-1) and glutamate aspartate transporter (GLAST) (Bak et al., 2006). The presence of extracellular glutamate itself induces an increase in GLAST expression on the cell surface, and thus, an elevation in transport capacities (Duan et al., 1999).

Astrocytes are organized in compartmentalized networks that are connected via gap junctions (involving connexin 30 and connexin 43) allowing fast communication and distribution of ions, metabolites, and neurotransmitters within the specific area (Giaume and Theis, 2010). The functionality of these astrocyte networks is of major importance as preventing their formation disrupts the functional development of the brain, while an interruption in adulthood impairs synaptic transmission, leading to defective memory formation and spatial learning (Hosli et al., 2022, Pannasch et al., 2011). One important role of astroglial networks is K^+ buffering, as

keeping extracellular K^+ low is indispensable for the electrochemical gradient that is necessary for neuronal function. In this regard, astrocytes can take up K^+ acutely in the situation of excess K^+ and temporarily accumulated it to be released at a later timepoint. Even more important is spatial K^+ buffering, which describes the mechanism of K^+ trafficking within astroglial networks from areas with elevated K^+ levels to areas low in K^+ (Kofuji and Newman, 2004).

Astrocytes communicate by releasing so called “gliotransmitters”, signaling molecules that can be sensed by cells in proximity to astroglial processes. Those include, but are not limited to, neurotransmitters like glutamate and ATP, metabolites like lactate and glucose, as well as neuromodulators, growth, and inflammatory factors. In general, astrocytes conduct their secretory properties by exocytosis but also through transporters and pores (Verkhratsky et al., 2016).

Astroglial activity also reaches beyond the microenvironment of the central nervous system, e.g., Marina and colleagues recently elucidated that astrocytes also possess properties akin that of baroreceptors, and respond to reduced cerebral blood flow by increasing heart rate and arterial blood pressure via activation of sympathetic outflow (Marina et al., 2020).

1.6.2 Glucose metabolism in astrocytes

A range of *in vitro* studies have shown that while neurons metabolize glucose and lactate with a preference for the latter, astrocytes preferably metabolize glucose leading to a release of lactate into the medium, the end-product of glycolysis (Itoh et al., 2003, Bouzier-Sore et al., 2006). The highly glycolytic properties of astrocytes are mediated by the high expression levels of several genes related to metabolism. For example, the enzyme fructose-2,6-bisphosphatase-3 (PFKFB3) is highly expressed in astrocytes, which allosterically activates the master regulator of glycolysis, phosphofructokinase-1 (PFK-1), via its product fructose-2,6-bisphosphate (Herrero-Mendez et al., 2009, Almeida et al., 2004). Furthermore, the activity of pyruvate dehydrogenase (PDH), the enzyme responsible for the conversion of pyruvate to acetyl-CoA to enter the citric acid cycle, seems to be barely expressed and/or tightly regulated in astrocytes, which suggests that pyruvate is rather used for the production of lactate (Itoh et al., 2003, Halim et al., 2010, Laughton et al., 2007). Conversely, lactate dehydrogenase-5 (LDH-5), the LDH with the fastest conversion rate of pyruvate to lactate and which is specifically expressed in glycolytic tissues, is enriched in astrocytes in humans ((Cahn et al., 1962, Bittar et al., 1996, Laughton et al., 2007). Interestingly, it has been demonstrated that inhibition of mitochondrial respiration in astrocytes, both *in vitro* (by complex I inhibitor rotenone) and *in vivo* (by KO of cytochrome c oxidase in GLAST+ astrocytes), does not affect the viability of either astrocytes or neurons, glial morphology, synapse density, or the expression of inflammatory markers (Supplie et al., 2017). However, the lactate levels of mice with inhibited mitochondrial respiration were increased when compared to controls, suggesting that, indeed, astrocytes can thrive on glycolysis only (Supplie et al., 2017). Additionally,

astrocytes are able to store glucose as glycogen; 3-12µmol/g tissue have been reported (Choi et al., 1999, Cruz and Dienel, 2002). Wender and colleagues demonstrated that glycogen granules are exclusively found in astrocytes in rat optic nerve fibers (Wender et al., 2000). When testing axon function in glucose deprivation, they found that the amount of glycogen corresponds to the amount of time it takes for the axon activity to be significantly impaired, suggesting that astroglial glycogen fuels neuronal activity (Wender et al., 2000). The same can be observed in cell culture, where astrocytic glycogen seems to protect neurons from being damaged by glucoprivation - a protection that could not be observed after glycogen depletion from astrocytes (Swanson and Choi, 1993). This is in line with the observation that brain areas with higher glycogen accumulation seem to be less affected by hypoglycemic brain damage (Sagar et al., 1987, Auer, 2004). Interestingly, blocking lactate transport reduced the time until failure of rat optic nerve axon function, indicating that the astroglial metabolic support through stored glycogen is brought to neurons via the release of lactate (Wender et al, 2000). In primary cell culture, astrocytes deplete glycogen stores in response to restricted glucose availability, releasing high amounts of lactate into the medium (Dringen et al 1993). It could even be demonstrated that inhibition of glycogenolysis interferes with the formation of long-term memory highlighting the importance of metabolic substrate supply by astrocytes (Suzuki et al., 2011).

1.6.3 Neuron-astrocyte lactate shuttle theory

It has been postulated that astrocytes respond to neuronal activation by providing lactate as an energy substrate to neurons after glycolytic breakdown of glucose (originally (Pellerin and Magistretti, 1994)) as illustrated in Fig. 6.

In vitro, treatment with the neurotransmitter glutamate, used as a surrogate for neuronal activity, resulted in an increased glucose uptake into glial fibrillary acidic protein (GFAP)-positive astrocytes (Loaiza et al., 2003) and in an increase in glycolytic rate (Bittner et al., 2010). A study based on genetically encoded FRET-based nanosensors in *ex vivo* brain slices proved that neuronal activity stimulates astroglial glucose uptake and induces an elevation in intracellular level of glucose metabolites pyruvate and lactate, a phenomenon that could be prevented by blocking neuronal activation or uptake of excitatory extracellular K^+ into astrocytes (Ruminot et al., 2019). Further supporting the observation that neuronal activity induces adaptive changes in astrocyte metabolism, spatiotemporal imaging of brain slices *ex vivo* demonstrated that neuronal activity was followed by an increased glycolytic metabolism in astrocytes (Kasischke et al., 2004). Additionally, by using a genetically encoded FRET sensor detecting lactate, Mächler and colleagues showed that the baseline of intracellular lactate levels in astrocytes is much higher than in neurons, which creates a lactate gradient that favors the hypothesis of a flux from astrocytes to neurons (Machler et al., 2016). The transport of lactate is carried out by monocarboxylate transporters (MCTs), which also

transport other monocarboxylates, such as ketone bodies and pyruvate. Astrocytes express MCT1, which is also expressed in other cell types like oligodendrocytes and endothelial cells, and MCT4, which is mostly expressed by astrocytes in the CNS (Pierre and Pellerin, 2005).

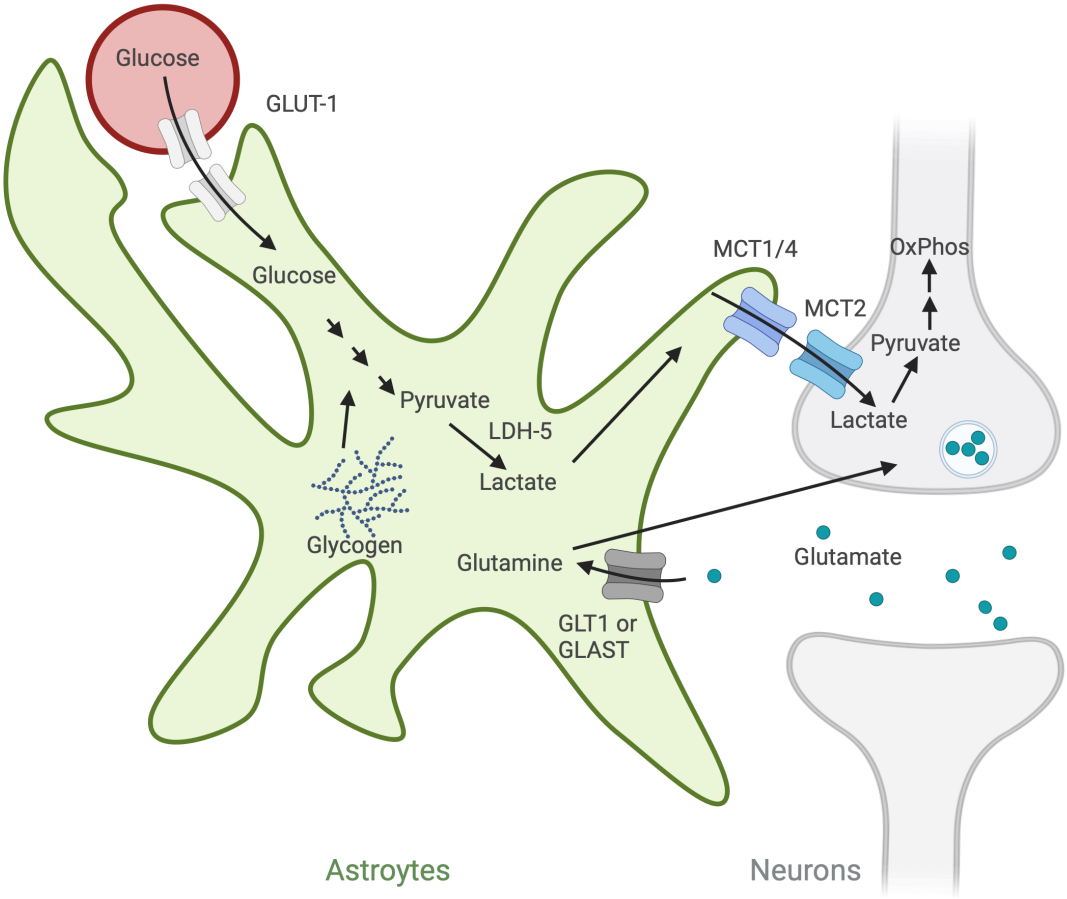

Figure 6 – Neuron-astrocyte lactate shuttle model

Neuronal activity is sensed by astrocytes via the uptake of the neurotransmitter glutamate. In response, lactate is generated from glucose and stored glycogen and released as an energy substrate for neurons. GLUT: Glucose transporter; MCT: monocarboxylate transporter LDH: lactate dehydrogenase; GLT1: glutamate transporter 1; GLAST: glutamate aspartate transporter; OxPhos: oxidative phosphorylation.

Neurons, on the other hand, express MCT2, which intriguingly accumulates in postsynaptic areas, an observation that could hint towards its involvement in the high energy demanding process of neurotransmission. As MCT2 has a significantly lower K_M value, which makes it predetermined for uptake processes, a transport from astrocytes to neurons is likely (Pierre and Pellerin, 2005). Interestingly, an antisense oligodeoxynucleotide knockdown approach of astroglial lactate transporters (MCT1 and MCT4) leads to memory impairments that were reversible with lactate injection into the brain, while an impairment by the knockdown of neuronal MCT2 could not be reversed by lactate (Suzuki et al., 2011). In the same study, inhibiting glycogenolysis could even be shown to block the formation of long-term memory, while the rise in lactate that was normally observed in the context of learning was blunted. In line, addition of lactate could rescue memory formation, suggesting that lactate is an important

energy substrate for high energy processes and that astroglial glycogenolysis is a fundamental source ((Suzuki et al., 2011)

In conclusion, astroglial glucose uptake, storage as glycogen, and release as lactate seem to be effectively fine-tuned to support neuronal energy supply, especially in times of high energy requirement.

1.6.4 Astrocytes in energy and glucose homeostasis

In the context of metabolic disease, changes in astrocytic morphology and upregulation of GFAP expression, so-called “astrogliosis”, have been linked to the inflammatory environment of high-fat diet feeding and diet-induced obesity in mice and humans (Schur et al., 2015, Thaler et al., 2012). These observations lead to the conclusion that astrocytes sense and respond to metabolic cues. In a recent study using electron microscopy and electrophysiology, an increase in glial ensheathment of AgRP neurons was linked to a higher activity in those neurons (Varela et al., 2021), suggesting that astrocytes are also part of the regulatory machinery of energy balance. In this regard, it was demonstrated that the activation of astrocytes in the dorsal vagal complex (DVC) by DREADDs diminished food intake under standard and fasting conditions, indicating a significant role of DVC astrocytes in provoking satiety (MacDonald et al., 2020).

Our group and others proved that astrocytes play a role in hormones and nutrients sensing by the brain, with an impact on whole body metabolism. More specifically, Kim and colleagues showed that deletion of the leptin receptor in astrocytes impaired the changes in food intake typically induced in response to leptin, ghrelin, or fasting (Kim et al., 2014). Additionally, our group found that astroglial insulin signaling is necessary for glucose sensing of POMC neurons, and its interference leads to impaired glucose tolerance due to blunted insulin secretion (Garcia-Caceres et al., 2016). Furthermore, NTS astrocytes seem to respond to glucose fluctuations as glucoprivation was followed by increased intracellular Ca^{2+}, a surrogate for astrocyte activation (McDougal et al., 2013a). Inhibiting astrocytic activity by fluorocitrate, a compound that inhibits the astroglial citric acid cycle, even prevented the enforcing effect of glucoprivation on gastric motility (McDougal et al., 2013b). Furthermore, other counterregulatory mechanisms like glucagon secretion depend on functional glucose sensing in astrocytes (Marty et al., 2005). This was shown by the restoration of 2DG-induced glucagon release by re-expressing GLUT-2 in GFAP-expressing astrocytes in a global GLUT-2 KO mouse model (Marty et al., 2005). Those results suggest that astrocytes are involved in the detection of changes in blood glucose levels. Interestingly, diabetic mouse models exhibit changes in the glial molecular profile of the retina, such as increased GFAP expression and decreased GLAST expression, in line with an accumulation of glutamate (Bogdanov et al., 2014). In humans, increased fasting insulin and HOMA-IR as a marker for insulin resistance

are positively associated with hypothalamic gliosis (Schur et al., 2015), further demonstrating that astrocytes are responding to impaired glucose homeostasis.

1.6.5 Glucose transporters in astrocytes

As described above, astroglial glucose uptake and metabolism play a major role in neuronal energy supply and could also be utilized as a part of glucose sensing. The main glucose transporter in astrocytes is glucose transporter-1 (GLUT-1), which belongs to the facilitative glucose transporters (GLUTs) of the membrane transporter major facilitator superfamily coded by the “SLC2” genes. GLUT-1 was the first of the glucose transporters to be closely investigated in 1985 and described to have the typical structure of 12 transmembrane domains with N- and C-termini facing the cytoplasm (Mueckler et al., 1985). In the brain, GLUT-1 can be found with different glycosylation levels: its most glycosylated version (55 kDa) is found in endothelial cells, while its least glycosylated version (45 kDa) is mainly found in astrocytes (Patching, 2017). Other glucose transporters have been found in astrocytes: GLUT-2, GLUT-4, GLUT-7, and the sodium/glucose-cotransporter 1 (SGLT-1) (Patching, 2017). Vannucci and colleagues demonstrated that GLUT-4 in the brain was upregulated in hyperinsulinemic mice (db/db mutation) and downregulated in hypoinsulinemic mice (streptozotocin-induced insulin-deficient diabetic mice and exercised mice) suggesting a regulation of GLUT-4 expression by metabolic cues (Vannucci et al., 1998).

Interestingly, lowering glucose availability in *ex vivo* brain slices or by injecting 2DG *in vivo* (glucoprivation), acutely increased the Ca^{2+} activity in local hindbrain astrocytes further suggesting an involvement in the regulation of glucose homeostasis (McDougal et al., 2013a, McDougal et al., 2013b). In this regard, astroglial GLUT-2 has been elegantly demonstrated to play a role in sensing and counterregulatory response to hypoglycemia by rescuing the phenotype via astrocyte-specific restoration of GLUT-2 in mice with a global GLUT-2 KO (Marty et al., 2005).

GLUT-1 is integrated in processes of metabolic adaptation, e.g., it is upregulated alongside SGLT-1 and MCT1 during short-term hypoxia (1d) in primary astrocyte culture, which then leads to increased glucose uptake and lactate release (Vega et al., 2006). Simpson and colleagues demonstrated significant upregulation of GLUT-1 expression in brain vasculature and elevated glucose transport across the BBB in response to hypoglycemia (Simpson et al., 1999). In astrocytes specifically, GLUT-1 expression and membrane translocation has been shown to be influenced by insulin signaling (Garcia-Caceres et al., 2016, Hernandez-Garzon et al., 2016). Furthermore, the energy sensor AMPK regulates GLUT-1 translocation in astrocytes which affects glucose uptake, lactate production, and neuronal survival (Muraleedharan et al., 2020). Therefore, as glucose availability is a negative regulator for AMPK, it inhibits GLUT-1 translocation. Accordingly, hyperglycemic conditions in diabetic rats

were associated with reductions in protein expression of GLUT-1 (Chari et al., 2011). However, in these diabetic rats, the suppression of peripheral gluconeogenesis induced by intra-hypothalamic glucose administration was blunted. Strikingly, normalization of blood glucose could be achieved by restoring GLUT-1 in hypothalamic GFAP-positive astrocytes (Chari et al., 2011).

In conclusion, glucose metabolism in astrocytes, in particular via GLUT-1, is emerging as a regulatory lever for both brain function and systemic glucose homeostasis. However, how astrocytes can impact local glucose sensing or if a disruption of astrocytic glucose metabolism impacts the whole-body metabolic phenotype, are still poorly understood.

1.7 Aim of the thesis

The hypothalamus plays a critical role in the regulation of systemic glucose homeostasis via the influence of peripheral systems. However, the cellular and molecular mechanisms by which the hypothalamus orchestrates the counterregulatory processes that are crucial for maintaining systemic glucose levels remain largely unknown. However, this function is particularly compromised in metabolic diseases such as obesity and T2D. Intrigued by this, and given the urgent need to identify better targets for future treatments of these diseases, the aim of my thesis was to advance knowledge of how both OT signaling and astrocyte glucose metabolism affects peripheral glucose levels and glucose homeostasis, and how these mechanisms are altered by diet-induced obesity (DIO), possibly contributing to the development of these metabolic diseases. To address this, I have divided my thesis into two lines of investigation:

Aim 1: To disentangle humoral from neural pathways by which hypothalamic OT neurons improve glucose tolerance.

Aim 2: To examine whether GLUT-1 expression in astrocytes plays a critical role maintaining systemic glucose homeostasis in conditions of high and low glucose.

2 Methods

2.1 Animal experiments

2.1.1 Animals

All animal experiments were approved by the Animal Ethics Committee of the government of Upper Bavaria, Germany following the guidelines of the Institutional Animal Care and Use Committee of the Helmholtz Center Munich, Bavaria, Germany. All mice had permanent access to water and were housed under standard conditions of 23 °C, with humidity-control and a 12 h-light-dark cycle. Mice were either fed a pelleted standard chow diet (5.6% fat, LM-485, Harlan Teklad) or high-fat-high-sucrose diet (HFHS) (D12331, 58% of calories from lipids; Research Diets, New Brunswick, NJ) ad libitum unless stated otherwise. Knockout (KO) and wildtype (WT) littermates were kept in mixed groups of 3-5 mice per cage in an enriched environment. Cohorts with AAV injections were randomly assigned to either of the respective groups. Tamoxifen-inducible knockout lines (CreERT2 allele) were bred according to heterozygous x wildtype regime resulting in randomized group composition (mendelian ratios) and the possibility to treat all mice the same, including with tamoxifen injections. Individual mice were ear-tagged for identification and genotyping.

To address the effect of OT in the peripheral versus central context, several mouse lines were generated. For chemogenetic activation of OT neurons, an AAV carrying hM3Dq (rAAV.hSyn.DIOflex.hM3D(Gq).mCherry or rAAV.hSyn.DIOflex.mCherry) was injected into the OT neuron expressing areas of the hypothalamus of OT-ires-Cre mice (B6; 129S-$Oxt^{tm1.1(cre)Dolsn/}$J, Jackson Laboratory). Injection sites on each hemisphere were chosen according to the Mouse Brain Atlas (Franklin and Paxinos, 2008), with coordinate orientation from bregma and the dura mater: PVN (±0.2, -0.7, -4,75) and the SON (±1.25, -0.6, -5.5). The islet-specific OTR KO was generated by crossbreeding OTRflx;Ins1Cre mice from OTRflx (B6.129(SJL)-Oxtrtm1.1.Wsy/J, Jackson Laboratory) and Ins1Cre mice (B6(Cg)-Ins1tm1.1(cre)Thor/J, Jackson Laboratoy). The VMH-specific OTR KO was induced with the help of adeno-associated viruses (AAV) that were commercially obtained (AAV-eSYN-mCherry-T2A-iCre-WPRE and AAV-eSYN-mCherry-T2A-WPRE, VectorBioLabs, Malvern, USA), expressing a Cre recombinase driven by a neuronal promotor (eSyn1). For OTR OE, C57Bl6J mice from Jackson Laboratory were injected with an AAV overexpressing OTR driven by a generic neuronal promotor (AAV1-hSyn1-m-OXTR-mCherry-WPRE or AAV1-hSyn1-mCherry-WPRE, VectorBioLabs, Malvern, USA). AAVs were injected bilaterally with the coordinates -1.5mm posterior, ±0.8 mm lateral to the bregma and -5,5mm and -5,1mm ventral from the dura mater to target the VMH according to “The Mouse Brain in Stereotaxic Coordinates” (Franklin and Paxinos, 2008).

To target GLUT-1 in astrocytes, we used the various approaches. For a brain-wide astroglial GLUT-1 KO, we crossbred Glut-1^{flx} mice (kindly provided by Jens Brüning after being developed by Wei and colleagues (Wei et al., 2015)) with the GLAST.CreER^{T2} which carries a Cre recombinase within the glutamate-aspartate transporter (GLAST) gene locus (Mori et al., 2006) (GLUT-$1^{i\Delta astro/GLAST+}$). To limit the KO of astroglial GLUT-1 to the mediobasal hypothalamus (MBH), I injected an AAV that expresses Cre recombinase or a green fluorescent protein (GFP) virus as driven by an astroglial promotor Gfa2 (rAAV.GFAPp.iCre and rAAV.GFAPp-eGFP-WPRE, VectorBioLabs, Malvern, USA) into the ARC (−1.5 mm posterior and ±0.25 mm lateral to the bregma and −5.7 mm ventral from the dura mater) and the VMH (−1.5 mm posterior and ±0.55 mm lateral to the bregma and −5.5 mm ventral from the dura mater) of GLUT-1flx mice (GLUT-$1^{AVV.Gfa.iCre}$). For GLUT-1 OE, an AAV that overexpresses GLUT-1 driven by GFAP promoter (AAV-GFAP-m-SLC2A1-P2A-EGFP or AAV-GFAP-P2A-EGFP, VectorBioLabs, Malvern, USA) was injected into the same specific region.

2.1.2 Tamoxifen injection

In mouse lines with inducible Cre recombinase expression, tamoxifen (10mg/kg bodyweight) was injected intraperitonially at 6 weeks of age for 5 consecutive days. For injections, tamoxifen was dissolved in ethanol and sterile sunflower oil (1:10) at 37°C resulting in a concentration of 10mg/ml.

2.1.3 Intrahypothalamic injections/ Stereotaxic surgeries

Mice were anesthetized by a mixture of ketamine/xylazine (100mg/kg and 7mg/kg bodyweight). Recombinant adeno-associated viruses (rAAV) generated from commercial distributers (VectorBiolabs, USA; VectorBuilder, Germany) were configured for cell-specific transgene expression. Firstly, serotypes specific for the respective cell population were chosen – serotype 2/5 for astrocytes and serotype 2/1 for neurons. Furthermore, cell-specific promotors were implemented; for astrocytes the synthetic 2.2kb promotor element Gfa2 (described by Brenner et al., 1994), and for neurons the human synapsin promotor (hSyn) or enhanced synapsin promotor (eSyn). rAAVs were injected bilaterally (max. 0.5µl/ hemisphere; 10^{12} viral particles/ml) into the mediobasal hypothalamus using a stereotactic device (David Kopf Instruments, USA), a binocular 3.5x-90x stereomicroscope (AMScope, USA), and pulled glass micropipettes (PCR Micropipets 1-10ul, Drummond Scientific, Broomall Pennsylvania, pulled with a micropipette puller from Narishige, Model PC-100, Japan). Injection speed was approximately 250 nl/min and a time-delayed (5min) slow retraction of the micropipette assured appropriate virus distribution. For postoperative analgesia, a subcutaneous (s.c.) injection of metamizol (200mg/kg bodyweight) was given acutely and meloxicam (1mg/kg bodyweight) was administered s.c. as postoperative care for three consecutive days with a close monitoring phase of 7 days.

2.1.4 Genotyping

Ear punches from mouse tagging were used for DNA isolation. 200 µl of NaOH (50mM) were added to ear punches from each mouse of interest followed by a 30-min- incubation period in the PCR cycler (Mastercycler, Model vapo.protect, Eppendorf, Germany) at 95 °C for lysis of the cell membranes. 20 µl of Tris buffer (1M, pH 8) was added to stabilize the pH. Isolated genomic DNA was stored at 4 °C until genotyping via polymerase chain reaction (PCR). Reagents and adapted protocols for the genes of interest (GLUT-1flx, GlastCreERT2, OT-Ires-Cre, Ins1Cre, OTRflx) are summarized in the supplementary material (see appendix).

2.1.5 Metabolic phenotyping

2.1.5.1 Bodyweight and body composition

If relevant, individual body weights were measured once a week. To determine the body composition (lean mass and fat mass), a quantitative magnetic resonance instrument (EchoMRI, USA), which relies on proton nuclear magnetic resonance (NMR), for whole body composition analysis was used.

2.1.5.2 Indirect calorimetry

For assessment of energy metabolism of mice, indirect calorimetry was applied, therefore we used a ventilated open circuit calorimeter (TSE PhenoMaster, TSE-Systems, Germany). Assignment to individual cages was randomized. Mice acclimated for 24h before food and water intake, O_2 consumption, CO_2 production, and locomotor activity of mice were evaluated. O_2 consumption and CO_2 production can be used to estimate energy expenditure and respiratory exchange ratio (RER).

2.1.5.3 Refeeding Experiments

For fasting and refeeding experiments, the food of single housed mice in metabolic cages was removed for 24h before refeeding. Blood measurements were conducted before and after fasting and 2h after refeeding. Glucose, ketones, and lactate were measured by handheld detection devices (for glucose: Freestyle, Abbott, Germany; for ketones: On Call, ACON Laboratories, USA; for lactate: Accutrend Plus, Roche Diagnostics, Germany).

2.1.5.4 Glucose tolerance test (GTT) and Glucose- induced insulin secretion (GSIS)

Mice were weighed and fasted for 5-6h with ad libitum access to water. Glycemia was measured in blood samples obtained from the tail vein with a handheld glucometer. Glycemia was measured before i.p. glucose injection (2g/kg bodyweight, dissolved at 25% in 1x PBS, pH 7.4) and 15, 30, 60, and 120 min after glucose injection.

Regarding the experiments to test the different roles of OT on glucose homeostasis, a series of glucose induced insulin secretion (GSIS) experiments were conducted without OT pretreatment as a baseline and pretreated with OT (Synthocinon; 1ug i.n., 20min before glucose injection or 500nmol/kg BW s.c., simultaneously to glucose injection). For GSIS,

additional blood was collected with EDTA-coated microcuvette tubes (Sarstedt, Germany) at the same timepoints as blood glucose measurements described above. Collected blood was centrifuged at 5000xg for 10min at 4°C to obtain plasma that was used to determine insulin concentration following the instructions of a commercially available insulin ELISA kit (see Materials 5.1). A baseline GSIS was followed by a GSIS with simultaneous s.c. OT injection (500nmol/kg bodyweight) and another GSIS with i.n. administered OT (1ng in 12ul, 6ul per nostril) 20 min before glucose injection. HOMA-IR was calculated from fasting glucose and fasting insulin values by the commonly used formula: HOMA-IR= [fasting insulin (mU/l) *fasting glucose (mg/dl)/405] (Matthews et al., 1985).

2.1.5.5 Insulin tolerance test (ITT)

For the insulin tolerance test, mice were fasted for 4h before insulin (0.75IU/kg BW in lean mice, 1.5IU/kg BW in DIO mice) was injected. Blood glucose was detected at timepoints 0, 5, 15, 30, 60, 90, 120, and 180min.

2.1.5.6 2-Deoxyglucose tolerance test (2DGTT)

2DG is a glucose analog which has a hydroxyl group (C2 position) exchanged with a hydrogen atom. This compound is absorbed and transported in the same manner as glucose while after uptake into the cell, it can only be metabolized into 2-deoxyglucose 6-phosphate via hexokinase. The resulting product inhibits the next step of glycolysis which would be the conversion to fructose 6-phosphate by phosphoglucose isomerase (Wick et al., 1955, Brown, 1962).

To test the response to 2DG-induced glucoprivation, food was removed for 2-3h before animals were subjected to an injection of 2DG (250 mg/kg BW). Blood glucose was detected at timepoints 0, 15, 30, 60, and 120min. Blood was sampled for further analysis at timepoints 0, 15, and 30min.

To test the hypothesis that sympathetic or parasympathetic enervation is involved, the nicotinergic antagonist hexomethonium, which does not penetrate the BBB, was used to block the peripheral nervous system. Hexomethonium (10mg/kg BW diluted in saline) was given i.p. at the same time as the 2DG injection and blood glucose was detected at timepoint 0, 15, 30, 60, and 120 min.

2.1.5.7 FDG PET (collaboration)

For the PET imaging, chow and HFHS diet fed C57Bl6J male mice were administered OT or saline intranasally 20min before an injection of glucose or vehicle. An Inveon preclinical PET/CT system (Siemens) was used, and it was performed as described in Jais et al., 2016. For the imaging, mice were anesthetized with 2% isoflurane in 65%/35% nitrous oxide/oxygen gas and positioned on a mouse carrier (MEDRES; Germany). Body temperature was kept at 37.0 ±0.5°C. The radiotracer (7-8MBq [18F]FDG in 50-100ul saline/ mouse) was injected intravascular into a catheter to the tail vain with a 30G cannula. Emission data was obtained

for 45min before mice were moved to the CT gantry for a CT scan (180 projections/360°, 200ms, 80kV, 500µA), which data was used for attenuation correction of the PET data while CT images of the skull were used for co-registration to the 3D mouse brain atlas (constructed from Paxinos and Franklin, 2013) with the imaging analysis software Vinci (Cízek et al, 2004). Plasma glucose levels were determined from the tail vein with a handheld glucometer (Bayer) after removing the catheters. PET data was histogrammed in timeframes of 12x30s, 3x60s 3x120s, 7x740s, fourier rebinned, and images were reconstructed with the help of MAP-SP algorithm provided by the manufacturer. For the kinetic modeling, an image-derived input function was extracted from PET data of the aorta, identified in the image of the first timeframe of each animal. Input function data was corrected for partial volume effect as in Green *et al*., 1998, assuming a standardized volume fraction of 0.6. Parametric images of [18F] FDG kinetic constants k1,k2,k3, and k4 were determined by a voxel-by-voxel fitting of data to a two-tissue-compartment kinetic model. The ratio of tissue and plasma glucose concentrations (C_E/C_p) is a measure for glucose transport and is given by C_E/C_p=k1/(k2+k3)/0.26.

2.1.5.8 Hyperglycemic clamp (collaboration)

In mice that express DREADD in OT neurons (PVN and SON, AAV injection as described in 2.1.1), catheters were attached to the *A. carotis* and *v.jugularis* to be able to clamp blood glucose to a chosen level. In the experiment, mice were injected with CNO to activate OT neurons 25min before the start of the clamp to a target glycemia of 270 mg/dl. Blood glucose was detected at 0, 5, 10, 15, 20, 30, 40, 50, and 60min after clamp start, blood for insulin measurements was taken at 0, 5,10, 15, 20, 40, and 60min. OT content in plasma was detected with a highly sensitive radioimmunoassay (RIAgnosis) as described before (Landgraf et al., 1995).

2.1.5.9 Perfusion

Mice were sacrificed with CO2 before perfusing PBS followed by ice-cold 4% PFA (0.08 M Na2HPO4; 0.02 M NaH2PO4 in ddH2O; pH 7.4). Liver tissues were taken during PBS perfusion and were immediately frozen on dry ice. After perfusing with 15 ml of 4% PFA, brains were dissected and post-fixed in 4% PFA overnight at 4°C. Subsequently, brains were changed into 30% sucrose (30 % sucrose, 0.05 % sodium azide in TBS 1x) until saturation.
Brains were glued to specimen discs with tissue freezing medium (O.C.T) and frozen at -20 °C for 30 min. Subsequently, brains were cut in 30-40 µm coronal sections with the cryostat (CM3050A, Leica, Germany). Slices were collected in 1x TBS at 4 °C for short-term storage.

2.2 *Ex vivo* measurements

2.2.1 Ca^{2+} imaging in ex vivo brain slice preparation and 2-photon excitation Ca^{2+} imaging (collaboration)

For neuronal Ca^{2+} imaging, I injected an AAV expressing the Ca^{2+} indicator GCaMP6 in neurons (pAAV-Syn-GCaMP6m.WPRE) into the VMH (+/-0.8/-1.5/-5.5 and -5.1) of adult

C57BL6J male mice. After recovery mice were sacrificed and brains were sliced at 250µm in ice-cold artificial cerebrospinal fluid (aCSF) (87mM NaCl, 2.69mM KCl, 1.25mM NaH2PO4, 26mM NaHCO3, 7mM MgCl2, 0.2mM CaCl2, 25mM D-glucose, and 75mM sucrose (330 mOsm/Kg H2O, pH 7.4 bubbled with a carbogen mixture of 95% O2 and 5% CO2)) in a vibratome chamber (VT1200, Leica Biosystems). Brain slices containing the VMH were incubated in aCSF (124mM NaCl, 2.69mM KCl, 1.25mM NaH2PO4, 26mM NaHCO3, 1.2mM MgCl2, 2mM CaCl2, 2.5mM D-glucose, and 7.5mM sucrose (298 mOsm/Kg H2O, pH 7.35 constantly bubbled with carbogen mixture)) for 30min at 32-33°C before the slices were changed to aCSF containing either 1 or 5 mM glucose and were incubated at room temperature for at least 1h for Ca^{2+} imaging experiments.

The cytosolic Ca^{2+} levels of neurons were then monitored by 2-photon excitation microscopy with the help of the AAV driven genetically encoded Ca^{2+} indicator GCaMP6f with an upright multiphoton laser scanner microscope (FVMPE-RS system, Olympus). Visualization of neurons was performed with a 25x water immersion objective, the excitation illumination was generated by the InSight X3 DUAL tunable laser system (Spectra-Physics) and image acquisition software (FluoView, FV31S-SW, Olympus) was used to tune the laser emission wavelength to 930nm to receive 2-photon absorption signals at an acquisition rate of ca. 0.5Hz. The setup of the Ca^{2+} imaging experiment contained a baseline recording (3min) before a bath application of OT (100nM), and finally the application of KCL (20mM) to investigate Ca^{2+} signal integrity as a readout for neuronal viability. Only responding neurons were considered for analysis. Changes in fluorescence intensity over baseline ($\Delta F/F_0$) were measured to estimate Ca^{2+} transients and $\Delta F/F_0$>3 standard deviations increase from baseline signal were recognized as a Ca^{2+} event. The amount of Ca^{2+} events per minute were plotted over time as a measure of frequency of OT-induced cytosolic Ca^{2+} transients.

For astroglial Ca^{2+} imaging, GLUT-1$^{i\Delta astro/GLAST+}$ mice and littermate controls were used. The *ex vivo* brain slices were incubated with the Ca^{2+}-sensitive dye Fluo-4, which is taken up by astrocytes. Experiments were conducted at 2.5 mM glucose and in the presence of tetanus toxin, to exclude neuronal interference. Baseline recording was followed by bath application of 2DG (10mM).

2.2.2 Elisas (Insulin, Glucagon, Catecholamines, Corticosteroids)

Hormones were detected in the serum with respective Elisa kits (see 5.1 Materials). In short, sampled blood was immediately stored on ice before being centrifuged for 15min at 4°C at 3000xg. Serum was stored at -80°C and handled according to the instructions of the kits.

2.2.3 Glycogen measurement

For the isolation and measurement of hepatic glycogen, the liver tissue was ground in a liquid nitrogen cooled mortar, incubated in KOH, and centrifuged after a 20min incubation period with 95% ethanol. The glycogen-containing pellet was resuspended in ultra-pure, sterile water for

measurement. 10µl of the suspension was diluted with 140µl of water in screw cap tubes, 150µl of 5% phenol and 750µl of sulfuric acid was added for a 10min incubation before they were transferred to a heating block for a further 10min of incubation at 25°C. The color change was detected at 490nm by UV-VIS spectrometry (Nanodrop 2000, Thermo Fisher Scientific).

2.2.4 Ex vivo GSIS with isolated islets (Collaboration)

The pancreas was perfused with collagenase P (6mg/ml) and dissolved in Hanks Balanced Salt Solution with Ca^{2+}/Mg^{2+} (HBSS). After separation by a gradient solution, islets were isolated and picked individually under a light-microscope. Islets were kept for recovery overnight in an incubator at 37°C 5% CO_2 in RPMI medium 1640 (11mM glucose) supplemented with 10% heat inactivated FBS and 1% penicillin/streptomycin.

For the *ex vivo* GSIS, islets were transferred to V-bottom 96-well plates and medium was exchanged with Krebs-Ringer bicarbonate buffer supplemented with HEPES (KRBH; 129mM NaCl, 4.8mM KCl, 1.2mM KH_2PO_4, 1.2mM $MgSO_4$ H_2O, 2mM $CaCl_2$, 24mM $NaHCO_3$, 6mM HEPES, and 0.2% bovine serum albumin; pH 7.4). Islets were equilibrated (KRBH, 2mM glucose) for 1h before the *ex vivo* GSIS.

Different glucose concentrations (2mM (low) and 16.8mM (high)) were applied for 1h each, together with OT at 0, 30, or 100nM at 37°C. The supernatants were collected for analysis of insulin secretion (see section “2.2.2 Elisa”). Islets were lysed for DNA quantification and DNA content was used for data normalization.

2.2.5 Histology and Imaging

2.2.5.1 Immunohistochemistry

Coronal sections corresponding to the region of interest were selected and incubated in primary antibodies diluted in SUMI (TBS, 0.5% TritonX 100, 0,25% gelatin) shaking overnight at 4°C. Next, brain sections were washed three times for 10min in 1x TBS before a 2-h incubation period in secondary antibodie(s) diluted in SUMI on a shaker at RT. Another three x 10min washes in 1x TBX, followed by a staining with DAPI in TBS for 10min in the end. The slices were mounted on gelatin-coated microscope slides (Superfrost Plus Adhesion Microscope Slides, Epredia, Germany), dried, and covered with mounting medium (Elvanol) and coverslips.

2.2.5.2 RNAscope

With the help of a multistep protocol, RNAscope allows for the visualization of single molecules of RNA. Therefore, the mice were perfused with RNAse-free PBS and 4% PFA. Brains were kept in 4% PFA overnight before they are transferred to 10% followed by 20% and 30% sucrose. After freezing, 10µm-slices were cut and directly mounted onto gelatin-coated microscope slides and stored at -80°C until further processing.

After a washing step in cell culture grade PBS, slides were baked for 30min at 60°C (HybEZ™ II oven, ACD, USA). Slides were postfixed (15min in 4% PFA at 4°C) and dehydrated stepwise

in 50%, 70%, and 100% ethanol for 5min each at RT. After drying, slides were treated with hydrogen peroxide solution for 10min at RT. For antigen retrieval, slides were steam-incubated for 5min (FS 5100, food steamer, Braun, Germany) in a target retrieval solution (RNAscope Target Retrieval Reagents, ACD, USA). After washing and drying, a barrier was drawn with a hydrophobic barrier pen (ImmEdge™, Vector Laboratories, Canada) around the slices of interest. Next, slides were incubated for 30min at 40°C with a protease (Protease III, provided in the kit) before washing and applying of probes (Channel 1(C1): GLUT-1; Channel 4 (C4): GLAST). The slides were incubated with the probes for 2h at 40°C. After washing, three amplification steps at 40°C (AMP1: 30min, AMP2: 30min, AMP3: 15min) were conducted separated by washing steps.

An amplification protocol was performed at 40°C (horseradish peroxidase (HRP)-C1 solution for 15min, C1-associated fluorophore (Opal™ 690) for 30min, and HRP Blocker solution for 15min) separated by washing and repeated for the C4-associated fluorophore (Opal™ 520). After the last washing step, the slides were incubated with DAPI for 30sec and mounted (Prolong Diamond Mountant, ThermoFisher).

2.2.5.3 Imaging and analysis

For KO validation by RNAscope, respective brain slices were sequentially scanned with a confocal microscope (Leica TCS SP8, Germany) using a glycerin-immersed 63x magnification objective with a 0.75µm step size. Analysis was conducted in ImageJ/Fiji, following the instructions of RNAscope. A 1.5x circle was drawn around Dapi-stained nuclei that were co-labelled by probes against GLAST. In the emerging area of interest, GLUT-1 RNA molecules labelled by the respective probe were counted. 4 astrocytes in 4 areas within the hypothalamus in 4 slices per animal of 5 mice per group were analyzed.

2.3 Cell culture

2.3.1 Primary astrocyte cell culture

The genetically modified GLUT-1$^{flox/flox}$ mouse line was used for primary astrocyte cell culture to be able to induce GLUT-1 knockout in primary astrocytes. 1–3-day-old mouse pups were decapitated. Heads were disinfected in 70% ethanol and in antibiotic-supplemented, ice-cold PBS, before the brains were removed from the skull into ice-cold PBS w/o Ca2+, Mg2+ (later referred to as DPBS for the rest of the paragraph) and freed from the meninges. Hypothalami were isolated under a dissecting microscope into a falcon tube containing ice-cold DPBS. Under a flow hood, DPBS was discarded and hypothalami were gently homogenized in 2-3 mL non-supplemented MEM (5.5mM glucose, 2mM L-Glutamine) using a micropipette. The homogenate was added onto a pre-wetted 40 µm nylon cell strainer (Falcon®/Corning, USA) for removal of undissociated pieces of tissue into a falcon tube containing MEM supplemented with 10% fetal bovine serum (FBS) and 1% antibiotics-antimycotics (Anti-Anti 100x, Gibco®/ThermoFisher Scientific, USA). The cell suspension was equally distributed into T175

cell culture flasks (2 hypothalami/flask) and the medium volume was brought up to 25mL. Mixed glia cells were kept in an incubator (37°C, 5% CO2, and 100% humidity) until confluence (2-3 weeks) with a cell culture medium change every 2-3 days. For passage into experimental plates (6-well: $10x10^5$ cells per well, 96-well: 24-well seahorse plate: $2x10^5$; 96-well seahorse plate: $5x10^4$), cells were trypsinized (0.05 % trypsin/0.02% EDTA solution; Biochrom GmbH, Germany) and mechanically unattached by gentle tapping. Before the experiment, the cells were treated with 200 µg/mL of clodronate liposomes (Clodrosome ®, Encapsulated Nano Sciences, USA) for 24h to remove microglial cells.

The GLUT-1 knockout was induced by an adenovirus carrying a Cre-Recombinase gene (Ad5-CMV-Cre-eGFP) and a Gfp gene only as a control (Ad5-CMV-eGFP). The viruses were added with a minimal medium (MEM, 2% FBS) for 16 h followed by a minimum of 72h of replication phase. As both AAVs express a fluorescent reporter, successful infection was confirmed with fluorescent microscopy (10x magnification, BZ-9000, Keyence, Corporation Itasca, USA).

2.3.2 Gene expression analysis

2.3.2.1 RNA isolation

RNA was isolated from respective tissues or primary astrocyte cell culture according to the instructions of the commercially available kit used (MicroRNeasy Kit). In more detail, tissues were frozen on dry ice immediately after dissection and stored at -80°. Tissue was homogenized in quiazol with a tissue lyzer and a metal beat at 300 rpm for 2-3 min. The homogenate was subjected to separating and cleaning steps of the kit, which allows to eluate RNA with ultra-pure water in the last step. The RNA concentration was detected with a microvolume UV-VIS spectrometer (NanoDrop, Thermo Fisher Scientific).

2.3.2.2 Reverse transcription

A commercially available kit (Quantitect, Qiagen, Germany) was taken advantage of to transcribe identical amounts of RNA into cDNA. Following the kit instructions, samples were diluted to contain the same amount of RNA and were treated with gDNA Wipeout buffer to eliminate any DNA contamination. After an incubation time (2 min at 42 °C), a mastermix containing reverse transcriptase, buffer, and primers was added for reverse transcription (30 min at 42 °C, followed by 3 min at 95 °C).

2.3.2.3 qPCRs

Applied Biosystems TaqMan Universal Master Mix (ThermoFisher Scientific) was used. It contains DNA polymerase, an internal standard, dNTPs, and dUTP, Uracil-DNA Glycosylase and optimized buffer components (https://www.thermofisher.com/order/catalog/product /4304437). For each tested gene, a mastermix was prepared containing the gene related TaqMan probe and the Universal Master Mix (1:10). For each well, 4 µl of mastermix was pipetted into 386-well plates. The cDNA was then diluted 5x and 1 µl of each sample was added in duplicates. The detection was performed using a qPCR cycler (ViiA 7 Real Time PCR

System, ThermoFisher Scientific). We applied the $2^{-\Delta\Delta Ct}$ method to visualize gene expression changes normalized to *Rpl32* or *Hrpt* as a housekeeper gene.

2.3.3 (Micro) BCA assay

For normalization, tissue and cells were lysed and protein concentration was detected in the lysate following the kit instructions of the bicinchoninic acid (BCA) assay (see 5.1 Material). In short, a working buffer is added to standards and samples, mixed, and after 30min incubation at 37°C, the absorbance was measured at 562 nm. For smaller protein amounts, a microBCA assay was used.

2.3.4 Glucose uptake measurements

To measure glucose uptake, a commercially available kit was used (see 5.1 Material) In short, cells were plated in a 96-well plate until confluent. After a starvation period (6h in serum-free MEM, 40min in Krebs Ringer Phosphate HEPES buffer), 2DG (1mM) was added for 10min. Lysis was performed with an extraction buffer and plates were frozen at -80°C. After thawing, 15ul were removed for normalization by protein content (see 2.3.2.4 ((Micro) BCA assay)). The leftover cell lysate was further prepared (see kit instructions) to finally detect 2DG/glucose uptake by measuring absorbance at 412nm.

2.3.5 Seahorse measurements

Cellular metabolism was investigated by using a Seahorse XF Analyzer (Extracellular Flux Analyser XF 24 and XF^e 96), which detects extracellular acidification rate (ECAR) and oxygen consumption rate (OCR) as measures for glycolysis and mitochondrial respiration.

In detail, primary astrocytes (GLUT-1flx) were plated in lysin-precoated cell culture microplates (Agilent Seahorse XF24 or XF 96-well plates), treated with clodrosome and adenovirus as described above. For a modified glycolytic stress test (compared to test design on Agilent.com), cells were incubated in glucose-free assay medium for 1.5h in a non-CO2 incubator at 37°C before conducting the assay with the respective Seahorse machine. During the assay, glucose is injected (5mM final concentration) and 12 measurements are taken for a prolonged baseline, followed by oligomycin (ATP synthase inhibitor), FCCP (10mM) as an uncoupler of the respiratory chain, and a mix of rotenone (complex I inhibitor), antimycin (complex III inhibitor) and 2DG (inhibitor of glycolysis), to stop respiration completely. Furthermore, a modified Mito Fuel Flex test (see 5.1 Materials) was used to investigate KO-induced changes in usage of glutamate as a fuel. Therefore, the compounds BPTES (inhibitor of glutamate oxidation), etomoxir (inhibitor of long chain fatty acid oxidation) and UK5099 (inhibitor of glucose oxidation) were used in different combinations to calculate capacity to metabolize and dependency on glucose and glutamate, while fatty acids were not part of our interest. Otherwise, the protocol was followed as suggested by the user manual (https://www.agilent.com/cs/library/usermanuals).

2.4 Statistical analysis

Data was organized and analyzed with the help of Microsoft Excel, ImageJ/Fiji, and GraphPad Prism (version 9). Normal distribution was tested using Shapiro-Wilk test. For normally distributed data, student's t-test, one-way, or two-way analysis of variance (ANOVA) was chosen accordingly. P-values lower than 0.05 were regarded as statistically significant. Data is shown as mean ± standard error of the mean (SEM). Exclusion criteria included misinjection of glucose (no change in blood glucose levels) and mistargeting of AAV injection.

3 Results

3.1 AIM 1: To disentangle humoral versus neural pathways by which OT neurons within the hypothalamus govern the improvement of glucose tolerance

3.1.1 Chemogenetic activation of OT neurons increases glucose disposal and first-phase insulin secretion

To investigate the glucoregulatory response to endogenous release of OT, we used adult male mice with Cre recombinase expression under the OT promoter (B6; 129S-Oxt$^{tm1.1(cre)Dolsn/}$J, Jackson Laboratory). These mice were bilaterally injected with an AAV in the PVN and SON. Control mice were injected with an AAV solely driving the expression of the fluorescent reporter mCherry in neurons (AAV-hSyn-DIO- mCherry) while the experimental group was injected with an AAV allowing the expression of not only the mCherry reporter, but a floxed activating DREADD (AAV-hSyn-DIO-hM3Dq-mCherry). DREADD is an artificial receptor that can be used to artificially stimulate specific cells, in my case OT neurons (hM3Dq^{OT}), *in vivo* via the injection of CNO (chemogenic activation). Subsequently, catheters were implanted in the *A.carotis* and the *V.jugularis* of these mice to perform clamp experiments in hyperglycemic conditions (270mg/dl) (Fig. 7A). This method provides information about the ability of a test subject to secrete insulin and dispose glucose, which can be estimated from the glucose infusion rate necessary to keep the blood glucose levels at the fixed hyperglycemic level. In the present setup, CNO was administered 25min before the start of the hyperglycemic clamp. It was confirmed that chemogenetic activation of OT neurons leads to an increased number of activated neurons in the MBH, as indicated by immunostaining for the protein cFos, a surrogate marker for neuronal activation (Fig 7C). This activation of OT neurons also led to significantly elevated OT plasma levels 20min post CNO injection (Fig. 7B). Furthermore, the hM3Dq^{OT} mice showed a rapid increase in insulin secretion observed within 5min of hyperglycemia (Fig. 7D). As expected, this increase in insulin secretion translated into a slight rise in glucose infusion (Fig. 7E). However, this was not accompanied by a higher insulin sensitivity indicated by the M/I ratio (Fig. 7F). This ratio is calculated from the average glucose infusion rate over the time of the clamp (M) divided by the average plasma insulin concentration during this period (I); a commonly used index from a hyperglycemic clamp for comparing insulin sensitivity.

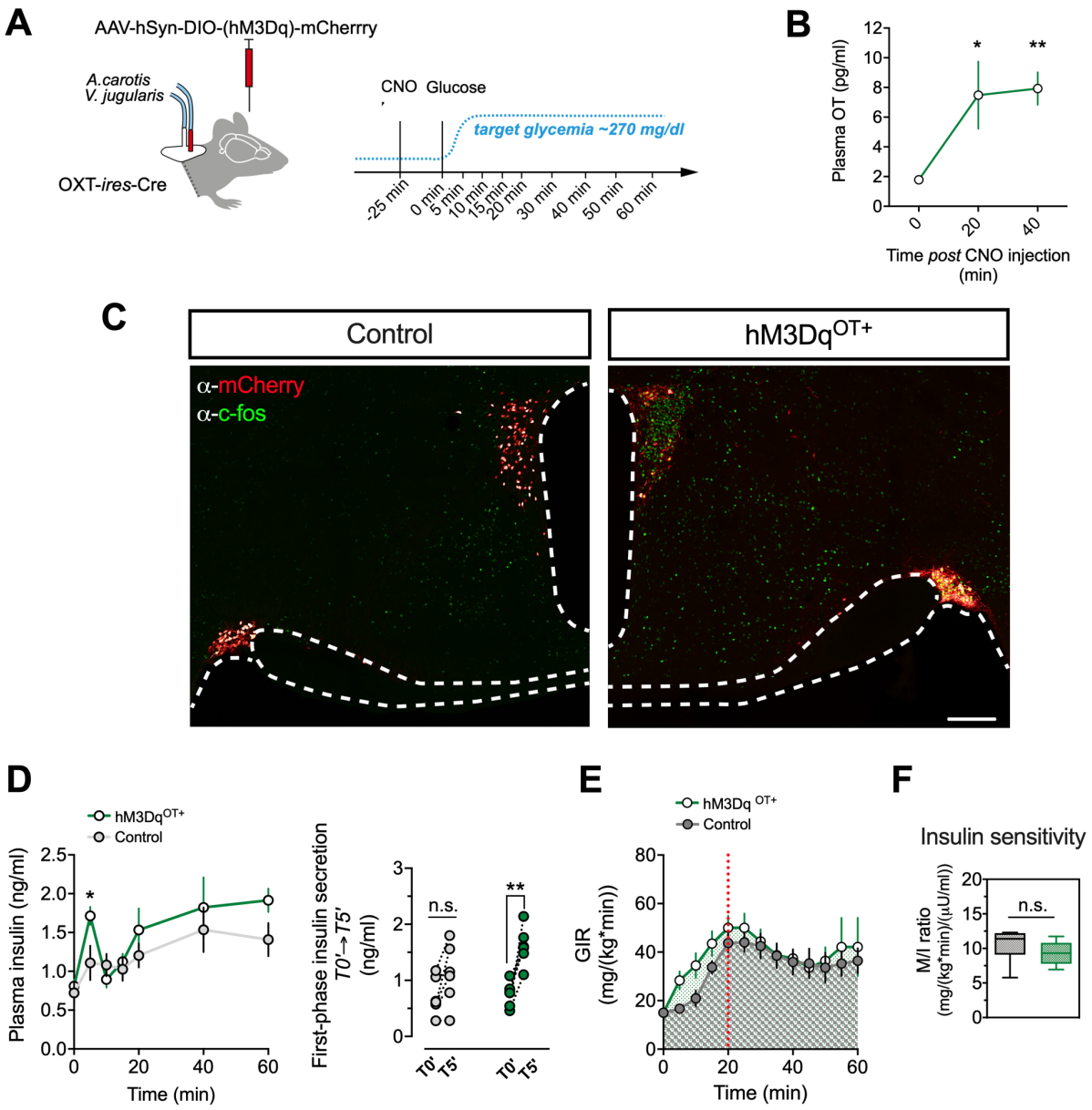

Figure 7 – Activation of OT neurons increases glucose disposal by first-phase insulin secretion.

*(A) Schematic representation of the experimental workflow: OT-ires Cre mice were injected with AAV- hSyn-DIO-(hM3Dq)-mCherry to chemogenetically activate OT neurons using DREADD (hM3Dq^{OT+} vs. control respectively). In the experiment, CNO was injected to activate OT neurons 25min before the start of the hyperglycemic clamp. (B) Activation of OT neurons by CNO resulted in release of OT into circulation, validating the model together with (C) co-immunostaining of OT neurons (mCherry, in red) in the mediobasal hypothalamus with cFos expression (in green) showing neuronal activation in the MBH. (D) CNO- induced activation of OT neurons led to an increased first-phase insulin secretion. (E) This resulted in an increased glucose infusion rate during the first 20 min of the hyperglycemic clamp. (F) Insulin sensitivity was not changed by OT neuronal activation. OT: Oxytocin; CNO: Clozapine-N-Oxide; DREADD: Designer receptors exclusively activated by designer drugs; MBH: Mediobasal hypothalamus; P-values: ** p<0.01; * p<0.05, ns: not significant (data obtained in collaboration)*

3.1.2 *Ex vivo* application of OT promotes insulin secretion in pancreatic islets under high glucose conditions

Preliminary experiments confirmed that OT administration to isolated pancreatic islets under high glucose conditions significantly augmented cytosolic Ca^{2+} transients as measured by epifluorescent time-lapse imaging after incubating with a Ca^{2+}-indicator (Fluo-4AM).

Consistently, administering OT into the medium significantly boosted insulin secretion under high glucose conditions in isolated pancreatic islets via the activation of OTR, while previously observed OT-mediated effects were lost in islets from mice genetically devoid of OTR ($OTR^{-/-}$) (Fig. 8A-C).

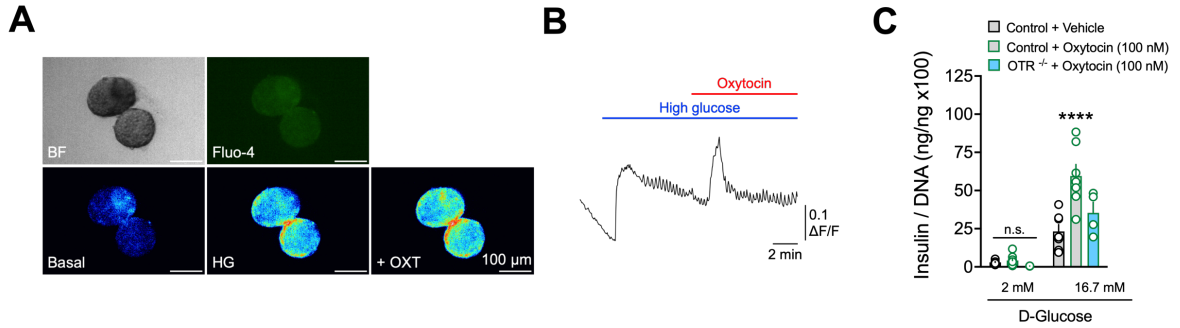

Figure 8 – Oxytocin promotes insulin secretion in pancreatic islets via OTR under high glucose conditions

(A)Visualization and (B) representative current of the Ca^{2+} activity increase in islets, that were incubated in Ca^{2+} indicator Fluo-4, in response to high glucose (HG) and after addition of OT. (C) In an ex vivo glucose-stimulated insulin secretion test, OT acted synergistically - an effect that was lost when OT receptor was removed.

3.1.3 OT triggers neuronal activity in the VMH of mice

To investigate if the VMH, as a major glucoregulatory hypothalamic region, is involved in OT's effect on glucose homeostasis, we applied OT to *ex vivo* brain slices and observed a significant rise in intracellular Ca^{2+} activity in VMH neurons (Fig. 9C and 9D). Notably, this increase was more pronounced with higher levels of glucose (5mM versus 1mM). Furthermore, *in vivo* experiments involving ^{18}FDG-PET, a method which uses changes in the uptake of a radio-labelled glucose into the brain as a surrogate to assess fluctuation in neuronal activity, revealed that i.n. administration of OT (1µg) resulted in higher glucose uptake, and thus, increased neuronal activity within the VMH (Fig. 9A and 9B).

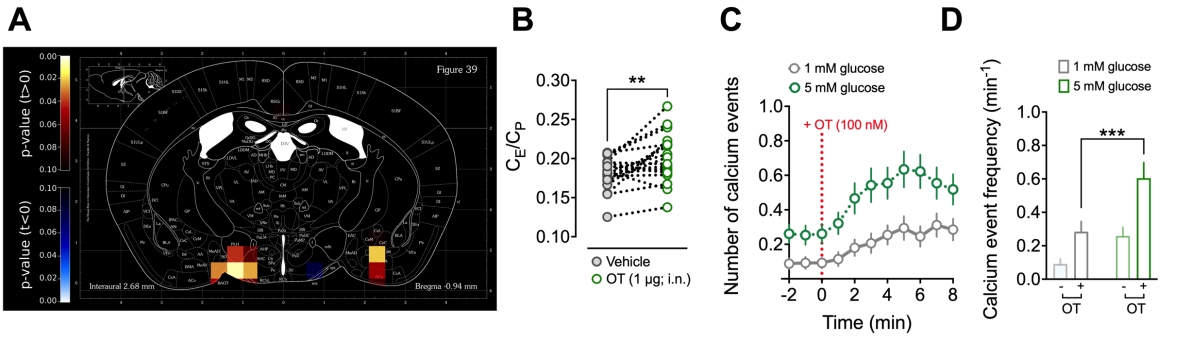

Figure 9 – OT triggers intracellular calcium and neuronal activation in the VMH of male mice

*(A) Visualization and (B) quantification of OT induced elevation in glucose uptake in the VMH in a ^{18}FDG-PET imaging experiment, where intranasal OT was administered 20min before measurement. (C) Bath-applied OT in ex vivo brain slices led to an increased number of Ca^{2+} events in VMH neurons. (D) Quantification of the Ca^{2+} event frequency revealed a significant increase under high but not low glucose conditions. OT: Oxytocin; OTR: Oxytocin receptor; i.n.: intranasal; P-values: **** p<0.001; *** p<0.001; ** p<0.01; * p<0.05; ns: not significant (data obtained in collaboration)*

These results suggest that both humoral and central signaling of OT affect glucoregulatory mechanisms. I therefore set out to disentangle the effects of each pathway.

3.1.4 Distinct central and peripheral OT effects on improving glucose tolerance: independency or requirement of OTR in β-cells and insulin secretion

To disentangle central and peripheral action of OT, I used a mouse model lacking OTR in β-cells specifically (OTR$^{\Delta Ins1}$) and subjected them to a series of GTTs following exogenous OT stimulation, administered either subcutaneously (s.c.) or i.n. (Fig. 10A). While the s.c. administration of OT mainly exerts peripheral effects due to its limited ability to penetrate the blood-brain barrier i.n. administration of OT predominantly elicits central-mediated effects (Ermisch et al., 1985, Lee et al., 2020). My findings revealed that centrally administered (i.n.) OT improved glucose tolerance in mice, regardless of the absence of OTR in β-cells (Fig 10B-10D).

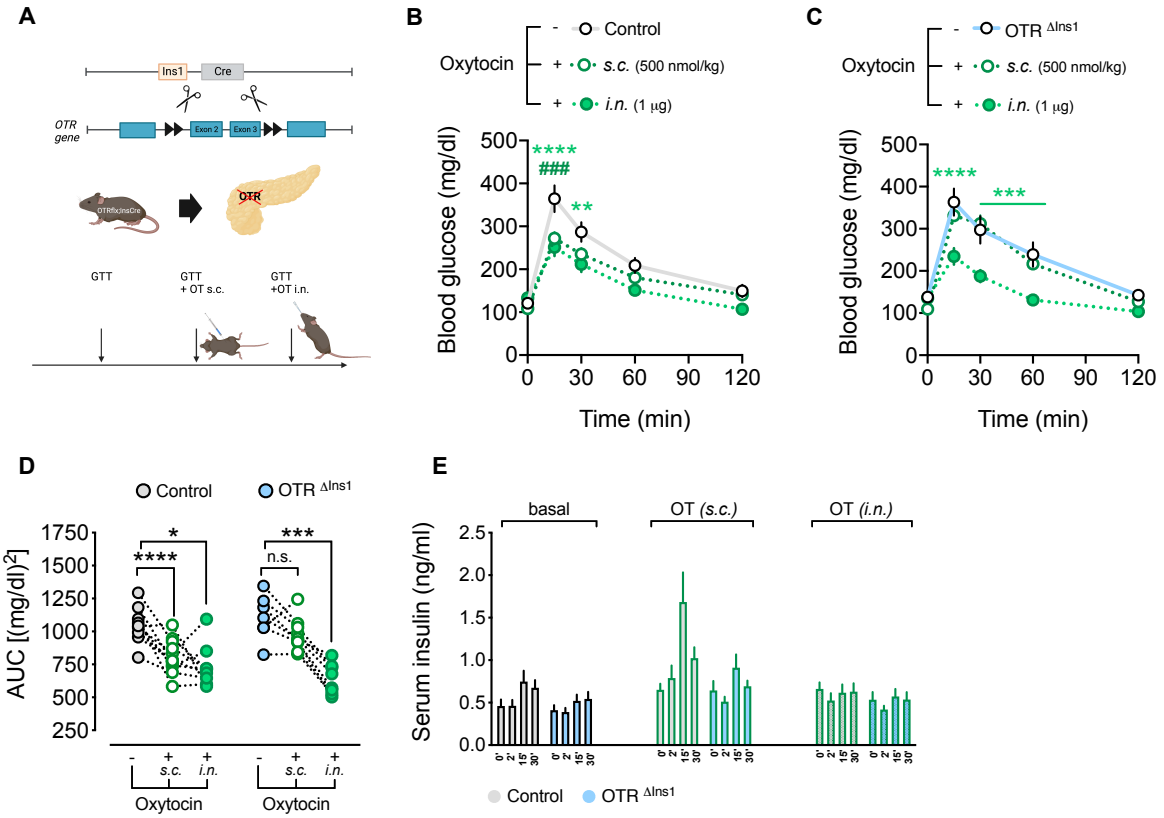

Figure 10 – Distinct central and peripheral OT effects on improvement in glucose tolerance in male mice.

*(A) OTRflx mice were crossed with mice heterozygous for Ins1Cre, Ins1 being a marker gene for β-cells, to generate mice lacking OTR in β-cells specifically (OTR$^{\Delta Ins1}$) and wildtype littermate controls. The mice were subjected to a baseline GTT without OT administration, compared to a GTT with OT applied s.c. and a GTT with OT applied i.n. (B) Control mice respond to OT administered s.c. (500nmol/kg) as well as i.n. (1ug) with an improved glucose tolerance. (C) OTR$^{\Delta Ins1}$ mice failed to respond to s.c. OT, however, i.n. OT still has the same effect. (D) Those results are further evidenced by the AUC of each respective group. (E) Serum insulin levels (ng/ml) were unaffected by the GTT without OT, but injecting OT in control mice led to increased insulin secretion, while this effect was lost in OTR$^{\Delta Ins1}$mice. Interestingly, i.n. OT did not lead to insulin secretion. GTT: Glucose tolerance test; i.n.: intranasal; s.c.: subcutaneous; OTR: Oxytocin Receptor; AUC: Area under the curve; P-values: **** p<0.001; *** p<0.001; ** p<0.01; * p<0.05*

In contrast, s.c. OT administration improved glucose tolerance only in mice expressing OTR in β-cells (Fig 10B-10D). These findings suggest that the pathways activated by central and peripheral OT signaling are distinct and contribute independently to the improvement in glucose tolerance. Interestingly, while s.c. OT administration increased insulin release in control mice – an effect that is abolished in $OTR^{\Delta Ins1}$ mice – i.n. OT failed to induce a detectable insulin release (Fig. 10E). This implies that the effect of centrally acting OT on glucose tolerance might involve an insulin-independent pathway.

3.1.5 The loss of OTR in the VMH induces glucose intolerance and insulin resistance in mice

Intrigued by the ^{18}FDG-PET and calcium imaging experiments that indicated OT-induced neuronal activity in VMH neurons (Fig. 9A-9D), my subsequent objective was to assess the impact of OT in the VMH on systemic glucose regulation. To accomplish this, I induced the knockout of OTR in the VMH of mice by injecting an AAV carrying a Cre recombinase (compared to an AAV carrying the fluorescent reporter mCherry as control) into the VMH of OTRflx/flx mice ($OTR^{\Delta VMH}$) (Fig. 11A). Under these conditions, the VMH-specific OTR KO resulted in strong glucose intolerance under basal conditions (Fig. 11B). Interestingly, these mice however responded to both s.c. and i.n. administered OT, as indicated by the analysis of the AUCs relative to the respective GTTs (Fig. 11C). Regarding serum insulin levels, no differences were detected between groups (Fig. 11D). Nevertheless, $OTR^{\Delta VMH}$ mice exhibited greater insulin resistance than controls (Fig. 11E), which was further confirmed by the HOMA-IR (Fig. 11F).

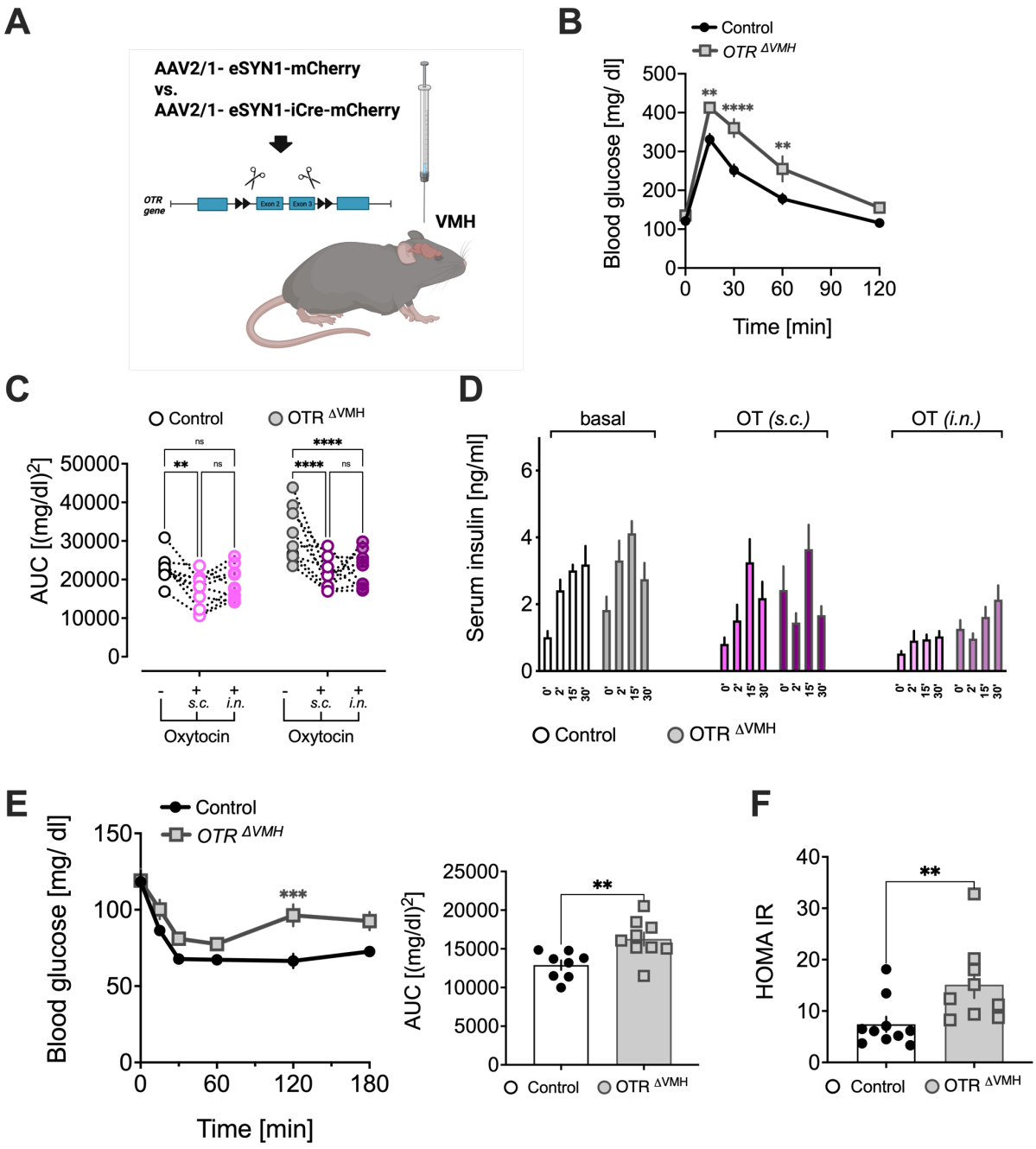

Figure 11 – The lack of OTR in the VMH (OTR $^{\Delta VMH}$) induces glucose intolerance and insulin resistance.

*(A) To generate VMH-specific KO mice (OTR $^{\Delta VMH}$), AAV2/1-eSYN1-iCre-mCherry vs. AAV2/1-eSYN1-mCherry (as control) were injected into the VMH of OTRflx mice. (B) In the baseline GTT, mice lacking OTR in the VMH were significantly more glucose intolerant. (C) Analysis of AUCs relative to the GTTs, in response to s.c. or i.n. OT. OTR $^{\Delta VMH}$ mice showed improved glucose tolerance. (D) Regarding serum insulin levels, no significant differences between groups were detected, however, a trend towards increased fasting insulin in OTR $^{\Delta VMH}$ mice was observed. (E) During an insulin tolerance test, OTR $^{\Delta VMH}$ mice revealed to be more insulin resistant than controls, (F) which was also confirmed by calculating the HOMA IR. AUC: area under the curve; GTT: glucose tolerance test; OTR: oxytocin receptor; VMH: ventrolateral hypothalamus; s.c.: subcutaneous; i.n.: intranasal; P-values: **** p<0.001; *** p<0.001; ** p<0.01; * p<0.05; ns: not significant*

3.1.6 The improvement in glucose tolerance mediated by central OT signaling is blunted in mice fed with a high-fat high-sugar diet (HFHS), but not in mice lacking OTR in β-cells

Next, I examined whether the impact of OT on glucose tolerance persisted in metabolically challenged animals that were fed a HFHS diet for 6 weeks.

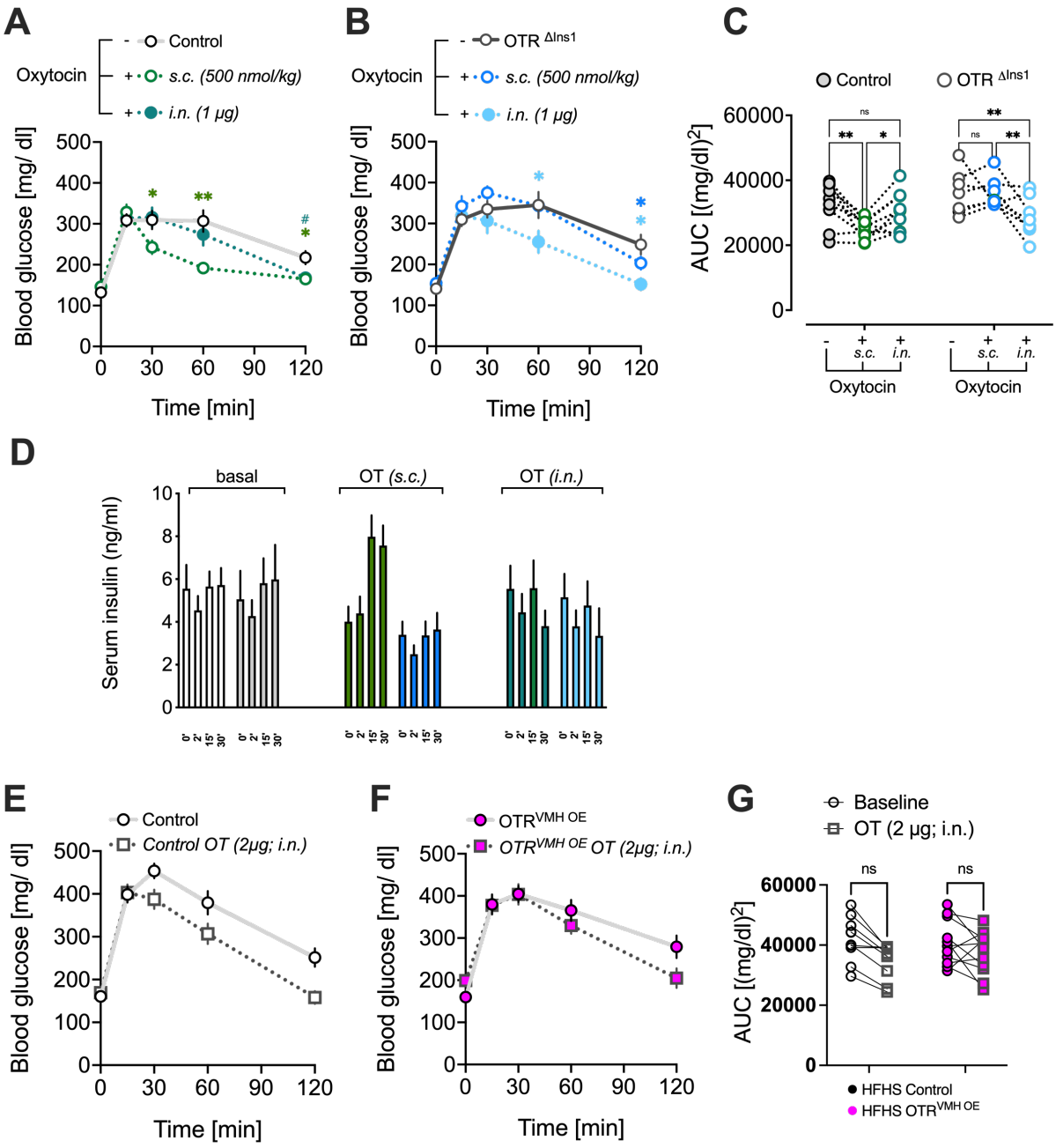

Figure 12 – The effect of i.n. OT on glucose tolerance is blunted in HFHS-diet fed mice.

*(A) HFHS diet fed control mice, have a blunted response to i.n. OT while s.c. OT still improves glucose tolerance. (B) Peripheral OT injection (s.c.) has no effect on OTR$^{\Delta Ins1}$ mice. However, there is an effect of intranasal OT unlike in the control mice. (C) AUC analysis confirming previously described results. (D) Insulin secretion of HFHS diet-fed control and OTR$^{\Delta Ins1}$ mice in response to s.c. and i.n. administered OT. (E) Blunted effect of intranasal OT (F) is not reversed in OTR$^{VMH\ OE}$ mice. (G) AUC analysis of glucose tolerance of control and OTR$^{VMH\ OE}$ mice fed HFHS diet for six weeks. P-values: ** p<0.01; * p<0.05*

I observed that while s.c.-administered OT retained its ability to enhance glucose tolerance through OTR in β-cells and augment insulin secretion under obesogenic conditions, the effectiveness of i.n. OT was blunted (Fig. 12A, 12C-12D), suggesting an impaired central signaling in obese mice. Paradoxically, administering i.n. OT to $OTR^{\Delta Ins1}$ mice exhibited an enhancement in glucose tolerance among mice fed with a HFHS diet (Fig. 12B-12D).

Intrigued by these results, I opted to conduct viral overexpression of OTR in the VMH to investigate whether this could potentially reverse the blunted effect of central OT HFHS diet-fed mice. Thus, male adult C57BL6J mice were either injected with an AAV overexpressing OTR ($OTR^{VMH\ OE}$) or a transgene control driven by a neuron-specific promotor (hSyn1) and fed HFHS for six weeks. However, the blunted response to i.n. administered OT in HFHS fed control mice (Fig. 12E-12G) could not be rescued in $OTR^{VMH\ OE}$ mice (Fig. 12F- 12G).

To sum up, I showed that central OT signaling improves glucose tolerance independently of peripheral OT signaling via OTR in pancreatic islets and concomitant insulin release. Blocking OT signaling in the VMH induces glucose intolerance and insulin resistance; however, i.n. OT still improves glucose tolerance, suggesting multiple signaling pathways in the brain. In HFHS diet-fed mice, central OT signaling is disrupted while peripheral OT administration is still effective, which needs to be considered when handling OT as a future drug candidate for diabetes.

3.3 AIM 2: To examine whether GLUT-1 expression in hypothalamic astrocytes plays a critical role in maintaining systemic glucose homeostasis in situations of high and low glucose levels

3.3.1 Generation of mice lacking GLUT-1 in GLAST-expressing astrocytes

To investigate the role of GLUT-1 in astrocytes, I used a postnatal tamoxifen-inducible knockout model, where the knockout was induced at 6 weeks of age (GLUT-1$^{i\Delta astro/GLAST+}$; Fig. 13A). This model facilitated the deletion of GLUT-1 from GLAST-expressing astrocytes throughout the entire brain. Through this approach, a reduction of GLUT-1 expression in GLAST- positive astrocytes of approximately 50% (average of counted mRNA molecules per astrocyte per mouse) was achieved (Fig. 13B), which translates to a reduced number of GLUT-1 mRNA molecules per astrocyte (Fig. 13C), as visualized by representative confocal images (Fig. 13D).

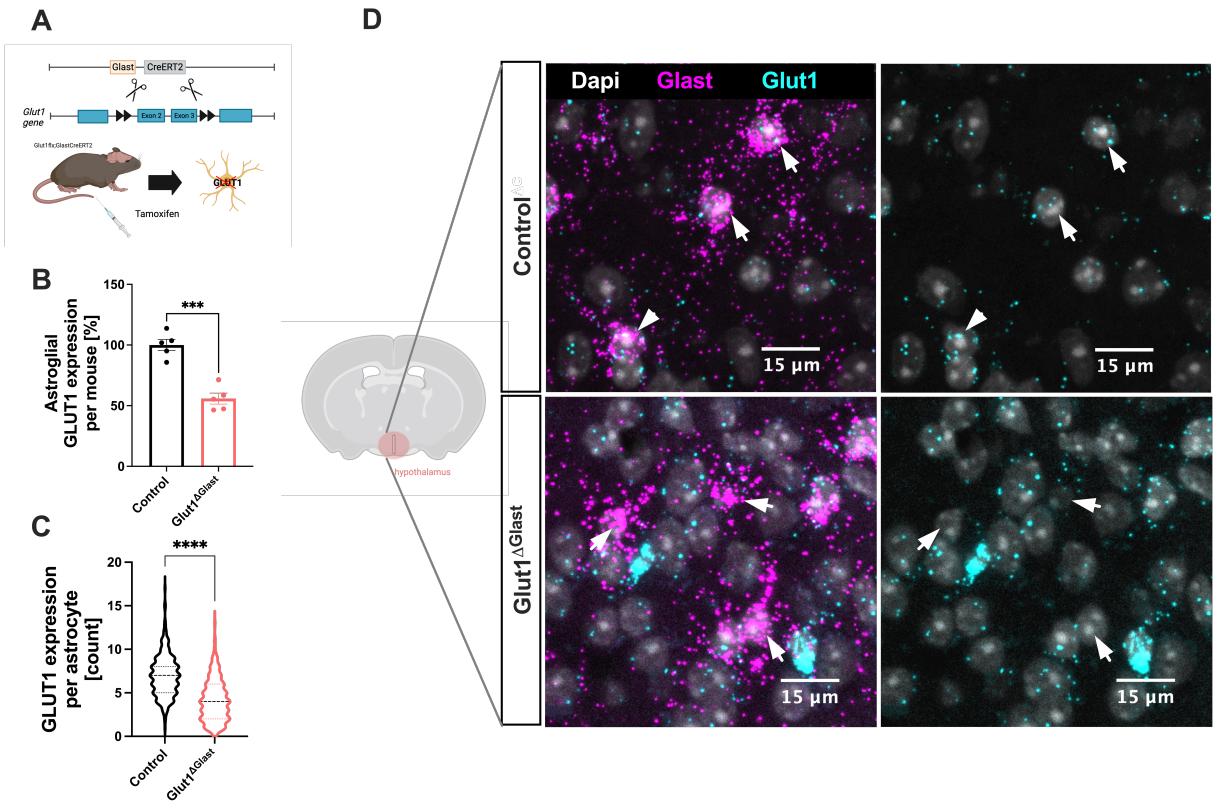

Figure 13 – Successful induction of tamoxifen-mediated deletion of GLUT-1 in GLAST-expressing astrocytes.

*(A) Schematics of tamoxifen-induced deletion of the Glut-1 gene in GLAST-expressing astrocytes in Glut-1flx;GlastCreERT2 mouse model. (B) Tamoxifen-induced deletion of the Glut-1 gene leads to a reduction of GLUT-1 expression by approximately 50% on average. (C) The deletion does result in a significantly reduced number of GLUT-1 mRNA molecules in astrocytes (D) Nuclei are stained with Dapi (white), astrocytes are visualized via GLAST expression (pink), Glut-1 mRNA is visualized in cyan – a large amount of astrocytes in Glut-1 KO mice have reduced or no Glut-1 expression; N=5, astrocytes per mouse: 64 = 4 (slices) x4 (hypothalamic areas) x4 (astrocytes); P-values: **** p<0.001; *** p<0.001*

3.3.2 Postnatal ablation of GLUT-1 in GLAST astrocytes does not impact energy homeostasis upon a standard chow diet

To assess whether the lack of GLUT-1 in GLAST-expressing astrocytes specifically impacts systemic energy metabolism, I subjected GLUT-1$^{i\Delta astro/GLAST+}$ mice to state-of-the-art metabolic phenotyping via indirect calorimetry (Fig. 14A). Three-month-old GLUT-1$^{i\Delta astro/GLAST+}$ mice fed a standard chow diet did not differ in bodyweight nor body composition when compared to littermate controls (Fig. 14B- 14D). Close monitoring of food intake, locomotor activity, RER and energy expenditure by means of metabolic cages did not reveal any differences between groups (Fig. 14E-14I). Measurements in BAT temperature with a thermal camera further confirmed that energy expenditure was unaffected (Fig. 14J).

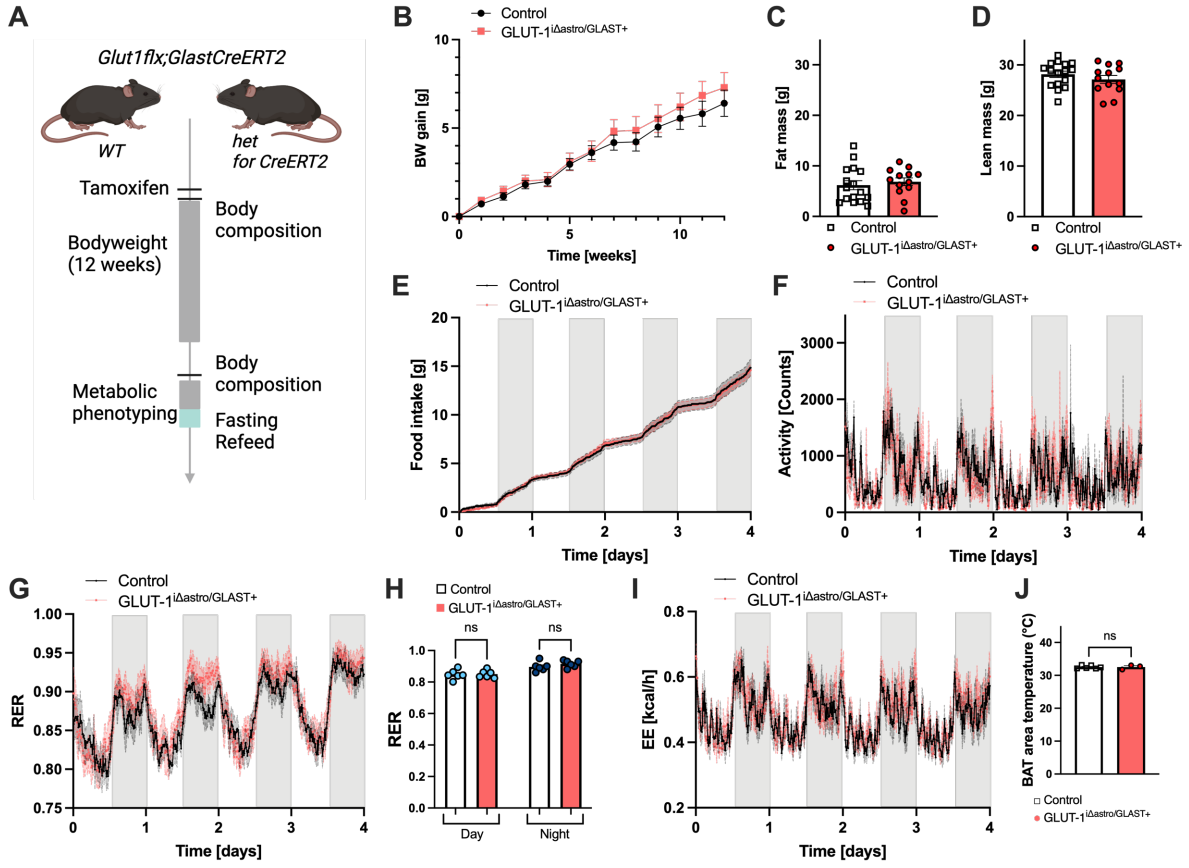

Figure 14 – GLUT-1$^{i\Delta astro/GLAST+}$ mice do not show a phenotype under physiological conditions.

(A) After induction of GLUT-1 knockout by tamoxifen, mice were subjected to state-of the art metabolic phenotyping. (B) Bodyweight gain did not differ from littermate control animals for 12 weeks. Moreover, no difference could be observed in (C) fat mass or (D) lean mass 18 weeks after tamoxifen injection. During a 4-day metabolic phenotyping in metabolic cages, no changes were observed regarding (E) food intake, (F) locomotor activity, (G) RER, (H) averaged RER during day and nighttime, (I) energy expenditure (EE), or (J) BAT temperature. BAT: Brown adipose tissue; EE: energy expenditure; RER: respiratory exchange ratio; ns: not significant; BW: body weight

3.3.3 Postnatal ablation of GLUT-1 in GLAST astrocytes does not impact energy homeostasis upon HFHS diet

Next, I exposed GLUT-1$^{i\Delta astro/GLAST+}$ mice to a HFHS diet for three months. Although the mice significantly gained weight, there were no observable alterations in bodyweight or in body

composition in GLUT-1$^{i\Delta astro/GLAST+}$ animals versus their corresponding littermate controls (Fig 15A-15C). Furthermore, no differences were found in other metabolic parameters such as FI, locomotor activity, RER, or energy expenditure between groups (Fig. 15D-15I).

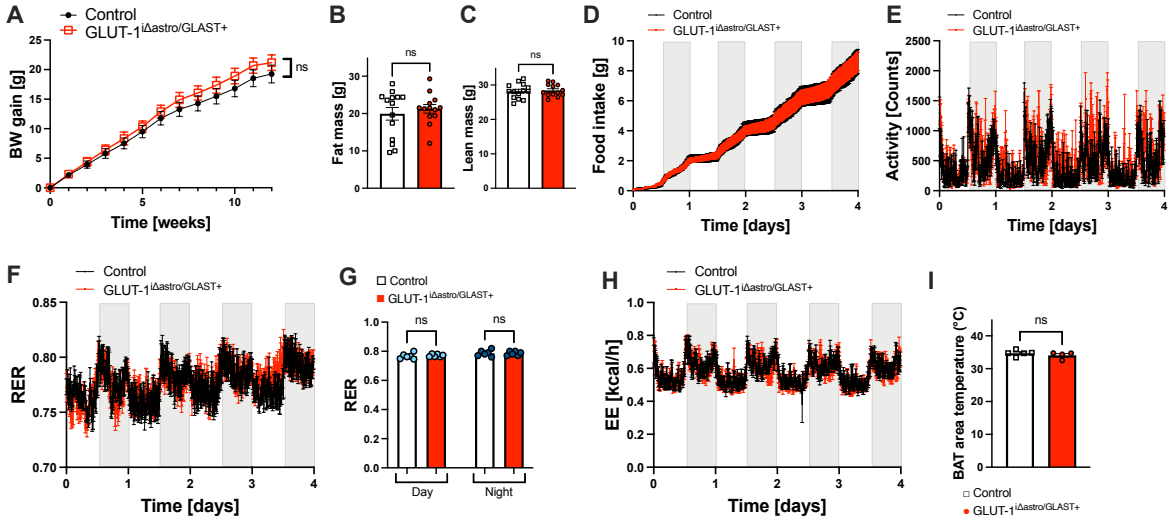

Figure 15 – The postnatal ablation of GLUT-1 in GLAST-expressing astrocytes did not result in differences in the overall metabolic phenotype in mice exposed to a HFHS diet.

(A) Bodyweight gain did not differ from HFHS diet-fed (12 weeks) littermate controls. No differences were observed in (B) fat mass or (C) lean mass 18 weeks after tamoxifen injection. During a 4-day metabolic phenotyping in metabolic cages, no changes in (D) food intake, (E) locomotor activity, (F) RER, (G) averaged RER during day- and night-time, (H) EE, or (I) BAT temperature were observed comparing HFHS-fed GLUT-1$^{i\Delta astro/GLAST+}$ mice and littermate control mice. BAT: brown adipose tissue; EE: energy expenditure; BW: bodyweight, RER: Respiratory exchange ratio

3.3.4 Mice lacking astroglial GLUT-1 exhibit normal metabolic response following prolonged fasting and refeeding

To explore the potential role of astroglial GLUT-1 in conditions of compromised glucose levels, we subjected GLUT-1$^{i\Delta astro/GLAST+}$ mice to an extended 24h fast, followed by a 2h refeeding period (Fig 16A). Under these conditions, metabolic adjustments of GLUT-1$^{i\Delta astro/GLAST+}$ mice did not differ from controls (Fig 16B-16D). Likewise, the response to 24-h fasting did not result in differences in rebound feeding in mice lacking astroglial GLUT-1 compared to littermate controls (Fig. 16E). Moreover, changes in blood lactate, ketone bodies, and glucose levels after the fasting period and the 2-h refeeding period did not show any differences between GLUT-1$^{i\Delta astro/GLAST+}$ and control mice (Fig. 16F-16H).

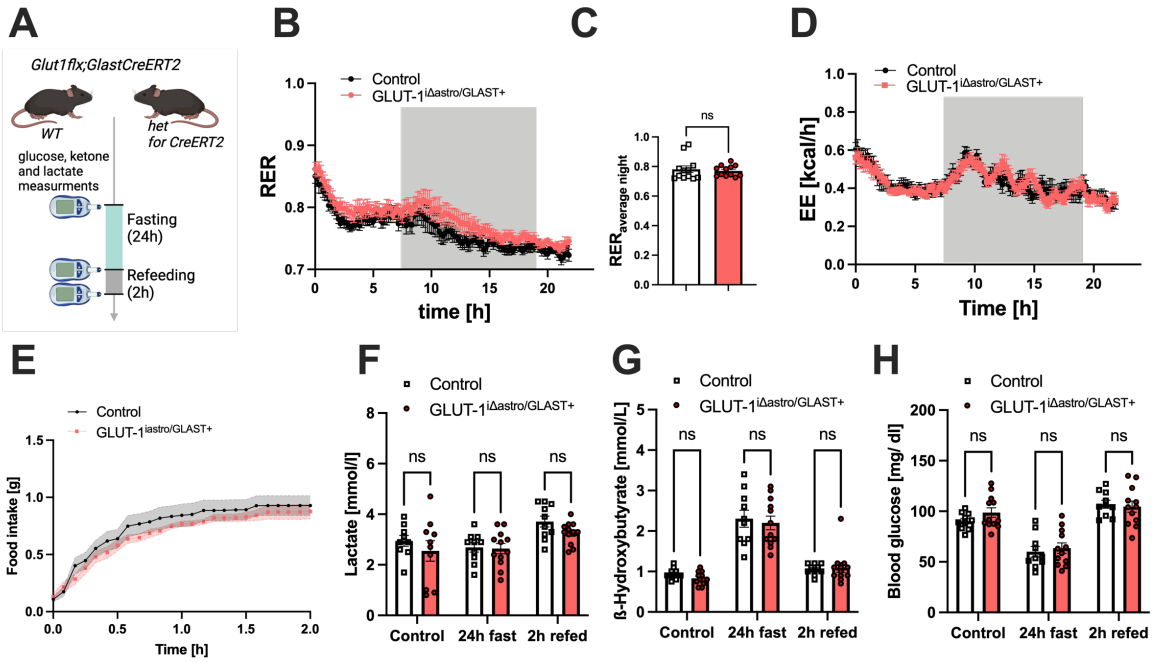

Figure 16 – Mice lacking astroglial GLUT-1 exhibit normal metabolic responses following prolonged fasting and refeeding.

(A) GLUT-1$^{i\Delta astro/GLAST+}$ and control mice were monitored in metabolic cages for a 24h fasting period and 2h of refeeding. Measurements of blood lactate, ketones, and glucose were taken before and after fasting as well as after refeeding. (B) RER, (C) averaged RER, and (D) EE were not significantly different between groups during fasting. (E) The 24h fasting period did not affect the food intake of GLUT-1$^{i\Delta astro/GLAST+}$ compared to control mice in a 2h refeeding period, (F) blood lactate, (G) or blood ketone bodies. (H)Blood glucose levels showed no difference after fasting or after refeeding between GLUT-1$^{i\Delta astro/GLAST+}$ and control mice. EE: energy expenditure; WT: wildype; RER: respiratory exchange ratio; ns: not significant

3.3.5 Postnatal ablation of GLUT-1 in astrocytes affects systemic glucose regulation *in glucoprivic conditions*

Despite not observing any metabolic differences under standard conditions, we investigated whether GLUT-1 in astrocytes plays a role in systemic glucose regulation under conditions of hyperglycemia or glucopenia. To do so, mice with or without GLUT-1 in GLAST-expressing astrocytes were subjected to an i.p. injection of glucose to induce hyperglycemia, and insulin or 2DG to induce glucoprivation (Fig. 17A). Under hyperglycemic conditions, mice lacking GLUT-1 in GLAST+ astrocytes displayed normal glycemic control and insulin sensitivity (Fig. 17B-17C). Intriguingly, GLUT-1$^{i\Delta astro/GLAST+}$ mice exhibited an aggravated counterregulatory glucose production compared to respective control mice in response to insulin and 2DG. More specifically, these mice showed a delayed response to insulin compared to littermate controls (Fig. 17D). Moreover, when these mice were subjected to 2DG, it resulted in an overcompensation of glucose production relative to controls (Fig. 17E).

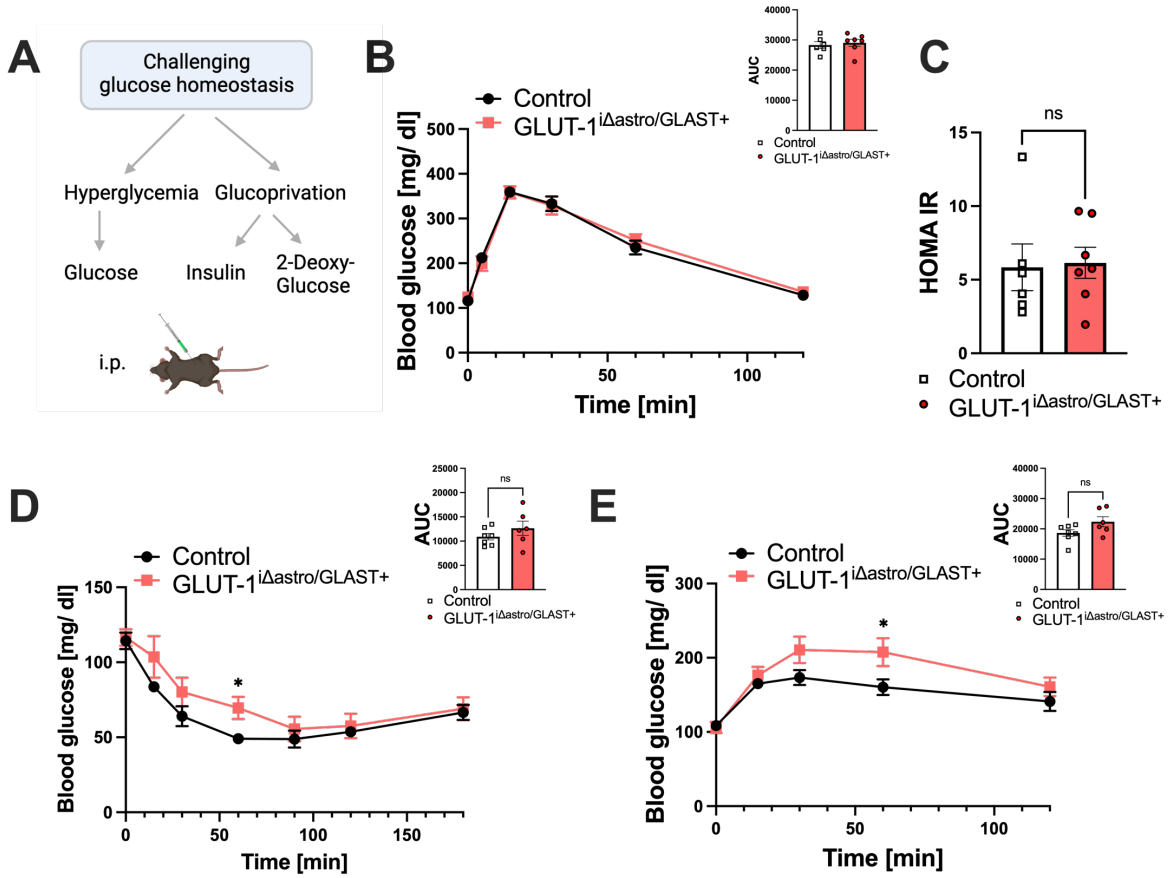

Figure 17 – Mice lacking GLUT-1 specifically in GLAST+ astrocytes showed alterations in glucose regulation in conditions of hypoglycemia.

*(A) Hyperglycemia was induced by intraperitonial (i.p.) glucose injections, glucoprivation by i.p. insulin and i.p. 2DG injections. (B) GLUT-1$^{iΔastro/GLAST+}$ mice displayed no difference in glucose tolerance as their WT littermates (C) and an unaffected insulin sensitivity as suggested by unchanged HOMA-IR values. (D) In response to insulin, GLUT-1$^{iΔastro/GLAST+}$ mice show a delayed decease in blood glucose compared to control animals after insulin injection. (E) 2DG injection resulted in an increase in blood glucose by endogenous glucose production in controls; however, the lack of GLUT-1 in astrocytes leads to an even higher glucose; 2DG: 2-deoxyglucose; i.p.: intraperitonial; WT: wildtype; P-values: * p<0.05*

3.3.6 Loss of astrocytic GLUT-1 in the MBH is sufficient to alter endogenous glucose production under an acute glucoprivation

Given that the ARC and VMH are pivotal brain regions regulating systemic glucose homeostasis and are situated in the MBH, I employed a viral approach to specifically knockout GLUT-1 in GFAP-expressing astrocytes exclusively in the MBH (GLUT-1$^{AVV.Gfa.iCre}$ mice). Similar to the observations in GLUT-1$^{iΔastro/GLAST+}$, metabolic adjustments to 24-h fasting and the 2-h refeeding did not result in differences regarding rebound feeding, ketone bodies, and glucose levels between GLUT-1$^{AVV.Gfa.iCre}$ and control mice, despite a delay in recovery of blood glucose levels after refeeding (Fig. 18A-18C). Following this, these mice received i.p. injections of insulin and 2DG to trigger the counterregulatory mechanism induced by glucoprivation. Similar to observations in mice lacking GLUT-1 in GLAST-expressing astrocytes throughout the entire brain (Fig. 17D), GLUT-1$^{AVV.Gfa.iCre}$ mice showed a significantly faster and more pronounced counterregulation against insulin-induced hypoglycemia compared to controls

(Fig. 18F). Additionally, a strong overcompensation of glucose production in GLUT-1$^{AVV.Gfa.iCre}$ mice compared to controls was observed (Fig. 18G). These findings collectively suggest that the loss of GLUT-1 specifically in hypothalamic astrocytes within the MBH is sufficient to disrupt the counterregulatory response to glucoprivation.

3.3.7 Loss of astrocytic GLUT-1 in the MBH also impairs glucose tolerance and insulin sensitivity

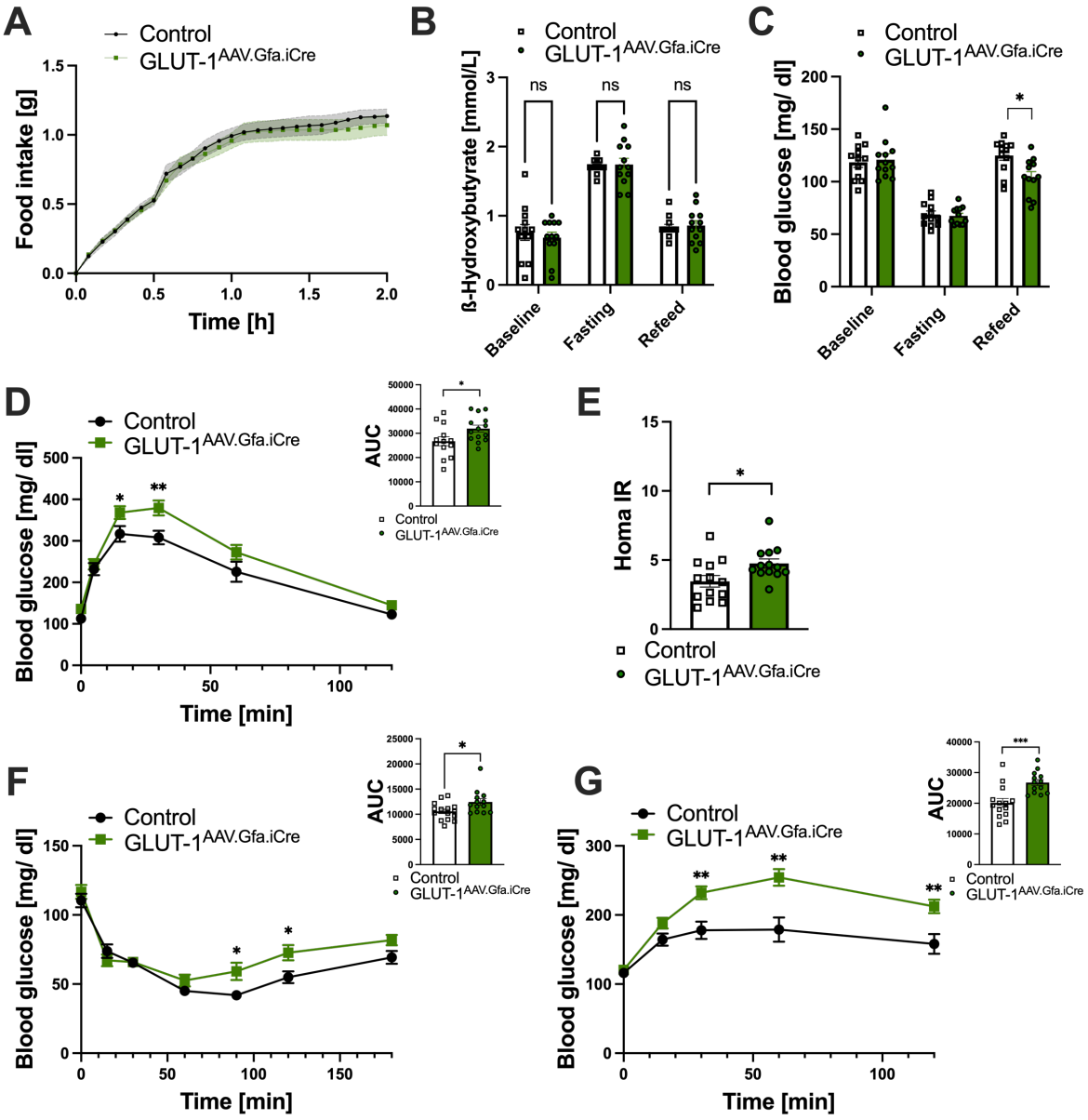

Figure 18 – Impaired glucose homeostasis in mice lacking GLUT-1 in MBH GFAP+ astrocytes.

(A) During refeeding after a 24h fast, food intake of GLUT-1$^{AVV.Gfa.iCre}$ mice did not differ from littermate controls. (B) Blood ketones increased with fasting in both groups; however, no difference was observed before and after fasting, or after refeeding (2h). (C) There was no difference between GLUT-1$^{AVV.Gfa.iCre}$ mice and controls after fasting; however, KO mice had significantly lower blood glucose values after 2h of refeeding. (D) GLUT-1$^{AVV.Gfa.iCre}$ mice showed a delayed clearing of glucose compared to WT controls (E), which might be due to increased insulin resistance further illustrated by a higher HOMA IR. (F) In response to insulin, the blood glucose of GLUT-1$^{AVV.Gfa.iCre}$ mice decreased comparably to WT controls but the return to baseline starts already at 60 min rather than 90 min after insulin injection. (G) 2DG injection resulted in an increase in blood glucose by endogenous glucose production

*in controls; however, the lack of GLUT-1 in astrocytes led to an even higher glucose release in GLUT-1$^{AVV.Gfa.iCre}$. 2DG: 2-Deoxy-glucose; KO: knockout; P-values: ** p<0.01; * p<0.05; ns: not significant*

Unlike mice lacking GLUT-1 in GLAST expressing astrocytes, we found that the lack of GLUT-1 in MBH GFAP-expressing astrocytes led to a significantly impaired glucose tolerance (Fig. 18D). Notably, insulin secretion in response to glucose injection did not differ between GLUT-1$^{AVV.Gfa.iCre}$ and controls, suggesting impairments in insulin sensitivity rather than a failure of insulin secretion. Indeed, the HOMA IR was increased in GLUT-1$^{AVV.Gfa.iCre}$ mice (Fig. 18E). These findings indicate a tendency towards slight (hepatic) insulin resistance in these mice, which could be responsible for the delayed glucose removal from the blood.

3.3.8 Overexpression of GLUT-1 in MBH GFAP-expressing astrocytes fails to rescue dysregulated glucose homeostasis in obese and diabetic mouse models

Based on previous observations showing the adverse effects of GLUT-1 deletion from MBH GFAP-expressing astrocytes on glucoregulation during glucoprivation, I sought to investigate the impact GLUT-1 overexpression (OE) in MBH astrocytes in models of diet-induced obesity and T2D (*db/db*), characterized by disruption of systemic glucose control.

To achieve this, I used 8-week-old HFHS diet-fed C57BL6J and db/db mice under standard chow diet conditions, which were injected with an AAV designed to specifically overexpress GLUT-1 in cells expressing the astrocyte marker GFAP (GLUT-1$^{MBH\ OE}$ and GLUT-1$^{db/db\ MBH\ OE}$) compared to controls injected with AAV driving the expression of GFP into the MBH. Subsequently, all mice underwent the previously conducted tolerance tests to assess glucose homeostasis. Notably, GLUT-1$^{MBH\ OE}$ mice did not display deviations in response to glucose, 2DG, or insulin tolerance tests compared to their respective (Fig. 19A-19B).

Indeed, GLUT-1$^{db/db\ MBH\ OE}$ mice showed similar intolerance to glucose and insulin as control mice, while an increase in HGP was shown in GLUT-1$^{db/db\ MBH\ OE}$ (Fig. 19C), demonstrating that astroglial GLUT-1 OE in the MBH is not able to rescue glucose homeostatic disturbances.

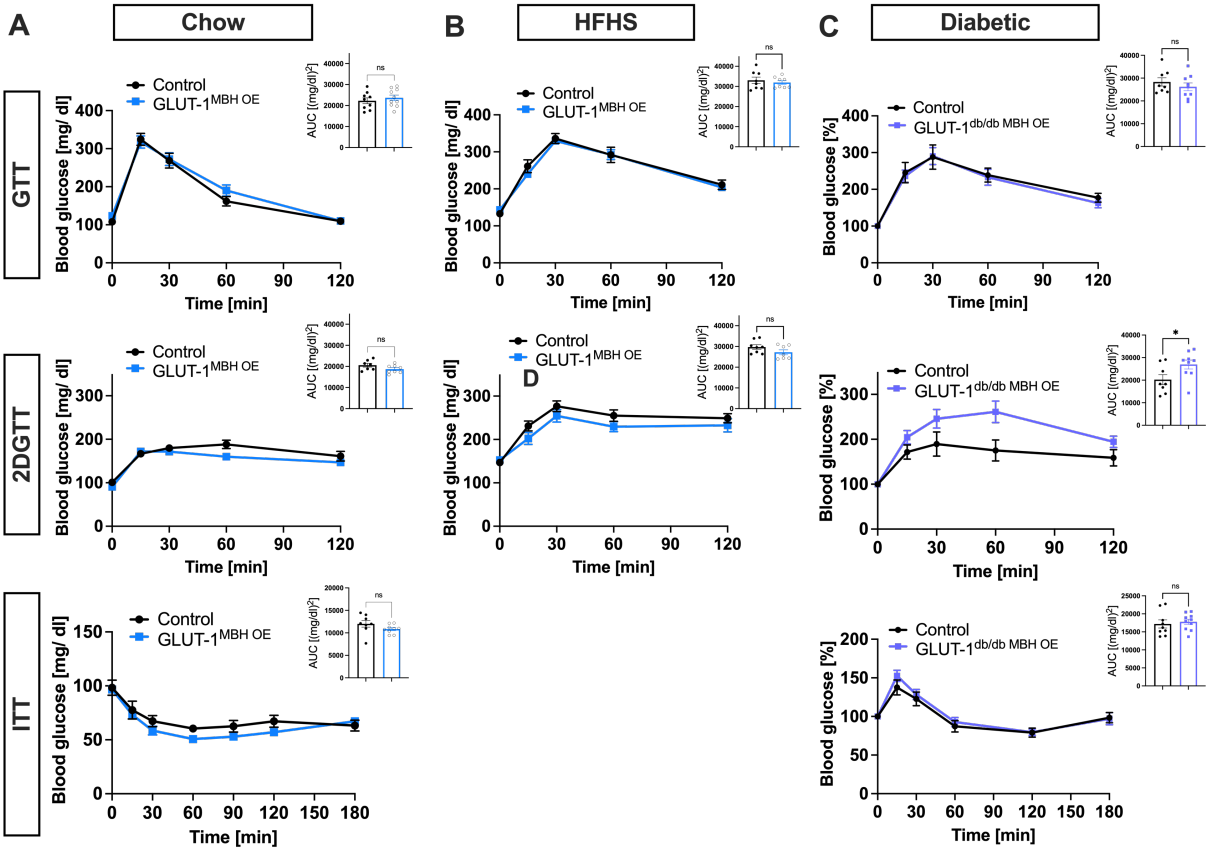

Figure 19 – GLUT-1 overexpression (OE) in the MBH does not rescue disturbed glucose homeostasis

*(A) Astroglial GLUT-1 OE did not change homeostatic response to glucose, 2DG, or insulin under chow-fed control conditions. (B) HFHS diet-fed GLUT-1$^{VMH\ OE}$ mice showed no improvements in glucose tolerance or response to 2DG compared to controls. (C) No changes could be observed in the glucose or insulin tolerance of diabetic GLUT-1$^{db/db\ VMH\ OE}$ mice compared to control mice, however, hepatic glucose output increased with GLUT-1 OE. P-values: * p<0.05*

3.3.9 The loss of GLUT-1 in astrocytes exacerbates counterregulatory response to glucoprivation via a mechanism involving autonomic innervation

Peripheral mechanisms responsible for counterregulatory HGP in response to hypoglycemia or glucoprivation include glucoregulatory hormones like catecholamines, glucagon, and corticosteroids ((Chevrier et al., 1982, Rappaport et al., 1982, Ishihara et al., 2009). While serum catecholamine levels remained unchanged 30 min after injection of 2DG in all groups (Fig. 20A), a significant increase in serum glucagon and corticosteroid levels following 2DG injections in both astroglial GLUT-1 KO models and controls was observed (Fig.20B and 20C). However, no differences were found between either astrocyte-specific GLUT-1 KO mouse models and their corresponding littermate controls concerning the extent of counterregulatory hormone release (Fig. 20B and 20C). Thus, we concluded that endocrine adaptations likely do not drive the exaggerated counterregulatory response previously observed in astrocyte GLUT-1 KO mice relative to littermate controls. Next, we assessed whether the loss of GLUT-1 in astrocytes leads to increased HGP by modulation of parasympathetic and sympathetic outflow, as a remaining putative alternative mechanism. To address this question, we injected

hexamethonium, a nicotinergic acetylcholine antagonist, that potently establishes a transient ganglionic blockade (i.e., silencing both branches of the autonomic nervous system). We were intrigued to see that hexamethonium eliminated the discrepancy in glucose production found between GLUT-1$^{i\Delta astro/GLAST+}$ and littermate controls (Fig. 20D and 20E), suggesting that GLUT-1 in astrocytes affects HGP via direct innervation of the liver.

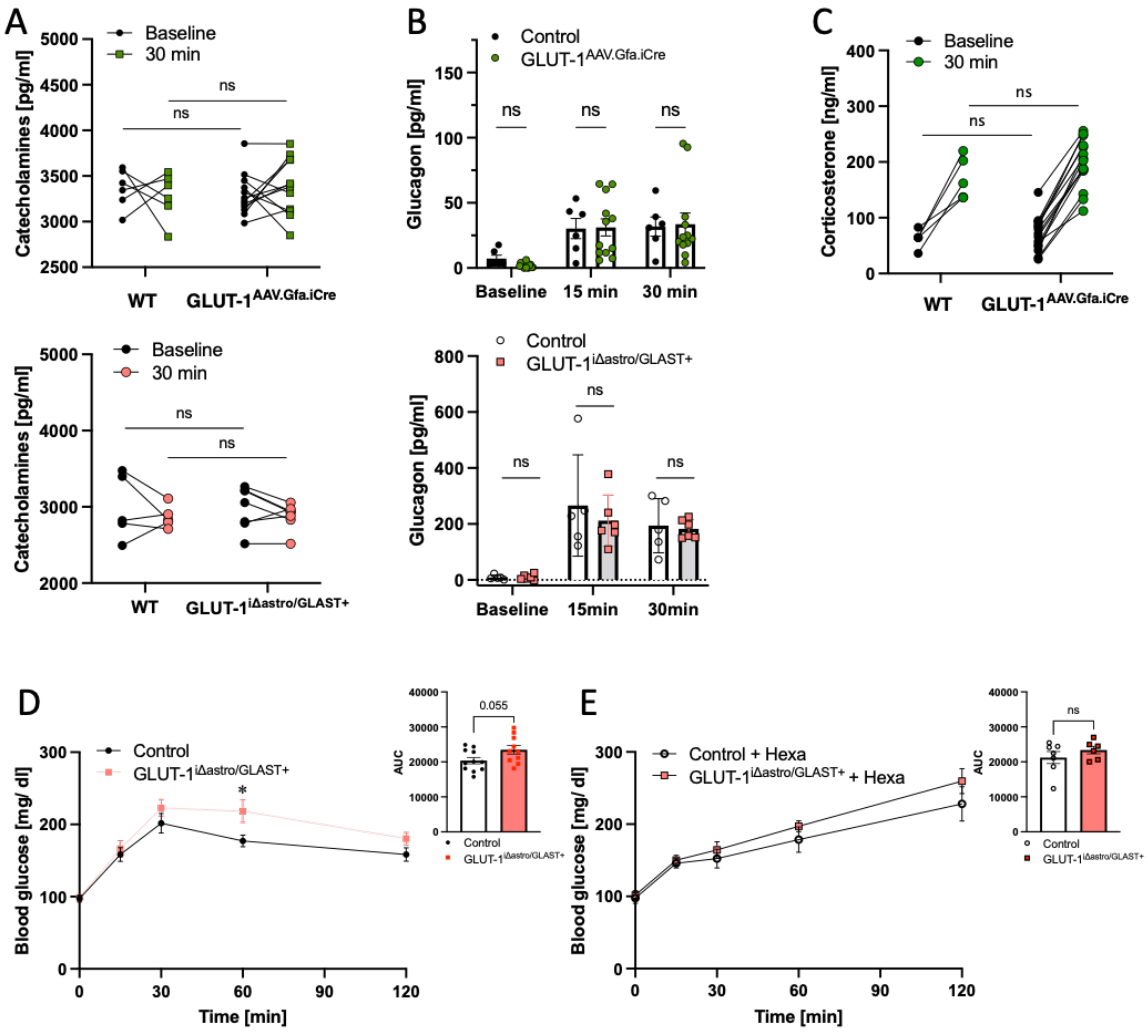

Figure 20 – Increased HGP in astroglial GLUT-1 KO mice is regulated by direct innervation of the liver

*(A) 30 min after 2DG injection, catecholamines are unchanged in both GLUT-1$^{i\Delta astro/GLAST+}$ and GLUT-1$^{AAV.Gfa.iCre}$ and respective WT controls (B) The glucagon output in response to 2DG after 15 and 30 min did not differ between WT controls and GLUT-1 KO models (C) Serum corticosterone increased to a similar extent in WT controls and GLUT-1$^{AAV.Gfa.iCre}$ mice. (D) 2DG injection alone led to a higher HGP in GLUT-1$^{i\Delta astro/GLAST+}$ mice compared to littermate controls. (E) Injections of hexamethonium resulted in a normalization of 2DG-induced HGP. HGP: hepatic glucose production; WT: wildtype; KO: knockout; 2DG: 2-deoxyglucose; P-values: * p<0.05, ns: not significant*

To shine light on the mechanism that is responsible for the differences in HGP production in response to 2DG, hepatic glycogen content and gene expression of major contributors to glycogenolysis and gluconeogenesis, as illustrated in Fig. 21A, were investigated. Hepatic glycogen content was not changed 90 min after 2DG injection in control or KO mice (Fig. 21B). In line with this, the rate limiting enzyme for gluconeogenesis, PYGL, was unaffected by astroglial GLUT-1 KO in both mouse models, as well as by 2DG injection (Fig. 21C). The most

important enzyme for hepatic gluconeogenesis, PEPCK, is upregulated in control mice of GLUT-1$^{AVV.Gfa.iCre}$, hinting towards a stronger involvement of the gluconeogenic pathway, although this is not seen in GLUT-1i$^{\Delta astro/GLAST+}$ (Fig. 21D). As both mouse models have strain differences, increased numbers would give more insights. However, as PEPCK expression in GLUT-1$^{AVV.Gfa.iCre}$ mice was lower compared to controls, it cannot explain the observed elevation in glucose output. G6P, which is necessary for glucose release from the liver, was non-significantly affected by 2DG, however, no differences between control and KO animals were detected (Fig. 21E). In summary, expressional changes of major regulatory enzymes do not seem to play a role in the significant difference in hepatic glucose release observed after 2DG, however faster adaptive processes like phosphorylation could be investigated in the future, as blood glucose differences are most pronounced at 30 and 60 min after injection.

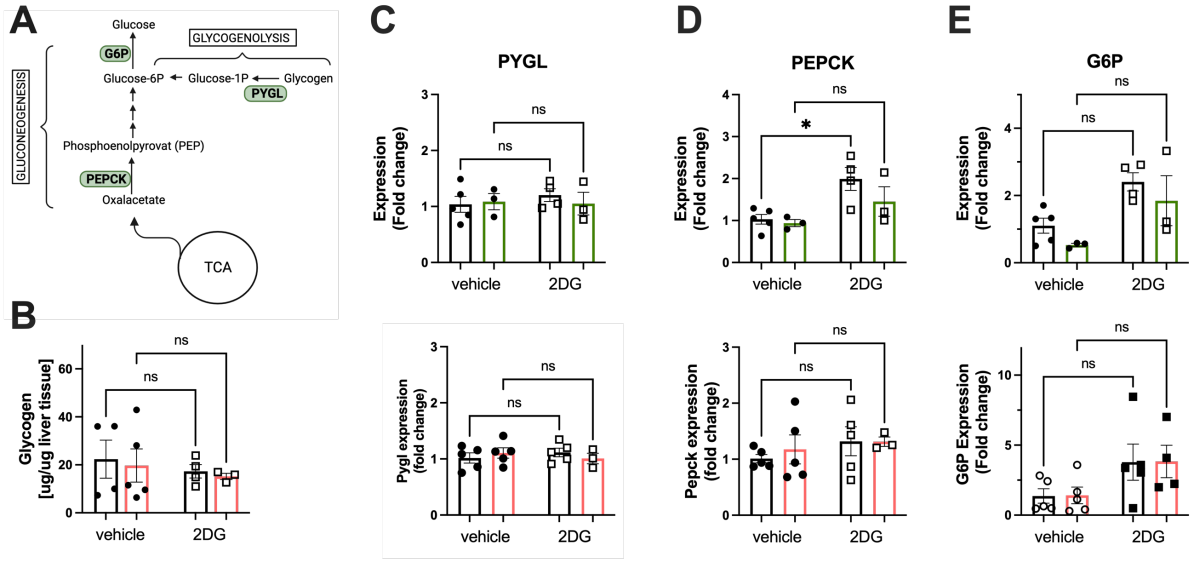

Figure 21 – Differences in hepatic glucose output cannot be explained by differences in expression of genes coding for glycogenolytic or gluconeogenic enzymes in the liver

*(A) HGP can happen via glycogenolysis or gluconeogenesis. Rate limiting enzymes are PYGL, PEPCK and G6P. (B) Hepatic glycogen content was not significantly changed in response to 2DG in controls or in GLUT-1$^{i\Delta astro/GLAST+}$ mice (C) which goes in line with no changes in PYGL expression. (D) PEPCK is significantly increased after 2DG injection in controls but not in GLUT-1$^{AVV.Gfa.iCre}$ mice, while there are no changes in GLUT-$^{1i\Delta astro/GLAST+}$ and their littermate controls. (E) G6P tends to be elevated after 2DG injection in both models, independently of astroglial GLUT-1 KO. HGP: hepatic glucose production; PYGL: liver glycogen phosporylase; PEPCK: phosphoenolpyrovat-carboxykinase; G6P: glucose-6-phosphatase; 2DG: 2-Deoxyglucose; P-values: * p<0.05*

3.3.1 Primary astrocyte cultures devoid of GLUT-1 exhibit reduced glucose uptake resulting in elevated basal respiration and inability to adapt to metabolic challenges

To test the direct impact of the absence of GLUT-1 on astrocytes in glucose metabolism, we generated hypothalamic primary astrocyte cultures from GLUT-1$^{lox/lox}$ animals and induced the loss of GLUT-1 using an adenovirus driving the expression of Cre recombinase (and the reporter GFP; KO astrocytes) compared to astrocytes infected with a control adenovirus driving the expression of GFP alone (WT astrocytes) (Fig. 22A). I first confirmed the successful

knockout of GLUT-1 in primary astrocytes (Fig. 22B). Next, I assessed whether the loss of GLUT-1 affects other glucose transporters previously described to be expressed in astrocytes. In this regard, GLUT-2 and GLUT-4 remained unchanged, whereas SGLT1 gene expression was significantly upregulated (Fig. 22B). No changes were observed in pyruvate-dehydrogenase kinase 2 (Pdk2), which regulates the conversion of pyruvate to acetyl-CoA, or in malic enzyme (Me1), which transforms malate into pyruvate to supply a substrate for lactate production or gluconeogenesis, both of which are relevant for glucoregulation.

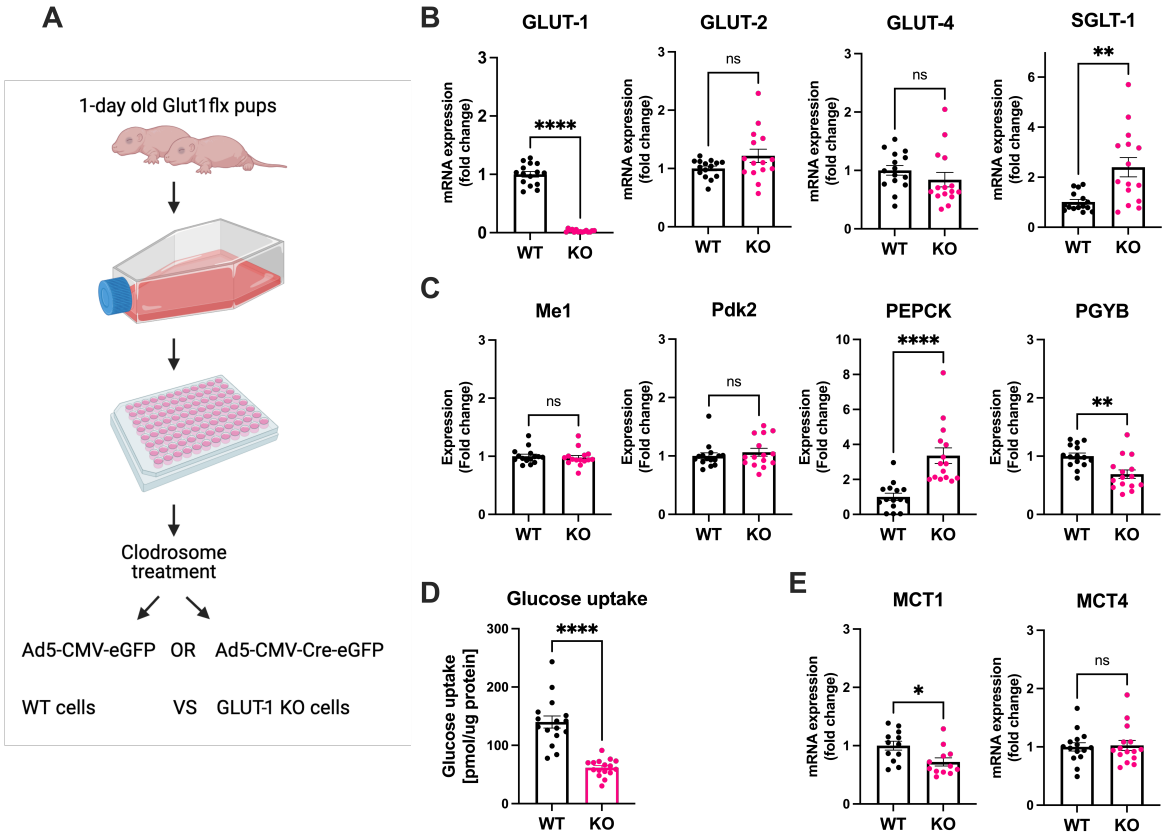

Figure 22 – GLUT-1 deficiency in astrocytes in vitro reduces glucose uptake, which is compensated by enhanced gluconeogenesis

*(A) For primary cell culture, hypothalami of 1–2-day-old pups from GLUT-1flx mice were used to generate an astrocyte-microglia mixed culture. After multiplying and plating, treatment with clodrosome removed microglia and an adenovirus allowing Cre expression induced the loss of GLUT-1 compared to cells treated with adenovirus allowing the expression of GFP. (B) GLUT-1 KO was confirmed by qPCR, expression of other GLUTs previously demonstrated to be present in astrocytes were unchanged (GLUT-2, GLUT-4); however, sodium gradient dependent SGLT1 expression was increased. (C) Regarding intracellular glucose production, Pdk2 and Me1 expression was unchanged, while PEPCK expression was upregulated. On the other hand, PYGB was downregulated. (D) Glucose uptake was significantly lower in GLUT-1 KO astrocytes. (E) From astroglial lactate transporters, MCT1 mRNA levels were decreased while MCT4 expression was unchanged. GFP: Green fluorescent protein; GLUT: Glucose transporter; SGLT1: sodium glucose cotransporter 1; MCT: Monocarboxylate Transporter; PEPCK: phosphoenolpyruvate carboxykinase; PYGB: brain glycogen phosphorylase; Pdk2: Pyruvate-Dehydrogenase Kinase Isoform 2; Me1: malic enzyme 1; P-values: **** p<0.001; ** p<0.01; * p<0.05*

However, an upregulation of another pyruvate-supplying enzyme PEPCK and a downregulation of the brain glycogen phosphorylase (PYGB), responsible for glycogen breakdown, was detected (Fig. 22C), suggesting a potential energetic compensation via

gluconeogenesis instead of glycogenolysis (Fig. 22C). Related to glucose uptake, KO astrocytes showed a significant reduction, although it was not totally abolished (Fig. 22D). Analysis of astroglial lactate transporter expression showed lower MCT1 mRNA transcript levels in GLUT-1 KO astrocytes while MCT4 expression did not change (Fig. 22E).

I next conducted extracellular flux analyses using the Seahorse XF24 instrument to determine the dynamic metabolic consequence of the loss of GLUT-1. Interestingly, basal respiration, measured by oxygen consumption, was augmented in GLUT-1 KO astrocytes (Fig. 23A and 23C), which is in line with a blunted glycolysis, measured by extracellular acidification rate (ECAR) (Fig. 23B and 23D). As the detected proton increase in the medium that is measured for the quantification of ECAR correlates with lactate release, it can be assumed the latter is also reduced.

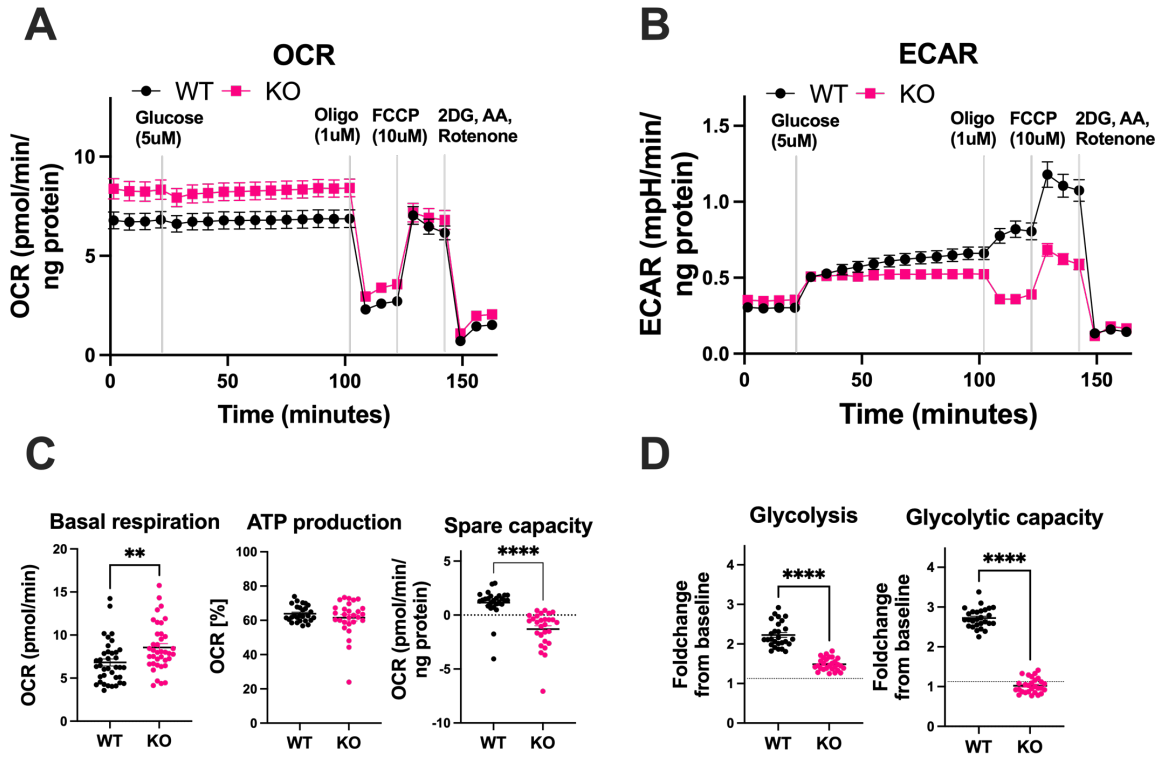

Figure 23 – GLUT-1 KO astrocytes are less metabolically flexible

*(A, C) GLUT-1 KO astrocytes (KO) could not increase ECAR at the same rate as WT astrocytes (WT) in response to 5µM glucose which is represented by a blunted glycolysis, and after inhibition of ATP synthase GLUT-1 KO astrocytes could not compensate by increasing glycolytic rate visualized as glycolytic capacity. (B, D) GLUT-1 KO astrocytes have an increased basal oxygen consumption rate, the basal respiration, which is significantly different. The ATP production is maintained, however, a metabolic deficit could be discovered calculating the spare capacity.WT: wildtype; KO: knockout; Oligo: Oligomycin; FCCP:; 2DG: 2-deoxyglucose; AA: Antimycin A; ECAR: extracellular acidification rate; OCR: oxygen consumption rate; P-values: **** p<0.001; ** p<0.01*

Specifically, I found that glycolysis of GLUT-1 KO astrocytes could not be elevated by the blockage of ATP-synthase by oligomycin, indicating the maximum has been reached. Furthermore, the displayed decrease in glycolytic capacity to produce energy suggests a mismatch between uptake and demand (Fig. 23D). While the ATP production by the electron

transport chain was maintained, GLUT-1 KO astrocytes exhibited no spare capacity (Fig. 23C). Taken together, these results highlight that the lack of GLUT-1 in astrocytes reduces glycolysis and glycolytic capacity, an effect that is compensated by an increased basal respiration.

3.3.2 Primary astrocytes lacking GLUT-1 rely on glutamate as fuel source

I then questioned whether the reduced utilization of glucose observed in GLUT-1 KO astrocytes affected the utilization of glutamate in these cells. Interestingly, GLUT-1 KO astrocytes had significantly increased their dependency on glutamate while reducing their dependency on glucose (Fig. 24A). Even though the capacity to use glucose is no different from control astrocytes, I observed a trend towards an increased capacity to use glutamate, which could hint towards a change in the intracellular metabolic machinery (Fig. 24B).

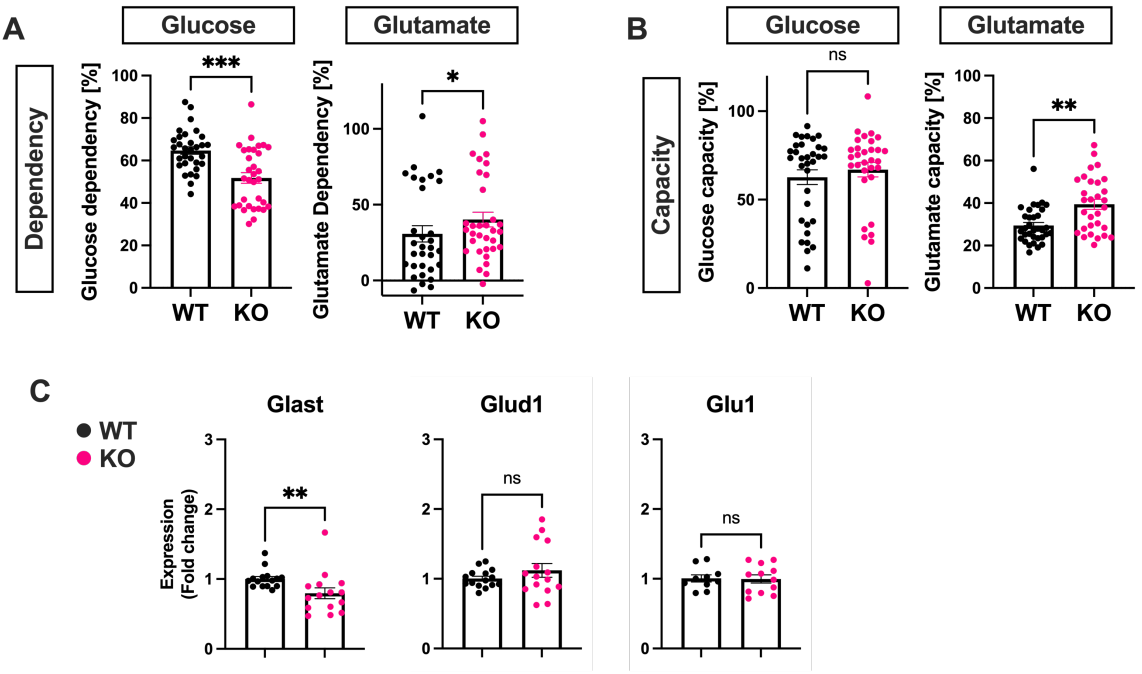

Figure 24 – GLUT-1 knockout astrocytes rely on metabolizing glutamate

*(A) Primary astrocytes lacking GLUT-1 have a reduced dependency on glucose while they increasingly depend on glutamate. (B) The capacity to use glucose is unchanged, however, there is a trend towards an increased capacity to utilize glutamate as a fuel in GLUT-1 KO primary astrocytes. (C) Enzymes involved in glutamate transport and metabolism are not changed (Glud1, Glu1), Glast expression is also decreased. WT: wildtype; KO: knockout; Glast: Glutamate Aspartate Transporter; Glud1: glutamate dehydrogenase 1; Glu1: glutamine synthetase; P-values: *** p<0.001; ** p<0.01; * p<0.05; ns: not significant*

To investigate if changes in glutamate metabolism resulted from upregulation of the respective machinery, I checked the expression of several genes involved such as GLAST, which is highly expressed in astrocytes and responsible for transporting glutamate into the cell (Huang et al., 2023). However, GLAST expression was reduced in astrocytes devoid of GLUT-1, therefore it would rather counteract the increased capacity to metabolize glutamate and the decrease of glucose dependency (Fig. 24C). Further important enzymes in glutamate metabolism are

glutamate dehydrogenase 1 (Glud1/Gdh), which deaminates glutamate to alpha-ketoglutarate to enter the citric acid cycle for metabolization, and glutamine synthetase (Glu1/GS), which catalyzes the production of glutamine from glutamate. Both enzymes were similarly expressed in WT and KO astrocytes, showing they do not mediate the changes in glutamate metabolism (Fig. 24C). Overall, a lack of GLUT-1 in astrocytes increases glutamate metabolism without obvious changes in the expression of the necessary enzymes.

3.3.3 The loss of GLUT-1 in MBH astrocytes elevates basal intracellular Ca^{2+} activity leading to an insensitivity to glucoprivation

Ex vivo brain preparations from GLUT-$1^{i\Delta astro/GLAST+}$ mice and littermate controls were used to investigate whether astroglial Ca^{2+} activity in the MBH is modulated by GLUT-1. This assessment involved employing Fluo-4 as a Ca^{2+} indicator, combined with sulforhodamine 101 (SR101) serving as an astrocytic marker (Fig. 25A). In the presence of tetrodotoxin (TTX) to block neuronal interference, we observed that MBH astrocytes of mice lacking astrocytic GLUT-1 showed a higher frequency of Ca^{2+} events than control astrocytes under basal conditions (Fig. 25B-25D).

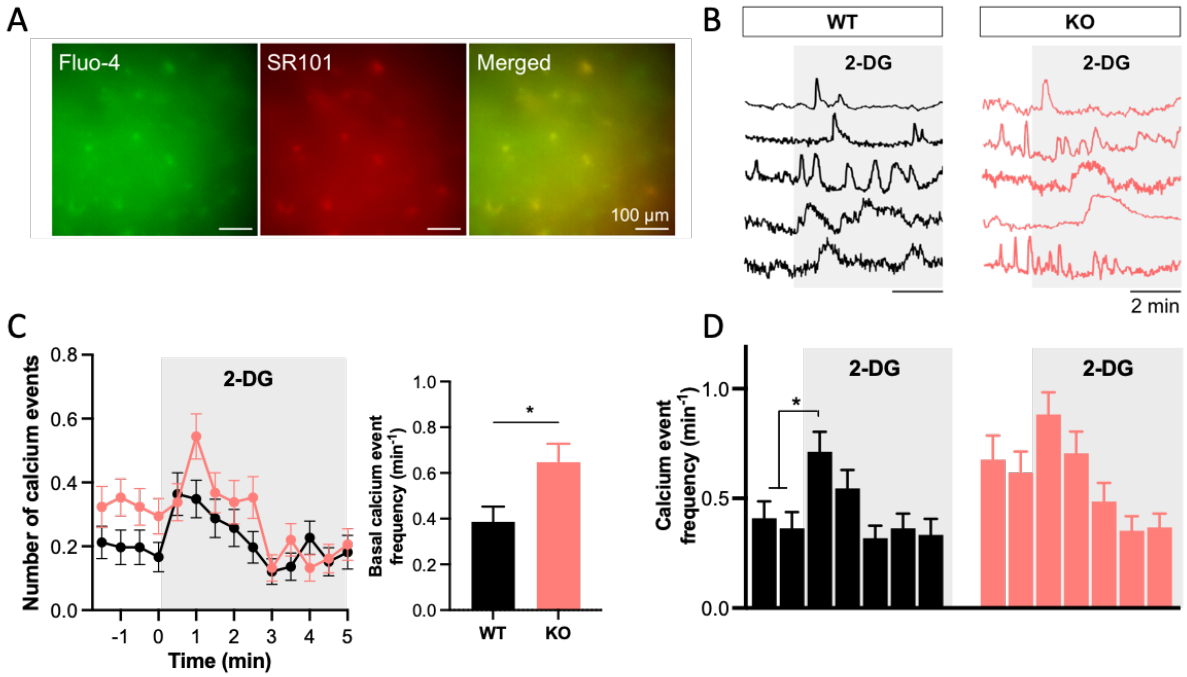

Figure 25 – Increased astrocytic Ca^{2+} activity in ex vivo brain slices of GLUT-$1^{i\Delta astro/GLAST+}$ mice

*(A) The astrocytes in MBH containing brain slices were labeled with sulforhodamine 101 (SR101) while Ca^{2+} activity can be visualized via the Ca^{2+} indicator Fluo-4 (B) Exemplary Ca^{2+} events of wildtype (WT, in black) and GLUT-1 knockout (KO, in red) astrocytes in brain slices in response to 10mM 2DG (grey area). (C) Number of Ca^{2+} events in WT (n=66, N=4) compared to KO astrocytes (n=68, N=5) before and after 2DG perfusion. The basal Ca^{2+} activity is significantly higher in GLUT-1 KO astrocytes while (D) the perfusion of 2DG only results in a significant increase of Ca^{2+} event frequency/min in WT astrocytes. (data obtained in collaboration); P-values: * p<0.05*

Then, astrocyte activity was studied after bath-applying 2DG to mimic glucopenia by means of recording Fluo-4. While SR101+ astrocytes of control mice significantly increased the number

of Ca^{2+} events upon perfusion with 2DG, such increase was not observed in astrocytes without GLUT-1 (Fig. 25B-25D).

In sum, GLUT-1 in astrocytes, especially in the hypothalamus, is required for functional regulatory properties of astrocytes in regard to systemic glucose homeostasis in conditions of hyper- and hypoglycemia. Disruption of regulation of glucose homeostasis in astroglial GLUT-1 KO mice is most likely due to metabolic adaptions within astrocytes leading to an increased basal activation, that does not allow further activation in acute changes of glucose availability. More research needs to be conducted to investigate changes in gliotransmitter release and the impact on neuronal activity.

4 Discussion

4.1 Improvement of glucose tolerance by OT receptor signaling

Glucose homeostasis is tightly regulated by brain-periphery communication through humoral, nutrient-mediated, immune, and nervous system signaling pathways. OT and OTR agonists have been shown to improve glucose tolerance in lean, obese and diabetic rodents (Zhang et al., 2013, Maejima et al., 2011, Maejima et al., 2015, Elnagar et al., 2022, Snider et al., 2019) and humans (Zhang et al., 2013, Klement et al., 2017). However, the exact mechanism of OT action concerning its effects on glucose tolerance remains to be elucidated. Studying different OTR KO mouse models and routes of OT administration, I demonstrated that central and peripheral OT signaling improves glucose tolerance through distinct pathways. While peripherally given OT seems to exclusively act through OTR signaling in pancreatic β-cells, intranasally administered OT seems to affect glucose homeostasis independent of insulin secretion.

4.1.1 Peripheral and central OT signaling improve glucose tolerance independently and by distinct mechanisms

In line with previous studies interested in *in vivo* and *ex vivo* pancreas (Snider et al., 2019, Maejima et al., 2015, Bobbioni-Harsch et al., 1995, Gao et al., 1991, Lee et al., 1995), I confirmed improved glucose tolerance by OT-induced insulin secretion, whether this was achieved through chemogenetically-induced endogenous OT release via the pituitary, or via s.c. peripheral administration of OT. Additionally, I further confirmed in isolated islets that the synergistic effect of OT on glucose-induced insulin secretion depends on its receptor, since OTR KO islets did not respond to the addition of OT. This result is in contrast to previous findings in *ex vivo* pancreas, which linked OT-induced insulin secretion to OT signaling via the more unspecific vasopressin receptor V1b (Lee et al., 1995). However, a β-cell specific KO of OTR completely abolished the effect of s.c. administered OT on glucose tolerance and insulin secretion, proving that OTR-specific signaling in the pancreas is responsible for the observed glucoregulatory improvements. These results also suggest that the findings previously made in *in vitro* studies supporting a direct effect of OT on glucose uptake in cardiomyocytes, skeletal muscle cells, and adipocytes (Florian et al., 2010, Lee et al., 2008), might not be as relevant *in vivo*.

Nevertheless, i.n. administered OT was able to improve glucose tolerance in both control and $OTR^{\Delta Ins1}$ animals to the same extent, without any detectable change in insulin secretion. Thus, we could demonstrate that central OT signaling improves glucose tolerance via a mechanism that is completely independent from peripheral OT effects. As described in the introduction, projections to various tissues can be activated to induce glucoregulatory changes in response to central sensing of the glucose status. Other studies have shown effects of OT treatment in

other tissues than the pancreas, e.g., a 7-day OT treatment normalized hepatic PEPCK expression in diabetic (db/db) mice (Elnagar et al., 2022), while a 12-week chronic OT administration improved cardiomyopathy in diabetic (db/db) mice (Plante et al., 2015), and a 14-day OT i.c.v. infusion increased oxidation of fatty acids (Deblon et al., 2011). However as, in these studies, either OT was administered was peripherally, or increased levels of circulating OT was detected, a direct effect of OT in the respective tissues cannot be excluded. Future investigations should evaluate which tissues and pathways are responsible for the effect of central OT signaling on peripheral glucose tolerance.

4.1.2 The loss of OTR in the VMH induces glucose intolerance and insulin resistance

In both *ex vivo* brain slice preparations and FDG-PET studies, VMH neurons displayed an increased activity in response to OT. Therefore, I set out to investigate the effect of VMH-specific OTR KO on the glucoregulatory effect of intranasally administered OT. Intriguingly, I observed that $OTR^{\Delta VMH}$ mice were glucose intolerant and insulin resistant, as demonstrated by an increase in HOMA-IR. Thus, OTR signaling in the VMH seems to be crucial for glucose homeostasis. However, intranasally administered OT still improved glucose tolerance, suggesting that additional brain areas contribute to the glucoregulatory effect of central OT signaling. This hints towards OTR signaling in other brain regions contributing to the effect of OT on glucose homeostasis. Studies have shown that i.n. administered OT reaches the striatum, the amygdala, the orbital cortex, the PVN, and the brain stem, among others (Maejima et al., 2015, Lee et al., 2020, Smith et al., 2019). As described in the introduction, OTRs are found in the PVN and several hindbrain nuclei, which are also involved in the regulation of glucose homeostasis (Kerem and Lawson, 2021, Jurek and Neumann, 2018, Routh et al., 2012). Interestingly, in the amygdala, another region where OTR is expressed, glucose sensing neurons have been shown to modulate glucose homeostasis as well (Devarakonda et al., 2018). Therefore, OT could possibly play a glucoregulatory role in those regions. Nevertheless, it is essential, among others, to explore co-expression of OTR and different players of the glucoregulatory machinery, or the impact of infusing OT directly into the relevant areas in order to substantiate this hypothesis.

4.1.3 Effect of OT in diet-induced obesity

As shown in several studies on rodents (Maejima et al., 2011, Maejima et al., 2015, Snider et al., 2019) and humans (Zhang et al., 2013, Klement et al., 2017, Ott et al., 2013), OT treatment significantly reduces food intake, leads to body weight loss, and improves glucose tolerance, all while displaying minimal side effects. These characteristics make it a potential candidate as an anti -obesity or -diabetes medication. Interestingly, I found that mice fed a HFHS diet for six weeks did not respond to i.n. OT. This hints towards a disruption of central OT signaling induced by this metabolic challenge. Accordingly, two human studies performed by M.

Hallschmid's group showed no effect of OT nasal spray on glucose tolerance and insulin levels in obese men (Brede et al., 2019), as well as no effect on obese diabetic patients (unpublished data, for poster abstract: (Röhm et al., 2023)). Interestingly, in DIO rats, glucose-induced sympathetic activity is increased compared to control animals that do not develop obesity in response to the diet (Levin and Sullivan, 1987, Levin and Sullivan, 1989). It was also observed that while glucose infusion resulted in increased cFos immunoreactivity in the PVN, VMH, dorsomedial nucleus, and ARC in control animals, this effect on neuronal activity was blunted in DIO rats (Levin et al., 1998). This phenomenon might be related to enhanced activation of the SNS. Indeed, central OT signaling has been suggested to act, at least partly, through sympathetic activation, e.g., in BAT thermogenesis (Roberts et al., 2017). Therefore, disrupted glucose sensing and elevated sympathetic activity in DIO in mice might lead to the disruption of the glucoregulatory effects of OT. Moreover, a recent human study examining intrahepatic nerve fiber endings revealed a reduction in both total and sympathetic nerve fibers in non-alcoholic steatohepatitis (Mizuno et al., 2021). This implies an alteration in innervation associated with the advancing inflammatory state in obesity. Hence, the loss of the central OT effect in HFHS-diet fed mice could be attributed to defective innervation, providing a hypothesis that warrants thorough investigation.

However, I showed that s.c. OT injection still led to increased glucose tolerance in HFHS diet-fed mice, comparably to that of lean controls. Additional studies have shown the impact of subcutaneously injected OT in prediabetic and diabetic rats. A 7-day treatment resulted to notable improvements in blood glucose, insulin, HOMA-IR, and lipid profile. Moreover, there was a reduction in tissue damage in the pancreas, liver, and kidneys, underscoring the continued efficacy of peripheral OT signaling (Elnagar et al., 2022). Moreover, a 12-week chronic OT delivery via osmotic pumps improved fasting glucose, glucose tolerance, and insulin sensitivity in diabetic (db/db) mice compared to saline treated controls (Plante et al., 2015). Interestingly, chronic central infusion (i.c.v, 14d) of OT in DIO rats was shown to induce fat oxidation and weight loss, as well as increased glucose tolerance, and insulin sensitivity (Deblon et al., 2011). However, elevated plasma OT was found, so the positive outcome could potentially be due to peripheral effects of OT (Deblon et al., 2011). While an exploration of the impact of chronically intranasally administered OT on glucose tolerance is worth considering, both my findings and existing research suggest that peripheral administration may be necessary compared to an easy-to-use nasal spray. Interestingly, looking at OT as an anti-obesity or anti-diabetic drug, it has been associated with reward and self-control over food intake (Kerem and Lawson, 2021), thus it might beneficially act against the drive to consume high-calorie, high reward foods. Studies in mice indicate that genetic loss of OT results in increased sucrose intake (Amico, 2005), whereas the administration of exogenous OT, whether peripherally (Olszewski et al., 2010, Rehn et al., 2022) or centrally (Mullis et al., 2013),

reduces sucrose intake. In humans, intranasal OT application has also been shown to decrease the consumption of reward-associated sweet snacks (Ott et al., 2013). Additionally, OT has been shown to promote energy expenditure by enhancing lipid metabolism, thermogenesis, and physical activity (Ong et al., 2017, Deblon et al., 2011, Roberts et al., 2017, Noble et al., 2014), presenting an additional beneficial effect in a state of excess body weight. Recent advancements in pharmaceutical approaches of treating diabetes and obesity involve the development of dual- or tri- agonists, enabling the simultaneous targeting of multiple signaling pathways. These innovations have showcased notable efficacy in addressing these health issues. For example, the approved GLP-1 and GIP dual-agonist tirzepatide has demonstrated superiority over commonly used GLP-1 mono-agonists and various insulin treatments in terms of lowering blood glucose, inducing weight loss, and ensuring safety (Zhou et al., 2023, Rosenstock et al., 2021, Del Prato et al., 2021, Frias et al., 2021). Thus, through its diverse glucoregulatory pathways and notable effects on the reward system and voluntary sugar intake, incorporating OT into combinatory treatment approaches or a multiagonism strategy holds promise for further therapeutic exploration.

Intrigued by the central resistance to OT effects in mice fed a hypercaloric diet, I overexpressed OTR in the VMH of 6-week-old HFHS fed-mice, but this did not rescue the disrupted OT signaling when OT was intranasally delivered. One explanation might be that the promoter used to drive the overexpression of OTR in neurons targets not only the neurons that readily express OTR, but all neurons. Indeed, the VMH harbors different neuronal subsets that are differentially involved in the regulation of hyper- or hypoglycemia. Therefore, it is possible that inducing the overexpression of the same OTR in two groups of neurons, whose activation has contradictory effects, leads to the effect of i.n. OT on blood sugar levels being simply canceled out.

Intriguingly, i.n. administration of OT to HFHS diet-fed mice becomes more effective with β-cell-specific KO. This observation hints towards a regulatory pathway via a feedback loop. Schwartz and colleagues suggested that islet-mediated and brain-mediated control of blood glucose are closely connected and compensate each other in the case that one is defective (Schwartz et al., 2013). Thus, a reduction in β-cell function and/or insulin secretion through β-cell-specific OTR KO might lead to a sensitization of the central glucoregulatory system. Vagal sensory neurons, emanating from the NTS, establish a direct connection between the pancreas and the brain (Makhmutova et al., 2021). The probable signaling molecule responsible is serotonin, which may even communicate information about the β-cell-secretory state to central structures, as it is co-released with insulin (Makhmutova et al., 2021). However, the precise mechanism by which β-cell specific OTR KO enhances central OT effects requires further investigations in future experiments.

4.2 Regulation of systemic glucose homeostasis by astroglial GLUT-1

Hypoglycemia is a life-threatening condition that is especially problematic for the brain as glucose is its major energy substrate. Thus, glucose homeostasis is tightly controlled, and blood glucose levels are monitored by glucose sensing mechanisms in the brain. Detection of low blood glucose results in the activation of a counterregulatory response. In diabetic patients treated with exogenous insulin, these counterregulatory mechanisms are dampened after recurrent hypoglycemic events. This leads to hypoglycemia unawareness, a neuroglycopenia without autonomic warning signs like sweating, palpitation, or tremors, which can be followed by hypoglycemia-associated autonomic failure and brain damage (Martin-Timon and Del Canizo-Gomez, 2015).

Strikingly, two distinct mouse models with deficiency of GLUT-1 in astrocytes both exhibit a blunted response to insulin and an exaggerated glucose production in response to 2DG-induced glucopenia. This underscores the involvement of astrocytic GLUT-1 in the regulatory processes of maintaining blood glucose homeostasis. Additionally, a mouse model devoid of GLUT-1 in MBH astrocytes specifically developed glucose intolerance and insulin insensitivity. This result suggests a potential role of astrocytes in the counterregulatory response to glucoprivation.

4.2.1 Astroglial GLUT-1 deletion interferes with peripheral counterregulation by affecting autonomic innervation

Artificially inducing hypoglycemia/glucopenia triggers an intracellular energy crisis, which prompts an increase in blood glucose through endogenous glucose production in the liver, commonly involving glycogenolysis and/or gluconeogenesis. This process is stimulated by direct innervation or by hormonal cues, including glucagon, corticosteroids, and catecholamines (Chevrier et al., 1982, Rappaport et al., 1982, Ishihara et al., 2009). In my studies, glucagon and corticosterone levels increased in response to 2DG, however, no significant differences could be detected between groups. This rules them out as putative contributors to the observed differences in glucose output.

Interestingly, 2DG retains its ability to interfere with SNS activity in adrenalectomized animals, indicating the involvement of direct innervation (Rappaport et al., 1982). It has been demonstrated that hexamethonium, a nicotinergic acetylcholine antagonist and an autonomic nervous system blocker, prevents hyperglycemia following injection of 2DG into the lateral cerebral ventricle (Yamamoto et al., 1988). When I injected hexamethonium and 2DG simultaneously, the difference in blood glucose output seen between mice lacking GLUT-1 in astrocytes and controls was eliminated. This suggests that the observed changes in HGP are due to the differential output of innervating nerves.

Looking at liver metabolism, analyzing of the gene expression of enzymes critical for hepatic gluconeogenesis and glycogenolysis (PEPCK, G6Pase, GYPL) did not reveal significant

differences between animals lacking astroglial GLUT-1 and their counterparts. However, since the changes in HGP were observed at 30 minutes and 60 minutes, with tissues collection occurring at 90 minutes, examining gluconeogenic machinery at an earlier timepoint and investigating protein levels could provide clarity on the underlying mechanism. Additionally, other factors influencing HGP could be explored. FOXO1 signaling is either suppressed or stabilized by phosphorylation, depending on the different signaling cascades of insulin and glucagon, respectively (Wu et al, 2018), suggesting FOXO1 as a potential target for further investigation. Furthermore, the upstream regulator of FOXO1, PPARχ coactivatior-1 (PGC-1α) is upregulated in the liver during fasting to provide energy substrate through the stimulation of fatty acid oxidation (Finck and Kelly, 2006). Operating independently of this pathway is the regulation of gluconeogenesis by STAT3 (Inoue et al., 2004). Hepatic STAT3 deficiency leads to insulin resistance and upregulation of gluconeogenic genes. Given the described mechanism for how hypothalamic insulin signaling affects HGP through hepatic STAT3 signaling (see introduction and figure 4) (Inoue et al., 2006), it emerges as a promising target for future investigations.

4.2.2 Counterregulatory signaling in the brain

While the observed metabolic changes are of peripheral nature, I see the most pronounced phenotypical changes when the astroglial GLUT-1 KO is limited to the MBH. Using intracellular Ca^{2+} imaging to assess astrocyte activity, we have observed that the lack of GLUT-1 in GLAST+ cells is associated with an increase in the basal activity of MBH astrocytes in *ex vivo* brain slices. Interestingly, when exposed to the glucoprivic agent 2DG, these astrocytes did not exhibit a further increase in Ca^{2+} activity, in contrast to the response observed in brain slices from control mice. This augmented basal activity, together with the inability to respond to metabolic cues like glucoprivation, might be responsible for the disrupted signaling to the liver. The consequences of the observed changes in astroglial activity are not completely clear. However, astrocytes are secretory cells, and in response to metabolic cues like insulin signaling, astrocytes respond with gliotransmitter release such as ATP, which results in changes in neuronal activity, and consequently, behavioral adaptions (Cai et al., 2018). Interfering with astrocyte sensing of metabolic signals, e.g., deleting receptors such as the leptin receptor or the IR, can impair energy homeostasis regulation through changes in activity of hypothalamic melanocortin neurons via remodeling of synapses (Kim et al., 2014, Garcia-Caceres et al., 2016). In particular, astroglial glucose uptake appears to play a central role, as it is controlled by IR and IGF-1R signaling, and any disturbances in this process can lead to disruptions in metabolic control (Garcia-Caceres et al., 2016, Hernandez-Garzon et al., 2016). A knockdown (via short hairpin RNA) of another glucose transporter, SGLT1, in the VMH ($SGLT1^{VMH}$), led to an increased HGP (Fan et al., 2015), which I also observed in my mouse

models lacking GLUT-1 in astrocytes. However, the increase in glucagon and epinephrine was not reproduced in mice lacking astroglial GLUT-1. The phenotype observed in $SGLT1^{VMH}$ mice could be, at least partly, due to astrocytes, as SGLT1 staining colocalized not only with some neuronal markers, but also with GFAP (Fan et al., 2015). Interestingly, SGLT1 mRNA is upregulated in primary GLUT-1 KO astrocytes, possibly as a compensatory effect.

The neuronal population and/or circuit involved in the exaggerated HGP in response to glucoprivation in the astroglial GLUT-1 KO models is yet to be identified. As the KO of astrocytic GLUT-1 is limited to the MBH in the $GLUT\text{-}1^{AVV.Gfa.iCre}$ model, it can be assumed that astrocytes and neurons in those hypothalamic regions are at least partly responsible for the observed phenotype. Several studies investigating the effect of activity changes in MBH neuronal populations on glucose homeostasis reveal similar glucoregulatory responses as my astroglial GLUT-1 KO models (Faber et al., 2018, Meek et al., 2016, Flak et al., 2020, Khodai et al., 2018). Therefore, these neuronal populations could be involved in the glucoregulatory changes seen in astroglial GLUT-1 KO mice. Within the hypothalamus, central administration of 2DG has been shown to increase neuronal activity, detected by cFos gene expression, including in the ARC, in which 20% of the activated neurons were shown to be NPY-positive (Minami et al., 1995). Interestingly, i.c.v. administration of NPY impedes the inhibitory action of insulin on HGP via sympathetic input, inferring an involvement of AgRP/NPY-expressing neurons and NPY release in the counterregulatory response (van den Hoek et al., 2008). Furthermore, optogenetic activation of $SF1^{VMH}$ neurons projecting to the aBNST led to a counterregulatory response including increased blood glucose, plasma corticosterone and glucagon, and increased hepatic PEPCK and G6Pase expression (Meek et al., 2016). I did not observe changes in the expression of hepatic gluconeogenic genes in the astroglial GLUT-1 KO models; however, optogenetic activation is described as supraphysiological compared to naturally induced neuronal activation (Khodai and Luckman, 2021). Thus, astroglial changes induced by GLUT-1 KO might only contribute to certain aspects of the observed phenotype. Similarly, optogenetic activation of VMH^{CCKBR} neurons induced hyperglycemia and increases in corticosterone and catecholamines, however without changes in glucagon (Flak et al., 2020). Interestingly, silencing of both $SF1^{VMH}$ and VMH^{CCKBR} neurons impaired the counterregulatory response, underscoring their relevance (Flak et al., 2020, Meek et al., 2016). Furthermore, optogenetic activation of NOS1-expressing VMH neurons results in severe hyperglycemia and in elevated glucagon and corticosterone levels compared to controls (Faber et al., 2018). However, the activation had no significant effect on an insulin-induced counterregulatory response, which is not the case in mice with astroglial GLUT-1 KO. The activation of $PACAP^{VMH}$ neurons did not affect blood glucose but induced glucose intolerance, which would be comparable to the $GLUT\text{-}1^{AVV.Gfa.iCre}$ model (Khodai et al., 2018). An explanation could stem from the observed decreases in plasma insulin levels in mice with

activated PACAP^{VMH} neurons, which have not been investigated yet in GLUT-1 KO mouse models. All these neuronal subsets need to be activated to induce an increase in HGP (Meek et al., 2016, Khodai et al., 2018, Faber et al., 2018). Therefore, an involvement of one of those neuronal populations in the overcompensation of HGP in astroglial GLUT-1 KO mice in response to glucoprivation would require that the lack of GLUT-1 in astrocytes leads to an increased activity in one or more of them. Interestingly, another neuronal population in the VMH expressing vGLUT2 exhibited a suppression of neuronal activity persisting up to 45min after injection of insulin or 2DG (Rawlinson et al., 2022). This population seems to be crucial for counterregulation against hypoglycemia, as a KO of vGLUT2 in SF1 neurons prevents HGP, glucagon release, and expression of gluconeogenic enzyme PEPCK (Tong et al., 2007). In this case, the lack of GLUT-1 in astrocytes would require to inhibit those neurons, which might be explained by a decreased in lactate release and an increase in glutamate metabolism. However, future experiments have to clarify changes in neuronal activity in astroglial GLUT-1 KO mice in the MBH to further investigate the circuits involved.

Comparing the two mouse models lacking GLUT-1 in astrocytes, GLUT-1$^{AVV.Gfa.iCre}$ mice, where the astroglial GLUT-1 KO limited to the MBH, exhibit a more pronounced phenotype, with a stronger counterregulatory response to glucoprivation and additional glucose intolerance and insulin resistance. Firstly, it needs to be considered that two different populations of astrocytes were targeted. While they partly overlap, both populations are comprised by distinct subtypes that might have functional differences. Recent findings suggest that astrocytes are functionally specialized depending on the considered specific brain region and neuronal circuits, while a high plasticity allows them to adapt to environmental changes (Holt, 2023). Our research group already observed in previous studies with other genetic targets, that mouse models relying on different astrocytic markers are not exchangeable ((Lutomska et al., 2022) and unpublished data). Especially in response to metabolic challenges, such as HFHS diet feeding, we noted variations in the expression of various astrocyte marker genes and distinct transcriptional adaptions in astrocytes, contingent on the brain region (Lutomska et al., 2022). Another explanation could be that the GLUT-1$^{i\Delta astro/GLAST+}$ model is targeting more astrocytes within more brain structures. Targeting astrocytes throughout different brain regions might imply complex interactions between different neuronal circuits mitigating the consequences of the astroglial GLUT-1 KO. Another area involved in glucoregulation, including counterregulation to hypoglycemia, is the hindbrain. Interestingly, 2DG administration in the 4V led to increased neuronal activity in the ARC and PVN, suggesting a close communication of the hindbrain and hypothalamus in response to glucoprivation (Sato et al., 2021). While chemogenetic activation of neurons in the VLM and NTS was demonstrated to induce a counterregulatory response leading to blood glucose elevations (Li et al., 2018, Zhao et al., 2017, Boychuk et al., 2019), activation of A1, C1, and A2 neurons by insulin-induced hypoglycemia was largely blunted by

L-lactate infusion in the 4V (Shrestha et al., 2014). This suggests that astroglial lactate release can interfere with counterregulatory signaling in these areas, which I observed to be reduced in primary astrocytes lacking GLUT-1. Lactate release also led to a normalization of catecholamines in different hypothalamic nuclei (Shrestha et al., 2014). Hence, changes in lactate release in the hindbrain can affect neuronal signaling in the hypothalamus and its impacts on peripheral glucose homeostasis. Hence, exploring the adaptions in astroglial metabolism triggered by GLUT-1 KO could provide additional insights into the mechanistic underpinnings of astroglial effects on neuronal signaling and subsequent phenotypes, as discussed in the following subsections.

4.2.3 Effects of metabolic changes in astrocytes

Investigating metabolic changes in primary astrocytes lacking GLUT-1 revealed a decrease in glycolysis detected by ECAR measurements. Those measurements depend on the release of protons (detected change in pH) and lactate. Therefore, a decrease in ECAR also indicates a reduction in lactate release. Interestingly, it has been shown that disruptions of astroglial metabolism leads to changes in affective behavior and spatial memory that can be reversed by lactate injection (Jouroukhin et al., 2018). Moreover, inhibition of astroglial lactate release results in a reduction in diabetes-induced inflammatory markers in the hypothalamus and in decreased food intake in streptozotocin-induced diabetic mice, which hints towards an involvement of astroglial lactate in the regulation of systemic glucose homeostasis (Rahman et al., 2020). Additionally, both lactate release by astrocytes and trafficking of lactate by the astrocyte network were demonstrated to be necessary for the functionality of hypothalamic neurons, especially during glucoprivation (Clasadonte et al., 2017). Remarkably, blunted GLUT-1 translocation seems to limit glucose uptake and lactate production and, thus, affect neuronal survival (Muraleedharan et al, 2020). Intriguingly, Borg and colleagues observed that perfusing the VMH with L-Lactate results in a decreased counterregulatory endogenous glucose production in response to hypoglycemia (Borg et al., 2003). This observation suggests that lactate availability is interfering with counterregulatory signaling. Indeed, Lam and colleagues could show that the negative feedback of hypothalamic glucose on HGP depends on its conversion to lactate (Lam et al., 2005).

A conceivable reason for the reduction of hypoglycemia-induced counterregulation is that the release of lactate by astrocytes is a necessary step to provide it as an energy substrate to neurons, as discussed by the astrocyte-neuron-lactate shuttle theory. On the other hand, lactate could also act as a signaling molecule. In the adipose tissue, the knockout of G-protein coupled lactate receptor GPR81/HCR1 demonstrated its necessity for insulin-induced inhibition of lipolysis and therefore shining light on its function as an autocrine and paracrine signaling molecule (Ahmed et al., 2010). The importance of lactate as a signaling molecule

has also been shown in the brain, as HCR1-expressing pericyte-like cells mediate cerebral angiogenesis in response to augmented lactate levels (Morland et al., 2017).

Generally, exposing primary astrocytes acutely to high glucose conditions results in increased lactate release (Rahman et al., 2020). Therefore, lactate availability might be recognized as a signal for glucose availability by other cell types, including neurons. Chronically challenging primary astrocytes with high concentrations of glucose led to higher glucose uptake, greater glycogen stores, and an increased probability for stored glycogen to be used in a situation of glucose shortage (Staricha et al., 2020).

Another way that metabolic changes in the brain influence peripheral homeostasis has been impressively demonstrated by Karaca and colleagues, who showed that a shutdown of glutamate oxidation in the brain via a glutamate dehydrogenase knockout led to increased glucose uptake in the brain and augmented peripheral energy production by sympathetic nervous system activity (Karaca et al., 2015). Vice versa, the knockout of GLUT-1 in astrocytes might be compensated by increased uptake and metabolization of glutamate. I observed an elevated basal respiration of GLUT-1 KO primary astrocytes accompanied by reduced glycolysis, which suggests a compensatory oxidative respiration. Moreover, I showed that GLUT-1 KO astrocytes show both an increased dependency on glutamate and a greater capacity to metabolize glutamate. Also, others show that astrocytes change metabolic properties like basal respiration in response to low glucose availability (Weightman Potter et al., 2022). Interestingly, the addition of glutamate prevented most adaptions of astrocytes to acute and recurrent low glucose availability (Weightman Potter et al., 2022), showing that astrocytes can, at least partly, circumvent glucose deficiency by metabolizing glutamate. In summary, the uptake and release of metabolites, which may also act as signaling molecules for glucose availability, are likely to play a role in astrocyte-neuron communication and peripheral glucoregulation. The use of new approaches such AAVs driving the expression of lactate or glutamate sensors should be able shine light on the fluctuation of those molecules.

4.2.4 Astroglial glucose metabolism as part of hypoglycemia detection

Through the overexpression of GLUT-1 in astrocytes, my aim was to investigate whether systemic glucose homeostasis could be regulated in a manner opposite to what I demonstrated in astroglial GLUT-1 KO mice, and potentially restore impaired glucose regulation in mice subjected to HFHS or with diabetes. However, I could not observe any effect of astroglial GLUT-1 OE on glucose homeostasis. An explanation could be that the astroglial mechanism affecting hepatic glucose output and insulin resistance is specifically designed to sense and respond to reduced glucose availability. For example, it has been shown that fasting increases sensitivity of NPY neurons to hypoglycemia by depolarization (Murphy et al., 2009), which could generally be secondary to astroglial sensing. Interestingly, the NPY neuron sensitizing effect of fasting is blunted by leptin (Murphy et al., 2009), which could explain the weakened

impact of astroglial GLUT-1 KO in DIO mice (data not shown) that have obesity-induced increases in leptin levels. Another explanation could be that both metabolic efficiency and capacity are reduced in astrocytes after long-term exposure to high glucose conditions (Staricha et al., 2020), which may contribute to dysregulated glucose homeostasis in diabetics.

In conclusion, the growing body of evidence supporting the active involvement of astrocytes and other glial cells in the regulation of glucose homeostasis is paving the way for personalized medication strategies tailored to individual patient predispositions clinical profiles. Additional research is essential to fully elucidate how targeting astrocytes can improve blood glucose control and homeostasis.

5 Conclusion

Altogether, the work presented in this thesis shines light on two glucoregulatory pathways which rely on functional circuits localized in the brain, and how interfering with them disrupts glucose homeostasis. Expanding our knowledge of cellular and molecular players involved in glucose intolerance in a diabetic state can help to further improve and fine-tune the treatment of the growing epidemic of both, obesity and diabetes. In this regard, the main findings of this thesis are:

- Peripheral OT increases glucose tolerance via pancreatic OTR receptor specifically, leading to increased insulin release.
- Central OT signaling has distinct and insulin-independent effects on improving glucose tolerance.
- VMH OTR signaling is required for the regulation of glucose homeostasis.
- The glucoregulatory effect of i.n. OT is blunted in mice fed a hypercaloric diet while s.c. OT is still effective.
- Glucose uptake in astrocytes via GLUT-1 is required for adequate counterregulatory response to glucopenia.
- Deletion of GLUT-1 in MBH astrocytes leads to glucose intolerance and insulin resistance.
- Changes in HGP induced by astroglial GLUT-1 deletion are mediated via autonomic innervation.
- Astrocytes lacking GLUT-1 exhibit a higher basal Ca^{2+} activity which prevents a further increase in activity by 2DG stimulation.

VII. List of references

ABI-SAAB, W. M., MAGGS, D. G., JONES, T., JACOB, R., SRIHARI, V., THOMPSON, J., KERR, D., LEONE, P., KRYSTAL, J. H., SPENCER, D. D., DURING, M. J. & SHERWIN, R. S. 2002. Striking differences in glucose and lactate levels between brain extracellular fluid and plasma in conscious human subjects: effects of hyperglycemia and hypoglycemia. *J Cereb Blood Flow Metab,* 22**,** 271-9.

AHMED, K., TUNARU, S., TANG, C., MULLER, M., GILLE, A., SASSMANN, A., HANSON, J. & OFFERMANNS, S. 2010. An autocrine lactate loop mediates insulin-dependent inhibition of lipolysis through GPR81. *Cell Metab,* 11**,** 311-9.

ALMEIDA, A., MONCADA, S. & BOLANOS, J. P. 2004. Nitric oxide switches on glycolysis through the AMP protein kinase and 6-phosphofructo-2-kinase pathway. *Nat Cell Biol,* 6**,** 45-51.

ALTHAMMER, F. & GRINEVICH, V. 2017. Diversity of oxytocin neurons: beyond magno- and parvocellular cell types? *J Neuroendocrinol*.

AMIN, M., WU, R. & GRAGNOLI, C. 2023. Novel Risk Variants in the Oxytocin Receptor Gene (OXTR) Possibly Linked to and Associated with Familial Type 2 Diabetes. *Int J Mol Sci,* 24.

ARAQUE, A., PARPURA, V., SANZGIRI, R. P. & HAYDON, P. G. 1999. Tripartite synapses: glia, the unacknowledged partner. *Trends Neurosci,* 22**,** 208-15.

ARNTFIELD, M. E. & VAN DER KOOY, D. 2011. beta-Cell evolution: How the pancreas borrowed from the brain: The shared toolbox of genes expressed by neural and pancreatic endocrine cells may reflect their evolutionary relationship. *Bioessays,* 33**,** 582-7.

AUER, R. N. 2004. Hypoglycemic brain damage. *Forensic Sci Int,* 146**,** 105-10.

BAK, L. K., SCHOUSBOE, A. & WAAGEPETERSEN, H. S. 2006. The glutamate/GABA-glutamine cycle: aspects of transport, neurotransmitter homeostasis and ammonia transfer. *J Neurochem,* 98**,** 641-53.

BANO, G. 2013. Glucose homeostasis, obesity and diabetes. *Best Pract Res Clin Obstet Gynaecol,* 27**,** 715-26.

BELL, B. B., HARLAN, S. M., MORGAN, D. A., GUO, D. F., CUI, H. & RAHMOUNI, K. 2018. Differential contribution of POMC and AgRP neurons to the regulation of regional autonomic nerve activity by leptin. *Mol Metab,* 8**,** 1-12.

BERGLUND, E. D., LIU, T., KONG, X., SOHN, J. W., VONG, L., DENG, Z., LEE, C. E., LEE, S., WILLIAMS, K. W., OLSON, D. P., SCHERER, P. E., LOWELL, B. B. & ELMQUIST, J. K. 2014. Melanocortin 4 receptors in autonomic neurons regulate thermogenesis and glycemia. *Nat Neurosci,* 17**,** 911-3.

BERGMAN, R. N., PHILLIPS, L. S. & COBELLI, C. 1981. Physiologic evaluation of factors controlling glucose tolerance in man: measurement of insulin sensitivity and beta-cell glucose sensitivity from the response to intravenous glucose. *J Clin Invest,* 68**,** 1456-67.

BERTHOUD, H. R. & JEANRENAUD, B. 1979. Acute hyperinsulinemia and its reversal by vagotomy after lesions of the ventromedial hypothalamus in anesthetized rats. *Endocrinology,* 105**,** 146-51.

BIGGERS, D. W., MYERS, S. R., NEAL, D., STINSON, R., COOPER, N. B., JASPAN, J. B., WILLIAMS, P. E., CHERRINGTON, A. D. & FRIZZELL, R. T. 1989. Role of brain in counterregulation of insulin-induced hypoglycemia in dogs. *Diabetes,* 38**,** 7-16.

BITTAR, P. G., CHARNAY, Y., PELLERIN, L., BOURAS, C. & MAGISTRETTI, P. J. 1996. Selective distribution of lactate dehydrogenase isoenzymes in neurons and astrocytes of human brain. *J Cereb Blood Flow Metab,* 16**,** 1079-89.

BITTNER, C. X., LOAIZA, A., RUMINOT, I., LARENAS, V., SOTELO-HITSCHFELD, T., GUTIERREZ, R., CORDOVA, A., VALDEBENITO, R., FROMMER, W. B. & BARROS, L. F. 2010. High resolution measurement of the glycolytic rate. *Front Neuroenergetics,* 2.

BLEVINS, J. E., GRAHAM, J. L., MORTON, G. J., BALES, K. L., SCHWARTZ, M. W., BASKIN, D. G. & HAVEL, P. J. 2015. Chronic oxytocin administration inhibits food intake, increases energy expenditure, and produces weight loss in fructose-fed obese rhesus monkeys. *Am J Physiol Regul Integr Comp Physiol,* 308**,** R431-8.

BOBBIONI-HARSCH, E., FRUTIGER, S., HUGHES, G., PANICO, M., ETIENNE, A., ZAPPACOSTA, F., MORRIS, H. R. & JEANRENAUD, B. 1995. Physiological concentrations of oxytocin powerfully stimulate insulin secretionin vitro. *Endocrine,* 3**,** 55-9.

BODEN, G. 1997. Role of fatty acids in the pathogenesis of insulin resistance and NIDDM. *Diabetes,* 46**,** 3-10.

BOGDANOV, P., CORRALIZA, L., VILLENA, J. A., CARVALHO, A. R., GARCIA-ARUMI, J., RAMOS, D., RUBERTE, J., SIMO, R. & HERNANDEZ, C. 2014. The db/db mouse: a useful model for the study of diabetic retinal neurodegeneration. *PLoS One,* 9**,** e97302.

BORG, M. A., SHERWIN, R. S., BORG, W. P., TAMBORLANE, W. V. & SHULMAN, G. I. 1997. Local ventromedial hypothalamus glucose perfusion blocks counterregulation during systemic hypoglycemia in awake rats. *J Clin Invest,* 99**,** 361-5.

BORG, M. A., TAMBORLANE, W. V., SHULMAN, G. I. & SHERWIN, R. S. 2003. Local lactate perfusion of the ventromedial hypothalamus suppresses hypoglycemic counterregulation. *Diabetes,* 52**,** 663-6.

BORG, W. P., SHERWIN, R. S., DURING, M. J., BORG, M. A. & SHULMAN, G. I. 1995. Local ventromedial hypothalamus glucopenia triggers counterregulatory hormone release. *Diabetes,* 44**,** 180-4.

BOURNAT, J. C. & BROWN, C. W. 2010. Mitochondrial dysfunction in obesity. *Curr Opin Endocrinol Diabetes Obes,* 17**,** 446-52.

BOUZIER-SORE, A. K., VOISIN, P., BOUCHAUD, V., BEZANCON, E., FRANCONI, J. M. & PELLERIN, L. 2006. Competition between glucose and lactate as oxidative energy substrates in both neurons and astrocytes: a comparative NMR study. *Eur J Neurosci,* 24**,** 1687-94.

BOYCHUK, C. R., SMITH, K. C., PETERSON, L. E., BOYCHUK, J. A., BUTLER, C. R., DERERA, I. D., MCCARTHY, J. J. & SMITH, B. N. 2019. A hindbrain inhibitory microcircuit mediates vagally-coordinated glucose regulation. *Sci Rep,* 9**,** 2722.

BREDE, S., FEHR, S., DALLA-MAN, C., COBELLI, C., LEHNERT, H., HALLSCHMID, M. & KLEMENT, J. 2019. Intranasal oxytocin fails to acutely improve glucose metabolism in obese men. *Diabetes Obes Metab,* 21**,** 424-428.

BROWN, C. H., LUDWIG, M., TASKER, J. G. & STERN, J. E. 2020. Somato-dendritic vasopressin and oxytocin secretion in endocrine and autonomic regulation. *J Neuroendocrinol,* 32**,** e12856.

BROWN, J. 1962. Effects of 2-deoxyglucose on carbohydrate metablism: review of the literature and studies in the rat. *Metabolism,* 11**,** 1098-112.

CAHN, R. D., ZWILLING, E., KAPLAN, N. O. & LEVINE, L. 1962. Nature and Development of Lactic Dehydrogenases: The two major types of this enzyme form molecular hybrids which change in makeup during development. *Science,* 136**,** 962-9.

CAI, W., XUE, C., SAKAGUCHI, M., KONISHI, M., SHIRAZIAN, A., FERRIS, H. A., LI, M. E., YU, R., KLEINRIDDERS, A., POTHOS, E. N. & KAHN, C. R. 2018. Insulin regulates astrocyte gliotransmission and modulates behavior. *J Clin Invest,* 128**,** 2914-2926.

CALINGASAN, N. Y. & RITTER, S. 1992. Hypothalamic paraventricular nucleus lesions do not abolish glucoprivic or lipoprivic feeding. *Brain Res,* 595**,** 25-31.

CAREY, M., LONTCHI-YIMAGOU, E., MITCHELL, W., REDA, S., ZHANG, K., KEHLENBRINK, S., KOPPAKA, S., MAGINLEY, S. R., ALEKSIC, S., BHANSALI, S., HUFFMAN, D. M. & HAWKINS, M. 2020. Central K(ATP) Channels Modulate Glucose Effectiveness in Humans and Rodents. *Diabetes,* 69**,** 1140-1148.

CATO, R. K., FLANAGAN, L. M., VERBALIS, J. G. & STRICKER, E. M. 1990. Effects of glucoprivation on gastric motility and pituitary oxytocin secretion in rats. *Am J Physiol,* 259**,** R447-52.

CHANG, H. H., CHANG, W. H., CHI, M. H., PENG, Y. C., HUANG, C. C., YANG, Y. K. & CHEN, P. S. 2019. The OXTR Polymorphism Stratified the Correlation of Oxytocin and Glucose Homeostasis in Non-Diabetic Subjects. *Diabetes Metab Syndr Obes,* 12**,** 2707-2713.

CHARI, M., YANG, C. S., LAM, C. K., LEE, K., MIGHIU, P., KOKOROVIC, A., CHEUNG, G. W., LAI, T. Y., WANG, P. Y. & LAM, T. K. 2011. Glucose transporter-1 in the hypothalamic glial cells mediates glucose sensing to regulate glucose production in vivo. *Diabetes,* 60**,** 1901-6.

CHEVRIER, C., HAMMICHE, N. & BRUDIEUX, R. 1982. Effects of 2-deoxy-D-glucose on plasma and adrenal concentrations of corticosterone and aldosterone in standard diet fed and potassium loaded rats. *Horm Metab Res,* 14**,** 94-7.

CHHABRA, K. H., ADAMS, J. M., FAGEL, B., LAM, D. D., QI, N., RUBINSTEIN, M. & LOW, M. J. 2016. Hypothalamic POMC Deficiency Improves Glucose Tolerance Despite Insulin Resistance by Increasing Glycosuria. *Diabetes,* 65**,** 660-72.

CHOI, I. Y., TKAC, I., UGURBIL, K. & GRUETTER, R. 1999. Noninvasive measurements of [1-(13)C]glycogen concentrations and metabolism in rat brain in vivo. *J Neurochem,* 73**,** 1300-8.

CHURUANGSUK, C., HALL, J., REYNOLDS, A., GRIFFIN, S. J., COMBET, E. & LEAN, M. E. J. 2022. Diets for weight management in adults with type 2 diabetes: an umbrella review of published meta-analyses and systematic review of trials of diets for diabetes remission. *Diabetologia,* 65**,** 14-36.

CLARET, M., SMITH, M. A., BATTERHAM, R. L., SELMAN, C., CHOUDHURY, A. I., FRYER, L. G., CLEMENTS, M., AL-QASSAB, H., HEFFRON, H., XU, A. W., SPEAKMAN, J. R., BARSH, G. S., VIOLLET, B., VAULONT, S., ASHFORD, M. L., CARLING, D. & WITHERS, D. J. 2007. AMPK is essential for energy homeostasis regulation and glucose sensing by POMC and AgRP neurons. *J Clin Invest,* 117**,** 2325-36.

CLASADONTE, J., SCEMES, E., WANG, Z., BOISON, D. & HAYDON, P. G. 2017. Connexin 43-Mediated Astroglial Metabolic Networks Contribute to the Regulation of the Sleep-Wake Cycle. *Neuron,* 95**,** 1365-1380 e5.

COWLEY, M. A., PRONCHUK, N., FAN, W., DINULESCU, D. M., COLMERS, W. F. & CONE, R. D. 1999. Integration of NPY, AGRP, and melanocortin signals in the hypothalamic paraventricular nucleus: evidence of a cellular basis for the adipostat. *Neuron,* 24**,** 155-63.

CRUZ, N. F. & DIENEL, G. A. 2002. High glycogen levels in brains of rats with minimal environmental stimuli: implications for metabolic contributions of working astrocytes. *J Cereb Blood Flow Metab,* 22**,** 1476-89.

DAMANHURI, H. A., BURKE, P. G., ONG, L. K., BOBROVSKAYA, L., DICKSON, P. W., DUNKLEY, P. R. & GOODCHILD, A. K. 2012. Tyrosine hydroxylase phosphorylation in catecholaminergic brain regions: a marker of activation following acute hypotension and glucoprivation. *PLoS One,* 7**,** e50535.

DE SOUZA CORDEIRO, L. M., ELSHEIKH, A., DEVISETTY, N., MORGAN, D. A., EBERT, S. N., RAHMOUNI, K. & CHHABRA, K. H. 2021. Hypothalamic MC4R regulates glucose homeostasis through adrenaline-mediated control of glucose reabsorption via renal GLUT2 in mice. *Diabetologia,* 64**,** 181-194.

DEBLON, N., VEYRAT-DUREBEX, C., BOURGOIN, L., CAILLON, A., BUSSIER, A. L., PETROSINO, S., PISCITELLI, F., LEGROS, J. J., GEENEN, V., FOTI, M., WAHLI, W., DI MARZO, V. & ROHNER-JEANRENAUD, F. 2011. Mechanisms of the anti-obesity effects of oxytocin in diet-induced obese rats. *PLoS One,* 6**,** e25565.

DEL PRATO, S., KAHN, S. E., PAVO, I., WEERAKKODY, G. J., YANG, Z., DOUPIS, J., AIZENBERG, D., WYNNE, A. G., RIESMEYER, J. S., HEINE, R. J., WIESE, R. J. & INVESTIGATORS, S.-. 2021. Tirzepatide versus insulin glargine in type 2 diabetes and increased cardiovascular risk (SURPASS-4): a randomised, open-label, parallel-group, multicentre, phase 3 trial. *Lancet,* 398**,** 1811-1824.

DENG, Y. & SCHERER, P. E. 2010. Adipokines as novel biomarkers and regulators of the metabolic syndrome. *Ann N Y Acad Sci,* 1212**,** E1-E19.

DEVARAKONDA, K., BAYNE, M., ALVARRSON, A. & STANLEY, S. 2018. Amygdala Glucose-Sensing Neurons Regulate Glucose Metabolism. *Diabetes,* 67.

DODD, G. T., DECHERF, S., LOH, K., SIMONDS, S. E., WIEDE, F., BALLAND, E., MERRY, T. L., MUNZBERG, H., ZHANG, Z. Y., KAHN, B. B., NEEL, B. G., BENCE, K. K., ANDREWS, Z. B., COWLEY, M. A. & TIGANIS, T. 2015. Leptin and insulin act on POMC neurons to promote the browning of white fat. *Cell,* 160**,** 88-104.

DUAN, S., ANDERSON, C. M., STEIN, B. A. & SWANSON, R. A. 1999. Glutamate induces rapid upregulation of astrocyte glutamate transport and cell-surface expression of GLAST. *J Neurosci,* 19**,** 10193-200.

ELNAGAR, A., EL-DAWY, K., EL-BELBASI, H. I., REHAN, I. F., EMBARK, H., AL-AMGAD, Z., SHANAB, O., MICKDAM, E., BATIHA, G. E., ALAMERY, S., FOUAD, S. S., CAVALU, S. & YOUSSEF, M. 2022. Ameliorative Effect of Oxytocin on FBN1 and PEPCK Gene Expression, and Behavioral Patterns in Rats' Obesity-Induced Diabetes. *Front Public Health,* 10**,** 777129.

ERMISCH, A., BARTH, T., RUHLE, H. J., SKOPKOVA, J., HRBAS, P. & LANDGRAF, R. 1985. On the blood-brain barrier to peptides: accumulation of labelled vasopressin, DesGlyNH2-vasopressin and oxytocin by brain regions. *Endocrinol Exp,* 19**,** 29-37.

FABER, C. L., MATSEN, M. E., VELASCO, K. R., DAMIAN, V., PHAN, B. A., ADAM, D., THERATTIL, A., SCHWARTZ, M. W. & MORTON, G. J. 2018. Distinct Neuronal Projections From the Hypothalamic Ventromedial Nucleus Mediate Glycemic and Behavioral Effects. *Diabetes,* 67**,** 2518-2529.

FAN, X., CHAN, O., DING, Y., ZHU, W., MASTAITIS, J. & SHERWIN, R. 2015. Reduction in SGLT1 mRNA Expression in the Ventromedial Hypothalamus Improves the Counterregulatory Responses to Hypoglycemia in Recurrently Hypoglycemic and Diabetic Rats. *Diabetes,* 64**,** 3564-72.

FERGUSON, A. V., LATCHFORD, K. J. & SAMSON, W. K. 2008. The paraventricular nucleus of the hypothalamus - a potential target for integrative treatment of autonomic dysfunction. *Expert Opin Ther Targets,* 12**,** 717-27.

FILIPPI, B. M., YANG, C. S., TANG, C. & LAM, T. K. 2012. Insulin activates Erk1/2 signaling in the dorsal vagal complex to inhibit glucose production. *Cell Metab,* 16**,** 500-10.

FINCK, B. N. & KELLY, D. P. 2006. PGC-1 coactivators: inducible regulators of energy metabolism in health and disease. *J Clin Invest,* 116**,** 615-22.

FLAK, J. N., GOFORTH, P. B., DELL'ORCO, J., SABATINI, P. V., LI, C., BOZADJIEVA, N., SORENSEN, M., VALENTA, A., RUPP, A., AFFINATI, A. H., CRAS-MENEUR, C., ANSARI, A., SACKSNER, J., KODUR, N., SANDOVAL, D. A., KENNEDY, R. T., OLSON, D. P. & MYERS,

M. G., JR. 2020. Ventromedial hypothalamic nucleus neuronal subset regulates blood glucose independently of insulin. *J Clin Invest,* 130**,** 2943-2952.
FLORIAN, M., JANKOWSKI, M. & GUTKOWSKA, J. 2010. Oxytocin increases glucose uptake in neonatal rat cardiomyocytes. *Endocrinology,* 151**,** 482-91.
FRIAS, J. P., DAVIES, M. J., ROSENSTOCK, J., PEREZ MANGHI, F. C., FERNANDEZ LANDO, L., BERGMAN, B. K., LIU, B., CUI, X., BROWN, K. & INVESTIGATORS, S.-. 2021. Tirzepatide versus Semaglutide Once Weekly in Patients with Type 2 Diabetes. *N Engl J Med,* 385**,** 503-515.
FROHMAN, L. A. & BERNARDIS, L. L. 1971. Effect of hypothalamic stimulation on plasma glucose, insulin, and glucagon levels. *Am J Physiol,* 221**,** 1596-603.
GAO, Z. Y., DREWS, G. & HENQUIN, J. C. 1991. Mechanisms of the stimulation of insulin release by oxytocin in normal mouse islets. *Biochem J,* 276 (Pt 1)**,** 169-74.
GARCIA-CACERES, C., QUARTA, C., VARELA, L., GAO, Y., GRUBER, T., LEGUTKO, B., JASTROCH, M., JOHANSSON, P., NINKOVIC, J., YI, C. X., LE THUC, O., SZIGETI-BUCK, K., CAI, W., MEYER, C. W., PFLUGER, P. T., FERNANDEZ, A. M., LUQUET, S., WOODS, S. C., TORRES-ALEMAN, I., KAHN, C. R., GOTZ, M., HORVATH, T. L. & TSCHOP, M. H. 2016. Astrocytic Insulin Signaling Couples Brain Glucose Uptake with Nutrient Availability. *Cell,* 166**,** 867-880.
GAVINI, C. K., JONES, W. C., 2ND & NOVAK, C. M. 2016. Ventromedial hypothalamic melanocortin receptor activation: regulation of activity energy expenditure and skeletal muscle thermogenesis. *J Physiol,* 594**,** 5285-301.
GBD 2015 OBESITY COLLABORATORS, AFSHIN, A., FOROUZANFAR, M. H., REITSMA, M. B., SUR, P., ESTEP, K., LEE, A., MARCZAK, L., MOKDAD, A. H., MORADI-LAKEH, M., NAGHAVI, M., SALAMA, J. S., VOS, T., ABATE, K. H., ABBAFATI, C., AHMED, M. B., AL-ALY, Z., ALKERWI, A., AL-RADDADI, R., AMARE, A. T., AMBERBIR, A., AMEGAH, A. K., AMINI, E., AMROCK, S. M., ANJANA, R. M., ARNLOV, J., ASAYESH, H., BANERJEE, A., BARAC, A., BAYE, E., BENNETT, D. A., BEYENE, A. S., BIADGILIGN, S., BIRYUKOV, S., BJERTNESS, E., BONEYA, D. J., CAMPOS-NONATO, I., CARRERO, J. J., CECILIO, P., CERCY, K., CIOBANU, L. G., CORNABY, L., DAMTEW, S. A., DANDONA, L., DANDONA, R., DHARMARATNE, S. D., DUNCAN, B. B., ESHRATI, B., ESTEGHAMATI, A., FEIGIN, V. L., FERNANDES, J. C., FURST, T., GEBREHIWOT, T. T., GOLD, A., GONA, P. N., GOTO, A., HABTEWOLD, T. D., HADUSH, K. T., HAFEZI-NEJAD, N., HAY, S. I., HORINO, M., ISLAMI, F., KAMAL, R., KASAEIAN, A., KATIKIREDDI, S. V., KENGNE, A. P., KESAVACHANDRAN, C. N., KHADER, Y. S., KHANG, Y. H., KHUBCHANDANI, J., KIM, D., KIM, Y. J., KINFU, Y., KOSEN, S., KU, T., DEFO, B. K., KUMAR, G. A., LARSON, H. J., LEINSALU, M., LIANG, X., LIM, S. S., LIU, P., LOPEZ, A. D., LOZANO, R., MAJEED, A., MALEKZADEH, R., MALTA, D. C., MAZIDI, M., MCALINDEN, C., MCGARVEY, S. T., MENGISTU, D. T., MENSAH, G. A., MENSINK, G. B. M., MEZGEBE, H. B., MIRRAKHIMOV, E. M., MUELLER, U. O., NOUBIAP, J. J., OBERMEYER, C. M., OGBO, F. A., OWOLABI, M. O., et al. 2017. Health Effects of Overweight and Obesity in 195 Countries over 25 Years. *N Engl J Med,* 377**,** 13-27.
GELLING, R. W., MORTON, G. J., MORRISON, C. D., NISWENDER, K. D., MYERS, M. G., JR., RHODES, C. J. & SCHWARTZ, M. W. 2006. Insulin action in the brain contributes to glucose lowering during insulin treatment of diabetes. *Cell Metab,* 3**,** 67-73.
GIAUME, C. & THEIS, M. 2010. Pharmacological and genetic approaches to study connexin-mediated channels in glial cells of the central nervous system. *Brain Res Rev,* 63**,** 160-76.
GIMPL, G. & FAHRENHOLZ, F. 2001. The oxytocin receptor system: structure, function, and regulation. *Physiol Rev,* 81**,** 629-83.
GONZALEZ OLMO, B. M., BETTES, M. N., DEMARSH, J. W., ZHAO, F., ASKWITH, C. & BARRIENTOS, R. M. 2023. Short-term high-fat diet consumption impairs synaptic plasticity in the aged hippocampus via IL-1 signaling. *NPJ Sci Food,* 7**,** 35.
GOTO, Y., CARPENTER, R. G., BERELOWITZ, M. & FROHMAN, L. A. 1980. Effect of ventromedial hypothalamic lesions on the secretion of somatostatin, insulin, and glucagon by the perfused rat pancreas. *Metabolism,* 29**,** 986-90.
HALIM, N. D., MCFATE, T., MOHYELDIN, A., OKAGAKI, P., KOROTCHKINA, L. G., PATEL, M. S., JEOUNG, N. H., HARRIS, R. A., SCHELL, M. J. & VERMA, A. 2010. Phosphorylation status of pyruvate dehydrogenase distinguishes metabolic phenotypes of cultured rat brain astrocytes and neurons. *Glia,* 58**,** 1168-76.
HASPULA, D. & CUI, Z. 2023. Neurochemical Basis of Inter-Organ Crosstalk in Health and Obesity: Focus on the Hypothalamus and the Brainstem. *Cells,* 12.
HE, Y., XU, P., WANG, C., XIA, Y., YU, M., YANG, Y., YU, K., CAI, X., QU, N., SAITO, K., WANG, J., HYSENI, I., ROBERTSON, M., PIYARATHNA, B., GAO, M., KHAN, S. A., LIU, F., CHEN, R.,

COARFA, C., ZHAO, Z., TONG, Q., SUN, Z. & XU, Y. 2020. Estrogen receptor-alpha expressing neurons in the ventrolateral VMH regulate glucose balance. *Nat Commun,* 11**,** 2165.
HENN, R. E., ELZINGA, S. E., GLASS, E., PARENT, R., GUO, K., ALLOUCH, A. A., MENDELSON, F. E., HAYES, J., WEBBER-DAVIS, I., MURPHY, G. G., HUR, J. & FELDMAN, E. L. 2022. Obesity-induced neuroinflammation and cognitive impairment in young adult versus middle-aged mice. *Immun Ageing,* 19**,** 67.
HERNANDEZ-GARZON, E., FERNANDEZ, A. M., PEREZ-ALVAREZ, A., GENIS, L., BASCUNANA, P., FERNANDEZ DE LA ROSA, R., DELGADO, M., ANGEL POZO, M., MORENO, E., MCCORMICK, P. J., SANTI, A., TRUEBA-SAIZ, A., GARCIA-CACERES, C., TSCHOP, M. H., ARAQUE, A., MARTIN, E. D. & TORRES ALEMAN, I. 2016. The insulin-like growth factor I receptor regulates glucose transport by astrocytes. *Glia,* 64**,** 1962-71.
HERRERO-MENDEZ, A., ALMEIDA, A., FERNANDEZ, E., MAESTRE, C., MONCADA, S. & BOLANOS, J. P. 2009. The bioenergetic and antioxidant status of neurons is controlled by continuous degradation of a key glycolytic enzyme by APC/C-Cdh1. *Nat Cell Biol,* 11**,** 747-52.
HOLT, M. G. 2023. Astrocyte heterogeneity and interactions with local neural circuits. *Essays Biochem,* 67**,** 93-106.
HOSLI, L., BININI, N., FERRARI, K. D., THIEREN, L., LOOSER, Z. J., ZUEND, M., ZANKER, H. S., BERRY, S., HOLUB, M., MOBIUS, W., RUHWEDEL, T., NAVE, K. A., GIAUME, C., WEBER, B. & SAAB, A. S. 2022. Decoupling astrocytes in adult mice impairs synaptic plasticity and spatial learning. *Cell Rep,* 38**,** 110484.
HUANG, H., HE, W., TANG, T. & QIU, M. 2023. Immunological Markers for Central Nervous System Glia. *Neurosci Bull,* 39**,** 379-392.
HUNG, L. W., NEUNER, S., POLEPALLI, J. S., BEIER, K. T., WRIGHT, M., WALSH, J. J., LEWIS, E. M., LUO, L., DEISSEROTH, K., DOLEN, G. & MALENKA, R. C. 2017. Gating of social reward by oxytocin in the ventral tegmental area. *Science,* 357**,** 1406-1411.
INOUE, H., OGAWA, W., ASAKAWA, A., OKAMOTO, Y., NISHIZAWA, A., MATSUMOTO, M., TESHIGAWARA, K., MATSUKI, Y., WATANABE, E., HIRAMATSU, R., NOTOHARA, K., KATAYOSE, K., OKAMURA, H., KAHN, C. R., NODA, T., TAKEDA, K., AKIRA, S., INUI, A. & KASUGA, M. 2006. Role of hepatic STAT3 in brain-insulin action on hepatic glucose production. *Cell Metab,* 3**,** 267-75.
INOUE, H., OGAWA, W., OZAKI, M., HAGA, S., MATSUMOTO, M., FURUKAWA, K., HASHIMOTO, N., KIDO, Y., MORI, T., SAKAUE, H., TESHIGAWARA, K., JIN, S., IGUCHI, H., HIRAMATSU, R., LEROITH, D., TAKEDA, K., AKIRA, S. & KASUGA, M. 2004. Role of STAT-3 in regulation of hepatic gluconeogenic genes and carbohydrate metabolism in vivo. *Nat Med,* 10**,** 168-74.
INOUE, S., CAMPFIELD, L. A. & BRAY, G. A. 1977. Comparison of metabolic alterations in hypothalamic and high fat diet-induced obesity. *Am J Physiol,* 233**,** R162-8.
ISHIHARA, K. K., HAYWOOD, S. C., DAPHNA-IKEN, D., PUENTE, E. C. & FISHER, S. J. 2009. Brain insulin infusion does not augment the counterregulatory response to hypoglycemia or glucoprivation. *Metabolism,* 58**,** 812-20.
ITOH, Y., ESAKI, T., SHIMOJI, K., COOK, M., LAW, M. J., KAUFMAN, E. & SOKOLOFF, L. 2003. Dichloroacetate effects on glucose and lactate oxidation by neurons and astroglia in vitro and on glucose utilization by brain in vivo. *Proc Natl Acad Sci U S A,* 100**,** 4879-84.
JARAMILLO, A. P., IBRAHIMLI, S., CASTELLS, J., JARAMILLO, L., MONCADA, D. & REVILLA HUERTA, J. C. 2023. Physical Activity as a Lifestyle Modification in Patients With Multiple Comorbidities: Emphasizing More on Obese, Prediabetic, and Type 2 Diabetes Mellitus Patients. *Cureus,* 15**,** e41356.
JOUROUKHIN, Y., KAGEYAMA, Y., MISHENEVA, V., SHEVELKIN, A., ANDRABI, S., PRANDOVSZKY, E., YOLKEN, R. H., DAWSON, V. L., DAWSON, T. M., AJA, S., SESAKI, H. & PLETNIKOV, M. V. 2018. DISC1 regulates lactate metabolism in astrocytes: implications for psychiatric disorders. *Transl Psychiatry,* 8**,** 76.
JUREK, B. & NEUMANN, I. D. 2018. The Oxytocin Receptor: From Intracellular Signaling to Behavior. *Physiol Rev,* 98**,** 1805-1908.
KARACA, M., FRIGERIO, F., MIGRENNE, S., MARTIN-LEVILAIN, J., SKYTT, D. M., PAJECKA, K., MARTIN-DEL-RIO, R., GRUETTER, R., TAMARIT-RODRIGUEZ, J., WAAGEPETERSEN, H. S., MAGNAN, C. & MAECHLER, P. 2015. GDH-Dependent Glutamate Oxidation in the Brain Dictates Peripheral Energy Substrate Distribution. *Cell Rep,* 13**,** 365-75.
KASISCHKE, K. A., VISHWASRAO, H. D., FISHER, P. J., ZIPFEL, W. R. & WEBB, W. W. 2004. Neural activity triggers neuronal oxidative metabolism followed by astrocytic glycolysis. *Science,* 305**,** 99-103.
KEREM, L. & LAWSON, E. A. 2021. The Effects of Oxytocin on Appetite Regulation, Food Intake and Metabolism in Humans. *Int J Mol Sci,* 22.

KHODAI, T. & LUCKMAN, S. M. 2021. Ventromedial Nucleus of the Hypothalamus Neurons Under the Magnifying Glass. *Endocrinology,* 162.
KHODAI, T., NUNN, N., WORTH, A. A., FEETHAM, C. H., BELLE, M. D. C., PIGGINS, H. D. & LUCKMAN, S. M. 2018. PACAP Neurons in the Ventromedial Hypothalamic Nucleus Are Glucose Inhibited and Their Selective Activation Induces Hyperglycaemia. *Front Endocrinol (Lausanne),* 9**,** 632.
KIM, J. G., SUYAMA, S., KOCH, M., JIN, S., ARGENTE-ARIZON, P., ARGENTE, J., LIU, Z. W., ZIMMER, M. R., JEONG, J. K., SZIGETI-BUCK, K., GAO, Y., GARCIA-CACERES, C., YI, C. X., SALMASO, N., VACCARINO, F. M., CHOWEN, J., DIANO, S., DIETRICH, M. O., TSCHOP, M. H. & HORVATH, T. L. 2014. Leptin signaling in astrocytes regulates hypothalamic neuronal circuits and feeding. *Nat Neurosci,* 17**,** 908-10.
KIMURA, K., TANIDA, M., NAGATA, N., INABA, Y., WATANABE, H., NAGASHIMADA, M., OTA, T., ASAHARA, S., KIDO, Y., MATSUMOTO, M., TOSHINAI, K., NAKAZATO, M., SHIBAMOTO, T., KANEKO, S., KASUGA, M. & INOUE, H. 2016. Central Insulin Action Activates Kupffer Cells by Suppressing Hepatic Vagal Activation via the Nicotinic Alpha 7 Acetylcholine Receptor. *Cell Rep,* 14**,** 2362-74.
KLEMENT, J., OTT, V., RAPP, K., BREDE, S., PICCININI, F., COBELLI, C., LEHNERT, H. & HALLSCHMID, M. 2017. Oxytocin Improves beta-Cell Responsivity and Glucose Tolerance in Healthy Men. *Diabetes,* 66**,** 264-271.
KNOBLOCH, H. S., CHARLET, A., HOFFMANN, L. C., ELIAVA, M., KHRULEV, S., CETIN, A. H., OSTEN, P., SCHWARZ, M. K., SEEBURG, P. H., STOOP, R. & GRINEVICH, V. 2012. Evoked axonal oxytocin release in the central amygdala attenuates fear response. *Neuron,* 73**,** 553-66.
KOEPSELL, H. 2020. Glucose transporters in brain in health and disease. *Pflugers Arch,* 472**,** 1299-1343.
KOFUJI, P. & NEWMAN, E. A. 2004. Potassium buffering in the central nervous system. *Neuroscience,* 129**,** 1045-56.
KUBLAOUI, B. M., GEMELLI, T., TOLSON, K. P., WANG, Y. & ZINN, A. R. 2008. Oxytocin deficiency mediates hyperphagic obesity of Sim1 haploinsufficient mice. *Mol Endocrinol,* 22**,** 1723-34.
KWON, E., JOUNG, H. Y., LIU, S. M., CHUA, S. C., JR., SCHWARTZ, G. J. & JO, Y. H. 2020. Optogenetic stimulation of the liver-projecting melanocortinergic pathway promotes hepatic glucose production. *Nat Commun,* 11**,** 6295.
LAM, T. K., GUTIERREZ-JUAREZ, R., POCAI, A. & ROSSETTI, L. 2005. Regulation of blood glucose by hypothalamic pyruvate metabolism. *Science,* 309**,** 943-7.
LAMY, C. M., SANNO, H., LABOUEBE, G., PICARD, A., MAGNAN, C., CHATTON, J. Y. & THORENS, B. 2014. Hypoglycemia-activated GLUT2 neurons of the nucleus tractus solitarius stimulate vagal activity and glucagon secretion. *Cell Metab,* 19**,** 527-38.
LANDGRAF, R., NEUMANN, I., HOLSBOER, F. & PITTMAN, Q. J. 1995. Interleukin-1 beta stimulates both central and peripheral release of vasopressin and oxytocin in the rat. *Eur J Neurosci,* 7**,** 592-8.
LARSON-MEYER, D. E., NEWCOMER, B. R., RAVUSSIN, E., VOLAUFOVA, J., BENNETT, B., CHALEW, S., CEFALU, W. T. & SOTHERN, M. 2011. Intrahepatic and intramyocellular lipids are determinants of insulin resistance in prepubertal children. *Diabetologia,* 54**,** 869-75.
LAUGHTON, J. D., BITTAR, P., CHARNAY, Y., PELLERIN, L., KOVARI, E., MAGISTRETTI, P. J. & BOURAS, C. 2007. Metabolic compartmentalization in the human cortex and hippocampus: evidence for a cell- and region-specific localization of lactate dehydrogenase 5 and pyruvate dehydrogenase. *BMC Neurosci,* 8**,** 35.
LAWSON, E. A., MARENGI, D. A., DESANTI, R. L., HOLMES, T. M., SCHOENFELD, D. A. & TOLLEY, C. J. 2015. Oxytocin reduces caloric intake in men. *Obesity (Silver Spring),* 23**,** 950-6.
LEE, B., YANG, C., CHEN, T. H., AL-AZAWI, N. & HSU, W. H. 1995. Effect of AVP and oxytocin on insulin release: involvement of V1b receptors. *Am J Physiol,* 269**,** E1095-100.
LEE, E. S., UHM, K. O., LEE, Y. M., KWON, J., PARK, S. H. & SOO, K. H. 2008. Oxytocin stimulates glucose uptake in skeletal muscle cells through the calcium-CaMKK-AMPK pathway. *Regul Pept,* 151**,** 71-4.
LEE, M. R., SHNITKO, T. A., BLUE, S. W., KAUCHER, A. V., WINCHELL, A. J., ERIKSON, D. W., GRANT, K. A. & LEGGIO, L. 2020. Labeled oxytocin administered via the intranasal route reaches the brain in rhesus macaques. *Nat Commun,* 11**,** 2783.
LEIBOWITZ, S. F., SLADEK, C., SPENCER, L. & TEMPEL, D. 1988. Neuropeptide Y, epinephrine and norepinephrine in the paraventricular nucleus: stimulation of feeding and the release of corticosterone, vasopressin and glucose. *Brain Res Bull,* 21**,** 905-12.
LENG, G. & SABATIER, N. 2017. Oxytocin - The Sweet Hormone? *Trends Endocrinol Metab,* 28**,** 365-376.

LEVIN, B. E., GOVEK, E. K. & DUNN-MEYNELL, A. A. 1998. Reduced glucose-induced neuronal activation in the hypothalamus of diet-induced obese rats. *Brain Res,* 808**,** 317-9.
LEVIN, B. E. & SULLIVAN, A. C. 1987. Glucose-induced norepinephrine levels and obesity resistance. *Am J Physiol,* 253**,** R475-81.
LEVIN, B. E. & SULLIVAN, A. C. 1989. Glucose-induced sympathetic activation in obesity-prone and resistant rats. *Int J Obes,* 13**,** 235-46.
LI, A. J., WANG, Q. & RITTER, S. 2018. Selective Pharmacogenetic Activation of Catecholamine Subgroups in the Ventrolateral Medulla Elicits Key Glucoregulatory Responses. *Endocrinology,* 159**,** 341-355.
LOAIZA, A., PORRAS, O. H. & BARROS, L. F. 2003. Glutamate triggers rapid glucose transport stimulation in astrocytes as evidenced by real-time confocal microscopy. *J Neurosci,* 23**,** 7337-42.
LUTOMSKA, L. M., MIOK, V., KRAHMER, N., GONZALEZ GARCIA, I., GRUBER, T., LE THUC, O., MURAT, C. D., LEGUTKO, B., STERR, M., SAHER, G., LICKERT, H., MULLER, T. D., USSAR, S., TSCHOP, M. H., LUTTER, D. & GARCIA-CACERES, C. 2022. Diet triggers specific responses of hypothalamic astrocytes in time and region dependent manner. *Glia,* 70**,** 2062-2078.
MA, Y., RATNASABAPATHY, R., DE BACKER, I., IZZI-ENGBEAYA, C., NGUYEN-TU, M. S., CUENCO, J., JONES, B., JOHN, C. D., LAM, B. Y., RUTTER, G. A., YEO, G. S., DHILLO, W. S. & GARDINER, J. 2020. Glucose in the hypothalamic paraventricular nucleus regulates GLP-1 release. *JCI Insight,* 5.
MACDONALD, A. J., HOLMES, F. E., BEALL, C., PICKERING, A. E. & ELLACOTT, K. L. J. 2020. Regulation of food intake by astrocytes in the brainstem dorsal vagal complex. *Glia,* 68**,** 1241-1254.
MACHLER, P., WYSS, M. T., ELSAYED, M., STOBART, J., GUTIERREZ, R., VON FABER-CASTELL, A., KAELIN, V., ZUEND, M., SAN MARTIN, A., ROMERO-GOMEZ, I., BAEZA-LEHNERT, F., LENGACHER, S., SCHNEIDER, B. L., AEBISCHER, P., MAGISTRETTI, P. J., BARROS, L. F. & WEBER, B. 2016. In Vivo Evidence for a Lactate Gradient from Astrocytes to Neurons. *Cell Metab,* 23**,** 94-102.
MAEJIMA, Y., IWASAKI, Y., YAMAHARA, Y., KODAIRA, M., SEDBAZAR, U. & YADA, T. 2011. Peripheral oxytocin treatment ameliorates obesity by reducing food intake and visceral fat mass. *Aging (Albany NY),* 3**,** 1169-77.
MAEJIMA, Y., RITA, R. S., SANTOSO, P., AOYAMA, M., HIRAOKA, Y., NISHIMORI, K., GANTULGA, D., SHIMOMURA, K. & YADA, T. 2015. Nasal oxytocin administration reduces food intake without affecting locomotor activity and glycemia with c-Fos induction in limited brain areas. *Neuroendocrinology,* 101**,** 35-44.
MAKHMUTOVA, M., WEITZ, J., TAMAYO, A., PEREIRA, E., BOULINA, M., ALMACA, J., RODRIGUEZ-DIAZ, R. & CAICEDO, A. 2021. Pancreatic beta-Cells Communicate With Vagal Sensory Neurons. *Gastroenterology,* 160**,** 875-888 e11.
MARINA, N., CHRISTIE, I. N., KORSAK, A., DORONIN, M., BRAZHE, A., HOSFORD, P. S., WELLS, J. A., SHEIKHBAHAEI, S., HUMOUD, I., PATON, J. F. R., LYTHGOE, M. F., SEMYANOV, A., KASPAROV, S. & GOURINE, A. V. 2020. Astrocytes monitor cerebral perfusion and control systemic circulation to maintain brain blood flow. *Nat Commun,* 11**,** 131.
MARTIN, B. C., WARRAM, J. H., KROLEWSKI, A. S., BERGMAN, R. N., SOELDNER, J. S. & KAHN, C. R. 1992. Role of glucose and insulin resistance in development of type 2 diabetes mellitus: results of a 25-year follow-up study. *Lancet,* 340**,** 925-9.
MARTIN-TIMON, I. & DEL CANIZO-GOMEZ, F. J. 2015. Mechanisms of hypoglycemia unawareness and implications in diabetic patients. *World J Diabetes,* 6**,** 912-26.
MARTY, N., DALLAPORTA, M., FORETZ, M., EMERY, M., TARUSSIO, D., BADY, I., BINNERT, C., BEERMANN, F. & THORENS, B. 2005. Regulation of glucagon secretion by glucose transporter type 2 (glut2) and astrocyte-dependent glucose sensors. *J Clin Invest,* 115**,** 3545-53.
MARTYN, J. A., KANEKI, M. & YASUHARA, S. 2008. Obesity-induced insulin resistance and hyperglycemia: etiologic factors and molecular mechanisms. *Anesthesiology,* 109**,** 137-48.
MATTHEWS, D. R., HOSKER, J. P., RUDENSKI, A. S., NAYLOR, B. A., TREACHER, D. F. & TURNER, R. C. 1985. Homeostasis model assessment: insulin resistance and beta-cell function from fasting plasma glucose and insulin concentrations in man. *Diabetologia,* 28**,** 412-9.
MCCORMACK, S. E., BLEVINS, J. E. & LAWSON, E. A. 2020. Metabolic Effects of Oxytocin. *Endocr Rev,* 41**,** 121-45.
MCDOUGAL, D. H., HERMANN, G. E. & ROGERS, R. C. 2013a. Astrocytes in the nucleus of the solitary tract are activated by low glucose or glucoprivation: evidence for glial involvement in glucose homeostasis. *Front Neurosci,* 7**,** 249.

MCDOUGAL, D. H., VIARD, E., HERMANN, G. E. & ROGERS, R. C. 2013b. Astrocytes in the hindbrain detect glucoprivation and regulate gastric motility. *Auton Neurosci,* 175**,** 61-9.
MCNAY, E. C. & GOLD, P. E. 2002. Food for thought: fluctuations in brain extracellular glucose provide insight into the mechanisms of memory modulation. *Behav Cogn Neurosci Rev,* 1**,** 264-80.
MEEK, T. H., NELSON, J. T., MATSEN, M. E., DORFMAN, M. D., GUYENET, S. J., DAMIAN, V., ALLISON, M. B., SCARLETT, J. M., NGUYEN, H. T., THALER, J. P., OLSON, D. P., MYERS, M. G., JR., SCHWARTZ, M. W. & MORTON, G. J. 2016. Functional identification of a neurocircuit regulating blood glucose. *Proc Natl Acad Sci U S A,* 113**,** E2073-82.
MELNICK, I. V., PRICE, C. J. & COLMERS, W. F. 2011. Glucosensing in parvocellular neurons of the rat hypothalamic paraventricular nucleus. *Eur J Neurosci,* 34**,** 272-82.
MINAMI, S., KAMEGAI, J., SUGIHARA, H., SUZUKI, N., HIGUCHI, H. & WAKABAYASHI, I. 1995. Central glucoprivation evoked by administration of 2-deoxy-D-glucose induces expression of the c-fos gene in a subpopulation of neuropeptide Y neurons in the rat hypothalamus. *Brain Res Mol Brain Res,* 33**,** 305-10.
MIRZADEH, Z., FABER, C. L. & SCHWARTZ, M. W. 2022. Central Nervous System Control of Glucose Homeostasis: A Therapeutic Target for Type 2 Diabetes? *Annu Rev Pharmacol Toxicol,* 62**,** 55-84.
MIZUNO, K., HAGA, H., OKUMOTO, K., HOSHIKAWA, K., KATSUMI, T., NISHINA, T., SAITO, T., KATAGIRI, H. & UENO, Y. 2021. Intrahepatic distribution of nerve fibers and alterations due to fibrosis in diseased liver. *PLoS One,* 16**,** e0249556.
MORGAN, D. A., MCDANIEL, L. N., YIN, T., KHAN, M., JIANG, J., ACEVEDO, M. R., WALSH, S. A., PONTO, L. L., NORRIS, A. W., LUTTER, M., RAHMOUNI, K. & CUI, H. 2015. Regulation of glucose tolerance and sympathetic activity by MC4R signaling in the lateral hypothalamus. *Diabetes,* 64**,** 1976-87.
MORI, T., TANAKA, K., BUFFO, A., WURST, W., KUHN, R. & GOTZ, M. 2006. Inducible gene deletion in astroglia and radial glia--a valuable tool for functional and lineage analysis. *Glia,* 54**,** 21-34.
MORLAND, C., ANDERSSON, K. A., HAUGEN, O. P., HADZIC, A., KLEPPA, L., GILLE, A., RINHOLM, J. E., PALIBRK, V., DIGET, E. H., KENNEDY, L. H., STOLEN, T., HENNESTAD, E., MOLDESTAD, O., CAI, Y., PUCHADES, M., OFFERMANNS, S., VERVAEKE, K., BJORAS, M., WISLOFF, U., STORM-MATHISEN, J. & BERGERSEN, L. H. 2017. Exercise induces cerebral VEGF and angiogenesis via the lactate receptor HCAR1. *Nat Commun,* 8**,** 15557.
MORTON, G. J., THATCHER, B. S., REIDELBERGER, R. D., OGIMOTO, K., WOLDEN-HANSON, T., BASKIN, D. G., SCHWARTZ, M. W. & BLEVINS, J. E. 2012. Peripheral oxytocin suppresses food intake and causes weight loss in diet-induced obese rats. *Am J Physiol Endocrinol Metab,* 302**,** E134-44.
MUECKLER, M., CARUSO, C., BALDWIN, S. A., PANICO, M., BLENCH, I., MORRIS, H. R., ALLARD, W. J., LIENHARD, G. E. & LODISH, H. F. 1985. Sequence and structure of a human glucose transporter. *Science,* 229**,** 941-5.
MULLIS, K., KAY, K. & WILLIAMS, D. L. 2013. Oxytocin action in the ventral tegmental area affects sucrose intake. *Brain Res,* 1513**,** 85-91.
MURALEEDHARAN, R., GAWALI, M. V., TIWARI, D., SUKUMARAN, A., OATMAN, N., ANDERSON, J., NARDINI, D., BHUIYAN, M. A. N., TKAC, I., WARD, A. L., KUNDU, M., WACLAW, R., CHOW, L. M., GROSS, C., RAO, R., SCHIRMEIER, S. & DASGUPTA, B. 2020. AMPK-Regulated Astrocytic Lactate Shuttle Plays a Non-Cell-Autonomous Role in Neuronal Survival. *Cell Rep,* 32**,** 108092.
MURPHY, B. A., FIORAMONTI, X., JOCHNOWITZ, N., FAKIRA, K., GAGEN, K., CONTIE, S., LORSIGNOL, A., PENICAUD, L., MARTIN, W. J. & ROUTH, V. H. 2009. Fasting enhances the response of arcuate neuropeptide Y-glucose-inhibited neurons to decreased extracellular glucose. *Am J Physiol Cell Physiol,* 296**,** C746-56.
NOBLE, E. E., BILLINGTON, C. J., KOTZ, C. M. & WANG, C. 2014. Oxytocin in the ventromedial hypothalamic nucleus reduces feeding and acutely increases energy expenditure. *Am J Physiol Regul Integr Comp Physiol,* 307**,** R737-45.
OBICI, S., FENG, Z., ARDUINI, A., CONTI, R. & ROSSETTI, L. 2003. Inhibition of hypothalamic carnitine palmitoyltransferase-1 decreases food intake and glucose production. *Nat Med,* 9**,** 756-61.
OBICI, S., ZHANG, B. B., KARKANIAS, G. & ROSSETTI, L. 2002. Hypothalamic insulin signaling is required for inhibition of glucose production. *Nat Med,* 8**,** 1376-82.
OGURTSOVA, K., DA ROCHA FERNANDES, J. D., HUANG, Y., LINNENKAMP, U., GUARIGUATA, L., CHO, N. H., CAVAN, D., SHAW, J. E. & MAKAROFF, L. E. 2017. IDF Diabetes Atlas: Global estimates for the prevalence of diabetes for 2015 and 2040. *Diabetes Res Clin Pract,* 128**,** 40-50.

OLSZEWSKI, P. K., KLOCKARS, A., OLSZEWSKA, A. M., FREDRIKSSON, R., SCHIOTH, H. B. & LEVINE, A. S. 2010. Molecular, immunohistochemical, and pharmacological evidence of oxytocin's role as inhibitor of carbohydrate but not fat intake. *Endocrinology,* 151**,** 4736-44.

ONG, Z. Y., BONGIORNO, D. M., HERNANDO, M. A. & GRILL, H. J. 2017. Effects of Endogenous Oxytocin Receptor Signaling in Nucleus Tractus Solitarius on Satiation-Mediated Feeding and Thermogenic Control in Male Rats. *Endocrinology,* 158**,** 2826-2836.

OSAKADA, T., YAN, R., JIANG, Y., WEI, D., TABUCHI, R., DAI, B., WANG, X., ZHAO, G., WANG, C. X., TSIEN, R. W., MAR, A. C. & LIN, D. 2022. A dedicated hypothalamic oxytocin circuit controls aversive social learning. *BioRxiv*.

OTT, V., FINLAYSON, G., LEHNERT, H., HEITMANN, B., HEINRICHS, M., BORN, J. & HALLSCHMID, M. 2013. Oxytocin reduces reward-driven food intake in humans. *Diabetes,* 62**,** 3418-25.

PADHI, S., NAYAK, A. K. & BEHERA, A. 2020. Type II diabetes mellitus: a review on recent drug based therapeutics. *Biomed Pharmacother,* 131**,** 110708.

PANNASCH, U., VARGOVA, L., REINGRUBER, J., EZAN, P., HOLCMAN, D., GIAUME, C., SYKOVA, E. & ROUACH, N. 2011. Astroglial networks scale synaptic activity and plasticity. *Proc Natl Acad Sci U S A,* 108**,** 8467-72.

PARTON, L. E., YE, C. P., COPPARI, R., ENRIORI, P. J., CHOI, B., ZHANG, C. Y., XU, C., VIANNA, C. R., BALTHASAR, N., LEE, C. E., ELMQUIST, J. K., COWLEY, M. A. & LOWELL, B. B. 2007. Glucose sensing by POMC neurons regulates glucose homeostasis and is impaired in obesity. *Nature,* 449**,** 228-32.

PATCHING, S. G. 2017. Glucose Transporters at the Blood-Brain Barrier: Function, Regulation and Gateways for Drug Delivery. *Mol Neurobiol,* 54**,** 1046-1077.

PELLERIN, L. & MAGISTRETTI, P. J. 1994. Glutamate uptake into astrocytes stimulates aerobic glycolysis: a mechanism coupling neuronal activity to glucose utilization. *Proc Natl Acad Sci U S A,* 91**,** 10625-9.

PINOL, R. A., JAMESON, H., POPRATILOFF, A., LEE, N. H. & MENDELOWITZ, D. 2014. Visualization of oxytocin release that mediates paired pulse facilitation in hypothalamic pathways to brainstem autonomic neurons. *PLoS One,* 9**,** e112138.

PLANTE, E., MENAOUAR, A., DANALACHE, B. A., YIP, D., BRODERICK, T. L., CHIASSON, J. L., JANKOWSKI, M. & GUTKOWSKA, J. 2015. Oxytocin treatment prevents the cardiomyopathy observed in obese diabetic male db/db mice. *Endocrinology,* 156**,** 1416-28.

POCAI, A., LAM, T. K., GUTIERREZ-JUAREZ, R., OBICI, S., SCHWARTZ, G. J., BRYAN, J., AGUILAR-BRYAN, L. & ROSSETTI, L. 2005a. Hypothalamic K(ATP) channels control hepatic glucose production. *Nature,* 434**,** 1026-31.

POCAI, A., OBICI, S., SCHWARTZ, G. J. & ROSSETTI, L. 2005b. A brain-liver circuit regulates glucose homeostasis. *Cell Metab,* 1**,** 53-61.

PRENTKI, M. & NOLAN, C. J. 2006. Islet beta cell failure in type 2 diabetes. *J Clin Invest,* 116**,** 1802-12.

QUINTANA, D. S., ROKICKI, J., VAN DER MEER, D., ALNAES, D., KAUFMANN, T., CORDOVA-PALOMERA, A., DIESET, I., ANDREASSEN, O. A. & WESTLYE, L. T. 2019. Oxytocin pathway gene networks in the human brain. *Nat Commun,* 10**,** 668.

RAHMAN, M. H., BHUSAL, A., KIM, J. H., JHA, M. K., SONG, G. J., GO, Y., JANG, I. S., LEE, I. K. & SUK, K. 2020. Astrocytic pyruvate dehydrogenase kinase-2 is involved in hypothalamic inflammation in mouse models of diabetes. *Nat Commun,* 11**,** 5906.

RAPPAPORT, E. B., YOUNG, J. B. & LANDSBERG, L. 1982. Effects of 2-deoxy-D-glucose on the cardiac sympathetic nerves and the adrenal medulla in the rat: further evidence for a dissociation of sympathetic nervous system and adrenal medullary responses. *Endocrinology,* 110**,** 650-6.

RAWLINSON, S., REICHENBACH, A., CLARKE, R. E., NUNEZ-IGLESIAS, J., DEMPSEY, H., LOCKIE, S. H. & ANDREWS, Z. B. 2022. In Vivo Photometry Reveals Insulin and 2-Deoxyglucose Maintain Prolonged Inhibition of VMH Vglut2 Neurons in Male Mice. *Endocrinology,* 163.

REHN, S., RAYMOND, J. S., BOAKES, R. A. & BOWEN, M. T. 2022. Sucrose intake by rats affected by both intraperitoneal oxytocin administration and time of day. *Psychopharmacology (Berl),* 239**,** 429-442.

RINAMAN, L. 1998. Oxytocinergic inputs to the nucleus of the solitary tract and dorsal motor nucleus of the vagus in neonatal rats. *J Comp Neurol,* 399**,** 101-9.

RITTER, S., LLEWELLYN-SMITH, I. & DINH, T. T. 1998. Subgroups of hindbrain catecholamine neurons are selectively activated by 2-deoxy-D-glucose induced metabolic challenge. *Brain Res,* 805**,** 41-54.

ROBERTS, Z. S., WOLDEN-HANSON, T., MATSEN, M. E., RYU, V., VAUGHAN, C. H., GRAHAM, J. L., HAVEL, P. J., CHUKRI, D. W., SCHWARTZ, M. W., MORTON, G. J. & BLEVINS, J. E. 2017.

Chronic hindbrain administration of oxytocin is sufficient to elicit weight loss in diet-induced obese rats. *Am J Physiol Regul Integr Comp Physiol,* 313**,** R357-R371.
ROH, E., SONG, D. K. & KIM, M. S. 2016. Emerging role of the brain in the homeostatic regulation of energy and glucose metabolism. *Exp Mol Med,* 48**,** e216.
RÖHM, N., MOSZKA, N., KANTARTZIS, K., PREISSL, H., FRITSCHE, L., FRITSCHE, A. & HALLSCHMID, M. 2023. Oxytocin does not acutely improve glucose homeostasis im men with type 2 diabetes. *59th EASD Annual Meeting.* Hamburg.
ROHNER-JEANRENAUD, F. & JEANRENAUD, B. 1980. Consequences of ventromedial hypothalamic lesions upon insulin and glucagon secretion by subsequently isolated perfused pancreases in the rat. *J Clin Invest,* 65**,** 902-10.
ROSARIO, W., SINGH, I., WAUTLET, A., PATTERSON, C., FLAK, J., BECKER, T. C., ALI, A., TAMARINA, N., PHILIPSON, L. H., ENQUIST, L. W., MYERS, M. G., JR. & RHODES, C. J. 2016. The Brain-to-Pancreatic Islet Neuronal Map Reveals Differential Glucose Regulation From Distinct Hypothalamic Regions. *Diabetes,* 65**,** 2711-23.
ROSENSTOCK, J., WYSHAM, C., FRIAS, J. P., KANEKO, S., LEE, C. J., FERNANDEZ LANDO, L., MAO, H., CUI, X., KARANIKAS, C. A. & THIEU, V. T. 2021. Efficacy and safety of a novel dual GIP and GLP-1 receptor agonist tirzepatide in patients with type 2 diabetes (SURPASS-1): a double-blind, randomised, phase 3 trial. *Lancet,* 398**,** 143-155.
ROUTH, V. H., DONOVAN, C. M. & RITTER, S. 2012. 2. Hypoglycemia Detection. *Transl Endocrinol Metab,* 3**,** 47-87.
ROUTH, V. H., HAO, L., SANTIAGO, A. M., SHENG, Z. & ZHOU, C. 2014. Hypothalamic glucose sensing: making ends meet. *Front Syst Neurosci,* 8**,** 236.
RUAN, H. B., DIETRICH, M. O., LIU, Z. W., ZIMMER, M. R., LI, M. D., SINGH, J. P., ZHANG, K., YIN, R., WU, J., HORVATH, T. L. & YANG, X. 2014. O-GlcNAc transferase enables AgRP neurons to suppress browning of white fat. *Cell,* 159**,** 306-17.
RUMINOT, I., SCHMALZLE, J., LEYTON, B., BARROS, L. F. & DEITMER, J. W. 2019. Tight coupling of astrocyte energy metabolism to synaptic activity revealed by genetically encoded FRET nanosensors in hippocampal tissue. *J Cereb Blood Flow Metab,* 39**,** 513-523.
SAGAR, S. M., SHARP, F. R. & SWANSON, R. A. 1987. The regional distribution of glycogen in rat brain fixed by microwave irradiation. *Brain Res,* 417**,** 172-4.
SAKAGUCHI, T. & BRAY, G. A. 1987. The effect of intrahypothalamic injections of glucose on sympathetic efferent firing rate. *Brain Res Bull,* 18**,** 591-5.
SAKAGUCHI, T. & BRAY, G. A. 1988. Sympathetic activity following paraventricular injections of glucose and insulin. *Brain Res Bull,* 21**,** 25-9.
SANDERS, N. M. & RITTER, S. 2000. Repeated 2-deoxy-D-glucose-induced glucoprivation attenuates Fos expression and glucoregulatory responses during subsequent glucoprivation. *Diabetes,* 49**,** 1865-74.
SARAVANI, R., ESMAEELI, E., TAMENDANI, M. & NEJAD, M. 2015. Oxytocin Receptor Gene Polymorphisms in Patients With Diabetes. *Gene, Cell and Tissue,* 2.
SATO, M., MINABE, S., SAKONO, T., MAGATA, F., NAKAMURA, S., WATANABE, Y., INOUE, N., UENOYAMA, Y., TSUKAMURA, H. & MATSUDA, F. 2021. Morphological Analysis of the Hindbrain Glucose Sensor-Hypothalamic Neural Pathway Activated by Hindbrain Glucoprivation. *Endocrinology,* 162.
SAYAR-ATASOY, N., LAULE, C., AKLAN, I., KIM, H., YAVUZ, Y., ATES, T., COBAN, I., KOKSALAR-ALKAN, F., RYSTED, J., DAVIS, D., SINGH, U., ALP, M. I., YILMAZ, B., CUI, H. & ATASOY, D. 2023. Adrenergic modulation of melanocortin pathway by hunger signals. *Nat Commun,* 14**,** 6602.
SCHUR, E. A., MELHORN, S. J., OH, S. K., LACY, J. M., BERKSETH, K. E., GUYENET, S. J., SONNEN, J. A., TYAGI, V., ROSALYNN, M., DE LEON, B., WEBB, M. F., GONSALVES, Z. T., FLIGNER, C. L., SCHWARTZ, M. W. & MARAVILLA, K. R. 2015. Radiologic evidence that hypothalamic gliosis is associated with obesity and insulin resistance in humans. *Obesity (Silver Spring),* 23**,** 2142-8.
SCHWARTZ, M. W., SEELEY, R. J., TSCHOP, M. H., WOODS, S. C., MORTON, G. J., MYERS, M. G. & D'ALESSIO, D. 2013. Cooperation between brain and islet in glucose homeostasis and diabetes. *Nature,* 503**,** 59-66.
SHIMAZU, T., FUKUDA, A. & BAN, T. 1966. Reciprocal influences of the ventromedial and lateral hypothalamic nuclei on blood glucose level and liver glycogen content. *Nature,* 210**,** 1178-9.
SHIMAZU, T. & OGASAWARA, S. 1975. Effects of hypothalamic stimulation on gluconeogenesis and glycolysis in rat liver. *Am J Physiol,* 228**,** 1787-93.
SHIUCHI, T., HAQUE, M. S., OKAMOTO, S., INOUE, T., KAGEYAMA, H., LEE, S., TODA, C., SUZUKI, A., BACHMAN, E. S., KIM, Y. B., SAKURAI, T., YANAGISAWA, M., SHIODA, S., IMOTO, K. &

MINOKOSHI, Y. 2009. Hypothalamic orexin stimulates feeding-associated glucose utilization in skeletal muscle via sympathetic nervous system. *Cell Metab,* 10**,** 466-80.
SHRESTHA, P. K., TAMRAKAR, P., IBRAHIM, B. A. & BRISKI, K. P. 2014. Hindbrain medulla catecholamine cell group involvement in lactate-sensitive hypoglycemia-associated patterns of hypothalamic norepinephrine and epinephrine activity. *Neuroscience,* 278**,** 20-30.
SILVER, I. A. & ERECINSKA, M. 1994. Extracellular glucose concentration in mammalian brain: continuous monitoring of changes during increased neuronal activity and upon limitation in oxygen supply in normo-, hypo-, and hyperglycemic animals. *J Neurosci,* 14**,** 5068-76.
SIMPSON, I. A., APPEL, N. M., HOKARI, M., OKI, J., HOLMAN, G. D., MAHER, F., KOEHLER-STEC, E. M., VANNUCCI, S. J. & SMITH, Q. R. 1999. Blood-brain barrier glucose transporter: effects of hypo- and hyperglycemia revisited. *J Neurochem,* 72**,** 238-47.
SMITH, A. S., KORGAN, A. C. & YOUNG, W. S. 2019. Oxytocin delivered nasally or intraperitoneally reaches the brain and plasma of normal and oxytocin knockout mice. *Pharmacol Res,* 146**,** 104324.
SNIDER, B., GEISER, A., YU, X. P., BEEBE, E. C., WILLENCY, J. A., QING, K., GUO, L., LU, J., WANG, X., YANG, Q., EFANOV, A., ADAMS, A. C., COSKUN, T., EMMERSON, P. J., ALSINA-FERNANDEZ, J. & AI, M. 2019. Long-Acting and Selective Oxytocin Peptide Analogs Show Antidiabetic and Antiobesity Effects in Male Mice. *J Endocr Soc,* 3**,** 1423-1444.
SONG, Z., LEVIN, B. E., MCARDLE, J. J., BAKHOS, N. & ROUTH, V. H. 2001. Convergence of pre- and postsynaptic influences on glucosensing neurons in the ventromedial hypothalamic nucleus. *Diabetes,* 50**,** 2673-81.
SONG, Z., LEVIN, B. E., STEVENS, W. & SLADEK, C. D. 2014. Supraoptic oxytocin and vasopressin neurons function as glucose and metabolic sensors. *Am J Physiol Regul Integr Comp Physiol,* 306**,** R447-56.
STANLEY, S., DOMINGOS, A. I., KELLY, L., GARFIELD, A., DAMANPOUR, S., HEISLER, L. & FRIEDMAN, J. 2013. Profiling of Glucose-Sensing Neurons Reveals that GHRH Neurons Are Activated by Hypoglycemia. *Cell Metab,* 18**,** 596-607.
STARICHA, K., MEYERS, N., GARVIN, J., LIU, Q., RARICK, K., HARDER, D. & COHEN, S. 2020. Effect of high glucose condition on glucose metabolism in primary astrocytes. *Brain Res,* 1732**,** 146702.
STECULORUM, S. M., RUUD, J., KARAKASILIOTI, I., BACKES, H., ENGSTROM RUUD, L., TIMPER, K., HESS, M. E., TSAOUSIDOU, E., MAUER, J., VOGT, M. C., PAEGER, L., BREMSER, S., KLEIN, A. C., MORGAN, D. A., FROMMOLT, P., BRINKKOTTER, P. T., HAMMERSCHMIDT, P., BENZING, T., RAHMOUNI, K., WUNDERLICH, F. T., KLOPPENBURG, P. & BRUNING, J. C. 2016. AgRP Neurons Control Systemic Insulin Sensitivity via Myostatin Expression in Brown Adipose Tissue. *Cell,* 165**,** 125-138.
STEVENSON, R. J., FRANCIS, H. M., ATTUQUAYEFIO, T., GUPTA, D., YEOMANS, M. R., OATEN, M. J. & DAVIDSON, T. 2020. Hippocampal-dependent appetitive control is impaired by experimental exposure to a Western-style diet. *R Soc Open Sci,* 7**,** 191338.
SUPPLIE, L. M., DUKING, T., CAMPBELL, G., DIAZ, F., MORAES, C. T., GOTZ, M., HAMPRECHT, B., BORETIUS, S., MAHAD, D. & NAVE, K. A. 2017. Respiration-Deficient Astrocytes Survive As Glycolytic Cells In Vivo. *J Neurosci,* 37**,** 4231-4242.
SUZUKI, A., STERN, S. A., BOZDAGI, O., HUNTLEY, G. W., WALKER, R. H., MAGISTRETTI, P. J. & ALBERINI, C. M. 2011. Astrocyte-neuron lactate transport is required for long-term memory formation. *Cell,* 144**,** 810-23.
SWAAB, D. F., PURBA, J. S. & HOFMAN, M. A. 1995. Alterations in the hypothalamic paraventricular nucleus and its oxytocin neurons (putative satiety cells) in Prader-Willi syndrome: a study of five cases. *J Clin Endocrinol Metab,* 80**,** 573-9.
SWANSON, L. W. & SAWCHENKO, P. E. 1983. Hypothalamic integration: organization of the paraventricular and supraoptic nuclei. *Annu Rev Neurosci,* 6**,** 269-324.
SWANSON, R. A. & CHOI, D. W. 1993. Glial glycogen stores affect neuronal survival during glucose deprivation in vitro. *J Cereb Blood Flow Metab,* 13**,** 162-9.
TANG, Q., LIU, Q., LI, J., YAN, J., JING, X., ZHANG, J., XIA, Y., XU, Y., LI, Y. & HE, J. 2022. MANF in POMC Neurons Promotes Brown Adipose Tissue Thermogenesis and Protects Against Diet-Induced Obesity. *Diabetes,* 71**,** 2344-2359.
THALER, J. P., YI, C. X., SCHUR, E. A., GUYENET, S. J., HWANG, B. H., DIETRICH, M. O., ZHAO, X., SARRUF, D. A., IZGUR, V., MARAVILLA, K. R., NGUYEN, H. T., FISCHER, J. D., MATSEN, M. E., WISSE, B. E., MORTON, G. J., HORVATH, T. L., BASKIN, D. G., TSCHOP, M. H. & SCHWARTZ, M. W. 2012. Obesity is associated with hypothalamic injury in rodents and humans. *J Clin Invest,* 122**,** 153-62.

TODA, C., KIM, J. D., IMPELLIZZERI, D., CUZZOCREA, S., LIU, Z. W. & DIANO, S. 2016. UCP2 Regulates Mitochondrial Fission and Ventromedial Nucleus Control of Glucose Responsiveness. *Cell,* 164**,** 872-83.

TODA, C., SHIUCHI, T., LEE, S., YAMATO-ESAKI, M., FUJINO, Y., SUZUKI, A., OKAMOTO, S. & MINOKOSHI, Y. 2009. Distinct effects of leptin and a melanocortin receptor agonist injected into medial hypothalamic nuclei on glucose uptake in peripheral tissues. *Diabetes,* 58**,** 2757-65.

TONG, Q., YE, C., MCCRIMMON, R. J., DHILLON, H., CHOI, B., KRAMER, M. D., YU, J., YANG, Z., CHRISTIANSEN, L. M., LEE, C. E., CHOI, C. S., ZIGMAN, J. M., SHULMAN, G. I., SHERWIN, R. S., ELMQUIST, J. K. & LOWELL, B. B. 2007. Synaptic glutamate release by ventromedial hypothalamic neurons is part of the neurocircuitry that prevents hypoglycemia. *Cell Metab,* 5**,** 383-93.

TRIBOLLET, E., CHARPAK, S., SCHMIDT, A., DUBOIS-DAUPHIN, M. & DREIFUSS, J. J. 1989. Appearance and transient expression of oxytocin receptors in fetal, infant, and peripubertal rat brain studied by autoradiography and electrophysiology. *J Neurosci,* 9**,** 1764-73.

VAN DEN BROEK-ALTENBURG, E., ATHERLY, A. & HOLLADAY, E. 2022. Changes in healthcare spending attributable to obesity and overweight: payer- and service-specific estimates. *BMC Public Health,* 22**,** 962.

VAN DEN HOEK, A. M., VAN HEIJNINGEN, C., SCHRODER-VAN DER ELST, J. P., OUWENS, D. M., HAVEKES, L. M., ROMIJN, J. A., KALSBEEK, A. & PIJL, H. 2008. Intracerebroventricular administration of neuropeptide Y induces hepatic insulin resistance via sympathetic innervation. *Diabetes,* 57**,** 2304-10.

VANNUCCI, S. J., KOEHLER-STEC, E. M., LI, K., REYNOLDS, T. H., CLARK, R. & SIMPSON, I. A. 1998. GLUT4 glucose transporter expression in rodent brain: effect of diabetes. *Brain Res,* 797**,** 1-11.

VARELA, L., STUTZ, B., SONG, J. E., KIM, J. G., LIU, Z. W., GAO, X. B. & HORVATH, T. L. 2021. Hunger-promoting AgRP neurons trigger an astrocyte-mediated feed-forward autoactivation loop in mice. *J Clin Invest,* 131.

VEGA, C., R. SACHLEBEN L, J., GOZAL, D. & GOZAL, E. 2006. Differential metabolic adaptation to acute and long-term hypoxia in rat primary cortical astrocytes. *J Neurochem,* 97**,** 872-83.

VERKHRATSKY, A., MATTEOLI, M., PARPURA, V., MOTHET, J. P. & ZOREC, R. 2016. Astrocytes as secretory cells of the central nervous system: idiosyncrasies of vesicular secretion. *EMBO J,* 35**,** 239-57.

WATANABE, S., WEI, F. Y., MATSUNAGA, T., MATSUNAGA, N., KAITSUKA, T. & TOMIZAWA, K. 2016. Oxytocin Protects against Stress-Induced Cell Death in Murine Pancreatic beta-Cells. *Sci Rep,* 6**,** 25185.

WATTS, A. G. & DONOVAN, C. M. 2010. Sweet talk in the brain: glucosensing, neural networks, and hypoglycemic counterregulation. *Front Neuroendocrinol,* 31**,** 32-43.

WEI, J., SHIMAZU, J., MAKINISTOGLU, M. P., MAURIZI, A., KAJIMURA, D., ZONG, H., TAKARADA, T., LEZAKI, T., PESSIN, J. E., HINOI, E. & KARSENTY, G. 2015. Glucose Uptake and Runx2 Synergize to Orchestrate Osteoblast Differentiation and Bone Formation. *Cell,* 161**,** 1576-1591.

WEIGHTMAN POTTER, P. G., ELLACOTT, K. L. J., RANDALL, A. D. & BEALL, C. 2022. Glutamate Prevents Altered Mitochondrial Function Following Recurrent Low Glucose in Hypothalamic but Not Cortical Primary Rat Astrocytes. *Cells,* 11.

WELCH, S., GEBHART, S. S., BERGMAN, R. N. & PHILLIPS, L. S. 1990. Minimal model analysis of intravenous glucose tolerance test-derived insulin sensitivity in diabetic subjects. *J Clin Endocrinol Metab,* 71**,** 1508-18.

WENDER, R., BROWN, A. M., FERN, R., SWANSON, R. A., FARRELL, K. & RANSOM, B. R. 2000. Astrocytic glycogen influences axon function and survival during glucose deprivation in central white matter. *J Neurosci,* 20**,** 6804-10.

WESS, J., NAKAJIMA, K. & JAIN, S. 2013. Novel designer receptors to probe GPCR signaling and physiology. *Trends Pharmacol Sci,* 34**,** 385-92.

WICK, A. N., DRURY, D. R. & MORITA, T. N. 1955. 2-Deoxyglucose; a metabolic block for glucose. *Proc Soc Exp Biol Med,* 89**,** 579-82.

YAMAMOTO, H., NAGAI, K. & NAKAGAWA, H. 1988. Time-dependent involvement of autonomic nervous system in hyperglycemia due to 2-deoxy-D-glucose. *Am J Physiol,* 255**,** E928-33.

YOSHIMATSU, H., NIIJIMA, A., OOMURA, Y., YAMABE, K. & KATAFUCHI, T. 1984. Effects of hypothalamic lesion on pancreatic autonomic nerve activity in the rat. *Brain Res,* 303**,** 147-52.

ZHANG, B., QIU, L., XIAO, W., NI, H., CHEN, L., WANG, F., MAI, W., WU, J., BAO, A., HU, H., GONG, H., DUAN, S., LI, A. & GAO, Z. 2021. Reconstruction of the Hypothalamo-Neurohypophysial System and Functional Dissection of Magnocellular Oxytocin Neurons in the Brain. *Neuron,* 109**,** 331-346 e7.

ZHANG, H., WU, C., CHEN, Q., CHEN, X., XU, Z., WU, J. & CAI, D. 2013. Treatment of obesity and diabetes using oxytocin or analogs in patients and mouse models. *PLoS One,* 8**,** e61477.
ZHAO, Z., WANG, L., GAO, W., HU, F., ZHANG, J., REN, Y., LIN, R., FENG, Q., CHENG, M., JU, D., CHI, Q., WANG, D., SONG, S., LUO, M. & ZHAN, C. 2017. A Central Catecholaminergic Circuit Controls Blood Glucose Levels during Stress. *Neuron,* 95**,** 138-152 e5.
ZHOU, Q., LEI, X., FU, S., LIU, P., LONG, C., WANG, Y., LI, Z., XIE, Q. & CHEN, Q. 2023. Efficacy and safety of tirzepatide, dual GLP-1/GIP receptor agonists, in the management of type 2 diabetes: a systematic review and meta-analysis of randomized controlled trials. *Diabetol Metab Syndr,* 15**,** 222.

VIII. Acknowledgements

First and for all I want to thank Cristina for supporting me and my projects at all times including sharing her expertise in long scientific discussions and comments as well as encouraging my ideas and my scientific development. I also want to thank my thesis committee, Ilona and Ali, who always gave me great comments on my ongoing work and reassurance to be on the right track. Thank you also to our collaborators Heiko Backes, Tobias Wiedemann, Manfred Hallschmid and Mostafa Bakthi for the productive collaboration and enlightening data.

Furthermore, I would like to say a big thank you to a great astrocyte-neuron-network team, especially my supervisors Ophélia and Tim, Beata for her constant help in cell culture studies and our great technical assistance from Nicole, Clarita and Cassie. Last but not least, I am very grateful to my friends and family, who did not always understand what I was up to and what my struggles are but who nevertheless tried to be as supportive as possible.

Overall, I feel very blessed for the friendly and welcoming environment that I was allowed to experience over the last few years at IDO before and while I was working on my Phd thesis. I am sure I will always think back to this time remembering all the good times and happy memories.

IX. Eidesstaatliche Erklärung

Ich erkläre an Eides statt, dass ich die am Wissenschaftszentrum Weihenstephan zur Promotionsprüfung vorgelegte Arbeit mit dem Titel:

“Deciphering the roles of hypothalamic oxytocin neurons and astrocytes in the regulation of systemic glucose homeostasis”

am Institut für Diabetes und Adipositas (Helmholtz Zentrum München) unter der Anleitung und Betreuung durch Prof. Ilona Grunwald Kadow und Prof. Dr. Cristina García-Cáceres ohne sonstige Hilfsmittel erstellt und bei der Abfassung nur die gemäß § 6 Abs. 6 und 7 Satz 2 angegebenen Hilfsmittel benutzt habe.

Ich habe keine Organisation eingeschaltet, die gegen Entgelt Betreuerinnen und Betreuer für die Anfertigung von Dissertationen sucht, oder die mir obliegenden Pflichten hinsichtlich der Prüfungsleistungen für mich ganz oder teilweise erledigt. Ich habe die Dissertation in dieser oder ähnlicher Form in keinem anderen Prüfungsverfahren als Prüfungsleistung vorgelegt.

Die vollständige Dissertation wurde noch nicht veröffentlicht.

Ich habe den angestrebten Doktorgrad noch nicht erworben und bin nicht in einem früheren Promotionsverfahren für den angestrebten Doktorgrad endgültig gescheitert.

Die öffentlich zugängliche Promotionsordnung der TUM ist mir bekannt, insbesondere habe ich die Bedeutung von § 28 (Nichtigkeit der Promotion) und § 29 (Entzug des Doktorgrades) zur Kenntnis genommen.

Ich bin mir der Konsequenzen einer falschen Eidesstattlichen Erklärung bewusst.

Mit der Aufnahme meiner personenbezogenen Daten in die Alumni-Datei bei der TUM bin ich einverstanden.

München, den 11.12.23 Franziska Lechner

X. Supplementary

5.1 Materials

Table 2 – Chemicals, kits and consumables

	Producer	**Catalogue Number**
RNAscope Wash Buffer Reagents	ACD	310091
RNAscope Target Retrieval Reagents	ACD	322000
NaOH	Carl Roth	6771
Tris	Carl Roth	4855
GoTaq G2 Flexi DNA Polymerase	Promega	M7806
KAPA2G fast genotyping mix	Sigma Aldrich	KK5121
Ultra-sensitive Mouse Insulin ELISA Kit	Crystalchem	900080
MicroRNeasy Kit	Qiagen	74106
Glucose	Gibco	15023-021
Collagenase P	Sigma-Aldrich	11213865001
Mouse Glucagon Elisa Kit	CrystalChem	81518
QuickDetect Catecholamine Mouse Elisa Kit	BioVision	E4462-100
Corticosterone Elisa Kit	Enzo	ADI-900-097
Hexamethonium chloride	Sigma Aldrich	H2138
2-Deoxy-Glucose	Sigma Aldrich	D8375
Synthocinon	Selleck Chemicals	P1029
RPMI medium 1640	Sigma Aldrich	R8758
Krebs-Ringer bicarbonate buffer	Sigma Aldrich	K4002
HBSS	ThermoFisher Scientific	
MEM	ThermoFisher Scientific	11095
Pierce™ BCA Protein Assay Kit	ThermoFisher Scientific	23227
Micro BCA ™ Protein Assay Kit	ThermoFisher Scientific	23235
Human insulin – Actrapid ® Penfill ®	Novo Nordisk	00536427
TritonX 100	Roche Diagnostics	11332481001
Gelantine	Sigma Aldrich	G1890
FBS heat-inactivated	Gibco®/ThermoFisher Scientific	
Prolong™ Diamond Mountant	ThermoFisher Scientific	P36965
Glucose Uptake Assay Kit (Colorimetric)	Abcam	Ab136955

Seahorse XF Mito Fuel Flex Test Kit	Agilent Technologies	103260-100
RNAscope® Multiplex Fluorescent Detection Reagents v2	ACD	323110
RNAscope® H2O2 and Protease Reagents	ACD	322381

5.2 Genotyping protocols

Table 3 – Genotyping GLUT-1flx - Mastermix

Substance	Concentration	Volume [µl]
H2O		6.6
Promega rxn buffer	5x	2.5
MgCl2		1
dNTP	2 mM	0.25
Glut1-fwd	0.2 mM	0.5
Glut1-rev	0.5 uM	0.5
Promega go taq flexi	0.01 U/ul	0.15

Glut1-loxP1 primer: TTGAGAGCCATCTGGAAGGGGG forward
Glut1-loxP1 primer: CAAGACTCTGAGGATGGTGGCCA reverse

Table 4 – Genotyping GLUT-1flx - PCR

Step	Temperature [°]	Time [min]	Cycles
Initial denaturation	95	3	1
Denaturation	95	0.5	
Annealing	60	0.5	39
Elongation	60	2	
Final Elongation	70	10	1

Table 5 – Genotyping GLASTCreERT2 - Mastermix

Substance	Concentration	Volume [µl]	
		Mutant Mix	WT Mix
H2O		5.625	5.625
Fast genotyping Mix		6.25	6.25
GLAST F8	20 µM	0.3125	0.3125
GLAST R3	20 µM		0.3125
CER1	20 µM	0.3125	

GLAST F8 *gag gca ctt ggc tag gct ctg agg a* *forward*

GLAST R3 *gag gag atc ctg acc gat cag ttg g* *reverse*

CER1 (Cre-ERT2 specific) *ggt gta cgg tca gta aat tgg aca t*

Table 6 – Genotyping GLASTCreERT2 - PCR

Step	Temperature [°]	Time [min]	Cycles
Initial denaturation	95	3	1
Denaturation	95	0.25	
Annealing	60	0.25	40
Elongation	72	0.25	
Final Elongation	72	1	1

Table 7 – Genotyping Ins1 Cre - Mastermix

Substance	Concentration	Volume [µl]
H2O		4.375
Fast genotyping Mix		6.25
Primer 26992	20 µM	0.625
Primer 26993	20 µM	0.625
Primer 26994	20 µM	0.625

Primer 26992 *GGA AGC AGA ATT CCA GAT ACT TG* *Common*

Primer 26993 *GTC AAA CAG CAT CTT TGT GGT C* *Wildtype forward*

Primer 26994 *GCT GGA AGA TGG CGA TTA GC* *Mutant forward*

Table 8 – Genotyping Ins1 Cre - PCR

Step	Temperature [°]	Time [min]	Cycles
Initial denaturation	95	3	1
Denaturation	95	0.25	
Annealing	60	0.25	40
Elongation	72	0.25	
Final Elongation	72	1	1

Table 9 – Genotyping OxtRflx - Mastermix

Substance	Concentration	Volume [µl]
H2O		10
Fast genotyping Mix	1x	13.75
OxtRflx F 13420	0.5 µM	0.625

OxtRflx R13421	0.5 µM	0.625

Primer 13420 *GCT GAG TCT TGG AAG CAG GA Forward*
Primer 13421 *GGT ACC TCC TTT GAG CTT CTG Reverse*

Table 10 – Genotyping OxtRflx - PCR

Step	Temperature [°]	Time [min]	Cycles
Initial denaturation	95	3	1
Denaturation	95	0.25	
Annealing	60	0.25	40
Elongation	72	0.25	
Final Elongation	72	1	1

Table 11 – Genotyping Oxt-ires-Cre - Mastermix

Substance	Concentration	Volume [µl]
H2O		3.6
Promega rxn buffer	5x	2.5
MgCl2	25mM	1.5
dNTP	10mM	0.25
13007	20µM	0.25
19178	20µM	0.25
19179	20µM	0.25
Betaine	5M	2.5
Promega go taq flexi	5U/µl	0.15

Primer 13007 *ACA CCG GCC TTA TTC CAA G* *Mutant*
Primer 19178 *TTT GCA GCT CAG AAC ACT GAC* *Common*
Primer 19179 *AGC CTG CTG GAC TGT TTT TG* *Wild type*

Table 12 – Genotyping Oxt-ires-Cre - PCR

Step	Temperature [°]	Time	Cycles
Initial denaturation	94	2min	1
Denaturation	94	20s	
Annealing	65	15s	10 (-0.5°C per cycle)
Elongation	68	10s	
Denaturation	94	15s	
Annealing	60	15s	28

Elongation	72	10s	
Final Elongation	72	2min	1

5.3 Probes, antibodies, adenoviruses

Table 13 – Taqman probes

Gene name	Acronym	Indentifier
Glucose transporter 1	Glut 1/ Slc2A1	Mm00441480
Glutamate aspartate transporter	Glast/Slc1A3	Mm00600697
Glutamate Dehydrogenase 1	Glud1	Mm00492353
Malic enzyme	ME1	Mm00782380
Glutamate Sythase	Glu1	Mm00725701
Glycogen Phosphorylase brain type	Pgyb	Mm00464080
Glutamine Synthetase	GS	Mm00725701
Glucose transporter 3	Glut3/ Slc2A3	Mm00441483
Glucose transporter 4	Glut4/ Slc2A4	Mm01245502
Phosphoenolpyrovate carboxykinase	Pepck/Pck1	Mm01247058
Monocarboxylate transporter 4	MCT4/SLC16A3	Mm00446102
Monocarboxylate transporter 1	MCT1/SLC16A1	Mm01306379
Pyrovate dehydrogenase kinase isoform 2	PDK2	Mm00446681
Ribosomal Protein L32	Rpl32	Mm02528467

Table 14 – Antibodies

Target	Host	Conjugate	Dilution	Product code	Provider
cFos	rabbit	-	1:500		Synaptic Systems
rabbit	donkey	647	1:1000	2420695	Invitrogen, ThermoFisher Scientific

Table 15 – RNAscope probes

Target	Channel	Product code	Provider
Slc2a1/GLUT-1	C1	458671	ACD
Slc1a3/Glast	C4	430781	ACD

Table 16 – Opal dyes

Conjugate	Dilution	Product code	Provider
520	1:1000	FP1487001KT	Opal™, Akoya Biosciences
690	1:1000	FP1497001KT	Opal™, Akoya Biosciences

Table 17 – Viral vectors

Name	Serotype	Promotor	Linker and Enhancer	Titer	Provider
AAV-eSYN-mCherry-T2A-WPRE	1	eSyn	2A linker; WPRE	10^{13}	Vector Biolabs, Malvern, USA
AAV-eSYN-mCherry-T2A-iCre-WPRE	1	eSyn	2A linker; WPRE	10^{13}	Vector Biolabs, Malvern, USA
rAAV.GFAPp.eGFP	2/5	Gfa2 (2.2kb)	WPRE	10^{13}	Vectorbiolabs, Malvern, USA
rAAV.GFAPp.iCre	2/5	Gfa2 (2.2kb)	WPRE	10^{13}	Vectorbiolabs, Malvern, USA
AAV-hSyn-DIO-hM3Dq-mCherry	5	hSyn (0.5kb)	2A linker	$3.8x10^{12}$	Horvath Lab, Yale, USA
AAV-hSyn-DIO-mCherry	5	hSyn (0.5kb)	2A linker	$3.8x10^{12}$	Horvath Lab, Yale, USA
AAV-GFAP-m-SLC2A1-P2A-EGFP	2/5	Gfap (0.7kb)		10^{12}	VectorBioLabs, Malvern, USA
AAV-GFAP-P2A-EGFP	2/5	Gfap (0.7kb)		10^{12}	VectorBioLabs, Malvern, USA
pAAV-Syn-GCaMP6m.WPRE		Syn	WPRE	$1.3x10^{13}$	Addgene

XI. Curriculum vitae